Adaptor binding sites in the clathrin terminal domain directly recruit the microtubule-stabilizing protein GTSE1 to the mitotic spindle

Inaugural-Dissertation

zur

Erlangung des Doktorgrades

Dr. rer. nat.

der Fakultät

für Biologie

an der

Universität Duisburg-Essen

vorgelegt von

Yu-Chih Lin

aus Taiwan

durchgeführt am

Max Planck Institut für molekulare Physiologie

Abteilung für mechanistische Zellbiologie

AG Bird

Februar 2018

Die der vorliegenden Arbeit zugrunde liegenden Experimente wurden am Max Planck Institut für molekulare Physiologie in der Abteilung für mechanistische Zellbiologie durchgeführt.

1. Gutachter: Prof. Dr. Andrea Musacchio
2. Gutachter: Prof. Dr. Hemmo Meyer

Vorsitzender des Prüfungsausschusses: Prof. Dr. Stefan Westermann

Tag der mündlichen Prüfung:
13. April 2018

Table of Contents

List of figures

List of tables

List of Abbreviations

ADP – Adenosine diphosphate

APC – Anaphase Promoting Complex

ATP – Adenosine triphosphate

BACs – Bacterial Artificial Chromosomes

bp – basepair

BSA– Bove Serum Albumin

CB – Coomassie Brilliant Blue

CCAN – Constitutive Centromere-Associated Network

Cdk – Cyclin Dependent Kinase

CHC– Clathrin Heavy Chain

CHC TD – Clathrin Heavy Chain Terminal Domain

ch-TOG – Colonic And Hepatic Tumor Over-Expressed Gene Protein

CIN – Chromosomal Instability

CPC – Chromosome Passenger Complex

CREST – Calcinosis, Raynaud's syndrome, Esophageal dysmotiliy, Sclerodactyly, Telangiectasia

DAPI – 4,6-diamidin-2-phenylindoldihydrochlorid

ddH_2O – double distilled water

DMEM – Dulbecco's Modified Eagle Medium

DMSO – Dimethyl sulfoxide

DNA – Deoxyribonucleic acid

D-TACC – Drosphila-Transforming Acid Coiled-coil Containing Protein 3

EB – End Binding Protein

FL – full-length

GAK– Cyclin G-associated kinase

GDP – Guanosine-5’-triphosphate

GFP – Green Fluorescent Protein

GTP – Guanosine-5’-triphosphate Index

GTSE1 – G2 and S phase expressed 1

GST – Glutathione-S-transferase

IF– immunofluorescence

IP–immunoprecipitation

kDa – kilo Dalton

KMN – KNL, Mis12, and Ndc80 Network

LB – Luria-Bertani medium

M-phase – Mitotic phase

mA – milli Ampere

MAPs – Microtubule Associated Proteins

Mad – Mitotic Arrest Deficient

MCAK – Mitotic Centromere Associated Kinesin

MCC – Mitotic Checkpoint Complex

MBP – Maltose binding protein

MT – Microtubule

NEBD – Nuclear Envelope Breakdown

PBS – Phosphate buffered saline

PCR – Polymerase Chain Reaction

PFA – Paraformaldehyde

PLA– Proximity Ligation Assay

Plk1 – Polo Like Kinase 1

S-phase – Synthesis phase

SAC – Spindle Assembly Checkpoint

SDS-page – Sodium Dodecyl Sulfate polyacrylamide gel electrophoresis

SEC – Size Exclusion Chromatography

TACC3 – Transforming Acid Coiled-coil Containing Protein 3

TGN – trans-Golgi network

TCEP – Tris-(2-carboxyethyl)-phosphine

TPX2 – Targeting Protein for Xklp2

V – Volts

WT – Wildtype

+TIP – Plus-tip Interacting Protein

Abstract

Proper microtubule stability is crucial to build normal bipolar spindles and align chromosomes correctly during mitosis. Clathrin heavy chain 17 (CHC) is required for microtubule stability during mitosis independent of its functions in interphase. CHC interacts with the protein TACC3, which permits the CHC-TACC3 complex to translocate onto mitotic spindles. A mutant on the CHC terminal domain (TD) affects neither the TACC3 interaction nor their spindle localization. However, this mutant further causes mitotic defects, suggesting that the CHC TD has unique functions during mitosis. Here, we found that GTSE1 binds directly to the CHC terminal domain (TD) via several LIDL-like motifs that resemble motifs in clathrin adaptor proteins for binding the CHC TD. A pair of different interactions with these motifs is required for stabilizing the CHC-GTSE1 complex. Using X-ray crystallography, we further gained insight into this interaction in a molecular resolution. Moreover, its direct interaction with CHC is required for GTSE1's recruitment to and functions on spindles. GTSE1 mutated at these CHC-binding motifs delocalizes from spindles and leads to defects in the spindle architecture, chromosome alignment and timely mitosis. We previously identified GTSE1 as a novel microtubule-stabilizing protein that inhibits the activity of the microtubule depolymerase MCAK. In this study, we reconstituted a microtubule-stabilizing complex including CHC, TACC3, ch-TOG and GTSE1 *in vitro*, and this complex can further interact with MCAK. Thus, one mechanism of how the CHC TD stabilizes spindle microtubules is by bringing GTSE1 to inhibit MCAK. Furthermore, we found that GTSE1 could weakly interact with the KMNZ network of kinetochores, dependent on Aurora B phosphorylation, and that GTSE1 occasionally colocalizes with MCAK on kinetochores. This recruitment might imply how GTSE1 regulates MCAK activity on kinetochores to maintain the proper microtubule-kinetochore attachment. In summary, here we showed that GTSE1 localizes on spindles via the CHC-TACC3 complex and is recruited to the outer kinetochores through the KMNZ complex, which globally regulates MCAK activity in mitosis to achieve a normal bipolar spindle and proper microtubule-kinetochore attachment.

Zusammenfassung

Die richtige Mikrotubilistabilität ist sowohl entscheidend für den Aufbau normaler bipolarer Spindeln als auch für die korrekte Ausrichtung der Chromosomen während der Mitose. Clathrin Heavy Chain 17 (CHC) wird, unabhängig von seinen Funktionen während der Interphase, während der Mitose zur Stabilisierung der Mikrotubuli benötigt. CHC interagiert mit dem Protein TACC3, was es dem CHC-TACC3 Komplex dann ermöglicht, sich auf mitotische Spindeln zu verlagern. Eine Mutation in der CHC Terminal Domäne (TD) beeinflusst weder die Interaktion mit TACC3 noch die Spindellokalisierung. Jedoch verursacht diese Mutation Defekte in der Mitose, was darauf hindeutet, dass die CHC TD einzigartige Funktionen während der Mitose ausübt. Hier konnten wir zeigen, dass GTSE1 durch mehrere LIDL Motive, die den Motiven von Clathrinadaptorproteinen ähneln, direkt die CHC TD bindet. Zur Stabilisierung dieses Komplexes werden dabei drei individuelle LIDL Motive benötigt. Mit Hilfe von Röntgenkristallographie konnten wir weitere Einblicke in diese Wechselwirkung in molekularer Auflösung gewinnen. Darüber hinaus ist die direkte Interaktion von CHC mit GTSE1 für die Rekrutierung von GTSE1 und die Lokalisierung an der mitotischen Spindel erforderlich. Mutationen von GTSE1 im Bereich dieser CHC Bindungsmotive führen zur Delokalisation von GTSE1 von der Spindel und Defekten in der Spindelarchitektur, Chromosomenausrichtung und verzögerter Mitose.

Zuvor konnten wir GTSE1 als neuartiges Mikrotubuli stabilisierendes Protein identifizieren, das die Depolymeraseaktivität von MCAK inhibiert. In dieser Studie rekonstruierten wir in vitro einen Mikrotubuli stabilisierenden Komplex aus CHC, TACC3, ch-TOG und GTSE1 und konnten zeigen, dass dieser des Weiteren mit MCAK interagieren kann. Demnach ist ein Mechanismus, durch den Spindelmikrotubuli stabilisiert werden, dass GTSE1 von CHC-TD rekrutiert wird und in Folge dessen MCAK inhibieren kann. Darüber hinaus fanden wir heraus, dass GTSE1 schwach mit dem KMNZ-Netzwerk von Kinetochoren in Abhängigkeit von Phosphorylierung durch Aurora B interagieren kann und dass GTSE1 sich vereinzelt mit MCAK an Kinetochoren kolokalisiert. Diese Rekrutierung könnte zeigen, wie GTSE1 die Aktivität von MCAK an Kinetochoren reguliert, um die korrekte Bindung zwischen Mikrotubuli und Kinetochoren aufrechtzuerhalten.

Zusammenfassend haben wir hier gezeigt, dass sich GTSE1 mit Hilfe des CHC-TACC3-Komplexes an Spindeln lokalisiert und durch den KMNZ-Komplex zu den äußeren Kinetochoren rekrutiert wird, wodurch die Aktivität von MCAK in der Mitose global reguliert

wird, um eine normale bipolare Spindel und korrekte Bindungen zwischen Mikrotubuli und Kinetochoren zu erreichen.

1. Introduction

The precise regulation of microtubule dynamics and stability ensures accurate chromosome segregation during cell division. Clathrin has recently emerged as an unexpected player to control mitotic microtubule stability. Clathrin heavy chain 17 (CHC) interacts with TACC3 in mitosis to form a complex that binds to microtubules and localizes to spindles. The CHC-TACC3 complex is important for microtubule stability and chromosome alignment, but the mechanisms by which this complex stabilizes microtubules are still being unraveled. This complex has been shown to recruit GTSE1 onto spindles, suggesting that GTSE1 could be functionally involved in the CHC-TACC3 complex. Our laboratory previously found GTSE1 as a novel microtubule-stabilizing protein that is required for maintaining proper microtubule stability, correct chromosome alignment, and timely mitosis. Additionally, we identified that the mechanism by which GTSE1 stabilizes microtubules is through the inhibition of MCAK. In this study, we aimed to ask if the GTSE1-MCAK complex could be a directly downstream effector of the CHC-TACC3 complex and understand how these protein complexes function together in stabilizing microtubules.

1.1 Tubulin dimer and microtubules

Microtubule dynamics is very important to regulate several cellular events such as cell migration and spindle integrity. The basic subunit of microtubule is tubulin dimer of one α- and one β-subunit that are tightly bound together. Each subunit of tubulin dimer binds GTP. The GTP bound to the α-tubulin is not hydrolyzed because it is trapped in the αβ-tubulin heterodimer. However, the GTP exposed on the β-tubulin is unstable and is hydrolyzed following polymerization (Akhmanova and Steinmetz, 2008). A protofilament is a polar polymer of the tubulin dimers in which the coming α-tubulin mainly adds onto the existing β-subunit of protofilament. The α-subunit-exposed end is designated as the minus end and the other β-subunit-exposed end is the plus end. In general, 13 protofilaments are laterally bound together and form a helically hollow cylinder called a microtubule that is approximately 25 μm in diameter (Akhmanova and Steinmetz, 2008). Microtubules show dynamic phases of growth and shrinkage/catastrophe at their plus ends where tubulin dimers are added or removed. The cycle between these two phases is termed dynamic instability (Mitchison and Kirschner, 1984). The GTP-containing end of microtubule (GTP-cap) is important for maintaining microtubule stability. If the GTP-cap is hydrolyzed, microtubule stops growing and depolymerizes. Once the GTP bound β-tubulin is added, this GTP-cap switches the

microtubule back to growth (Brouhard and Sept, 2012). In cells the minus ends of microtubules are captured and stabilized by microtubule organizing centers (MTOCs) and the plus ends show the growth and shrinkage of dynamics instability. However, in mitosis if the microtubule plus end is captured by chromosome, it is stabilized and the dynamic instability is suppressed (Heald and Khodjakov, 2015).

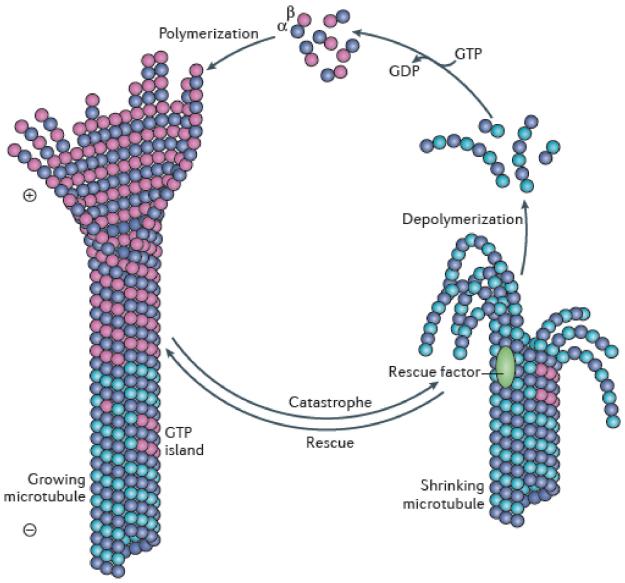

Figure 1-1. The cycle of tubulin assembly and disassembly

The GTP-bound tubulin dimer (purple) incorporates into the growing end (+) of microtubule. This process is called polymerization. GTP-bound β-tubulins on the plus end are termed a GTP-cap, which stabilizes the microtubule. Once the GTPs bound to β-tubulins are hydrolyzed (lightly blue), the tubulin dimers are removed from the plus end and undergo depolymerization/catastrophe, resulting in rapid shrinkage of the microtubule. When a rescue factor (e.g. a protein) approaches or new GTP-bound tubulin dimers are added on the plus end, the microtubule stops shrinking and repolymerizes again. The cycle between microtubule growth and catastrophe is termed "dynamic instability". Figure is adapted from Akhmanova and Steinmetz, 2015.

1.2 Microtubule associated proteins (MAPs)

MAPs are a group of proteins which associate with the tubulin subunit, the microtubule lattice or microtubule ends (Olmsted, 1986). Since microtubules are highly dynamic, MAPs generally either stabilize or destabilize microtubules. Recently, some MAPs have been found to accumulate specifically at the plus-end of microtubules, termed "+TIPs". EB (End binding) proteins are well known +TIPs. EB1 is an evolutionarily conserved protein that directly binds the microtubule plus end and controls microtubule dynamics (Vaughan, 2005). Proteins that contain SxIP motif (Ser-any amino acid-Ile-Pro) have been characterized as potential EB1

binding-proteins (Honnappa et al., 2009). Therefore, the tip tracking ability of some +TIPs is due to the interaction with EB proteins, but does not necessarily bind directly to the microtubule plus end. Other MAPs, motor proteins, utilize the energy from ATP and generate mechanical movement along microtubules. According to the movement on microtubules, motors are divided into kinesin or dynein. Kinesin usually moves toward the plus end and dynein moves toward the minus end. Due to the microtubule binding and the movement of motors, some motors generate a pull force to slide antiparallel microtubules apart and drive chromosome movement such as Kinesin-5 (Prosser and Pelletier, 2017). Additionally, some motor proteins form homodimer that bundle and stabilize microtubules, for example, kinesin-14 (Braun et al., 2009). The kinesin-13 family does not walk on microtubules, but acts as depolymerase to destabilize microtubules (Prosser and Pelletier, 2017).

1.3 Mitotic spindle microtubules

The mitotic spindle contains hundreds of microtubules in mammalian cells. Depending on whether they connect to kinetochores or not, microtubules can be simply divided into kinetochore fibers (k-fibers) or non-kinetochore fibers. In comparison with K-fibers, non-k-fibers are the major microtubules in mammalian spindles and are required for spindle shape and spindle stability (Mastronarde et al., 1993). Parallel microtubules originating from centrosomes, which form bundles that end at kinetochores, are known as K-fibers (discussed in detail in 1.4). Non-K-fiber microtubules, which do not interact with kinetochores, include astral microtubules, polar microtubules and bridging microtubules (Prosser and Pelletier, 2017; Tolic, 2017). Microtubules that grow from centrosomes towards the cell cortex are defined as astral microtubules. Polar microtubules are spindle microtubules that come from poles and have free ends. Recently, bridging microtubules/ fibers have been observed. They contain 10-15 microtubules originating from poles and pass the sister chromosomes, which are important for maintaining spindle integrity (Kajtez et al., 2016).

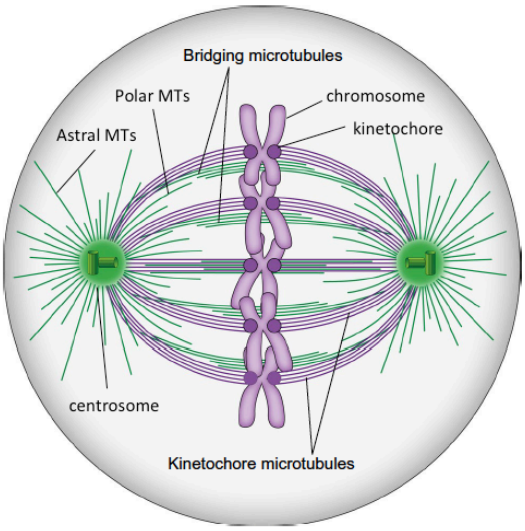

Figure 1-2. The mitotic spindle microtubules

The composition of microtubules in metaphase. K-fibers are indicated in purple lines. Non-kinetochore microtubules including astral microtubules (MTs), polar microtubules and bridging microtubules are labeled in green lines. Figure is adapted from Tolic, 2017

1.4 kinetochore fiber (K-fiber)

A K-fiber is a bundle of 20-40 parallel microtubules in which one end is located at the centrosome and the other end attaches to the kinetochore. Due to the connection between chromosome and kinetochores, K-fibers are essential for chromosome movement and segregation. K-fibers are remarkably more stable than the other spindle microtubules (Rieder, 1981). The higher stability of k-fibers is considered to mainly be due to the protection of the plus-ends from catastrophe when attached to kinetochores. Some proteins can bundle pairs of microtubules and thereby stabilize microtubules. For example, Eg5, PRC-1 and kinesin-14 are known to slide cross-linked anti-parallel microtubules, potentially contributing to k-fiber stability by coupling some degree of non K-fibers with K-fibers (Manning and Compton, 2008; Peterman and Scholey, 2009). However, due to the fact that microtubules are parallel inside K-fibers, these motors/proteins might not prefer to bundle microtubules and stabilize K-fibers *per se*. Additionally, they are barely found to decorate the entire K-fiber in cells. More recently, a clathrin-TACC3-ch-TOG complex has been shown to be associated with K-fibers and to control microtubule stability (Hood and Royle, 2009; Hood et al., 2013; Nixon et al., 2015). (discuss in detail in 1.12). Additionally, TPX2, which localizes to K-fibers, has been shown to bundle microtubules *in vitro*. However, it is not clear if TPX2 could cross-link inner-microtubules within K-fibers in cells (Alfaro-Aco et al., 2017; Bird and Hyman, 2008).

1.5 Mitotic phase

Mitotic phase is a stage of the cell cycle that consists of mitosis and cytokinesis. Replicated chromosomes are segregated and delivered into two new cells during mitosis. At cytokinesis the cytoplasm, organelles, nuclei and cell membranes are finally equally split into two daughter cells. The process of mitosis can be divided into five distinct phases: **In Prophase**, chromosomes start to condense and the nuclear envelope breaks down. Meanwhile, motor proteins walk along microtubules and generate pulling forces by which centrosomes are pushed away from each other and will eventually form two spindle poles. **During Prometaphase**, microtubules are mainly nucleated from centrosomes and chromatin, which generate a microtubule spindle apparatus. Microtubules asynchronously and stochastically capture kinetochores to align them. **In metaphase**, all chromosomes are aligned at the center of the bipolar spindle known as metaphase plate. Each kinetochore chromosome has to be attached by microtubules from opposite poles, forming a status defined as the bi-orientation, to initiate anaphase. **During anaphase**, the cyclin B1 and securin are degraded, leading to inactivation of Cdk1 and liberation of separase. Separase cleaves cohesins between sister chromosomes. A pulling force, which is generated by depolymerization of kinetochore fibers at the pole and the kinetochore, segregates chromosomes towards opposite poles. **In telophase**, a new nuclear envelope surrounding the chromosomes is formed that completes mitosis (Asbury, 2017; Cheeseman and Desai, 2008).

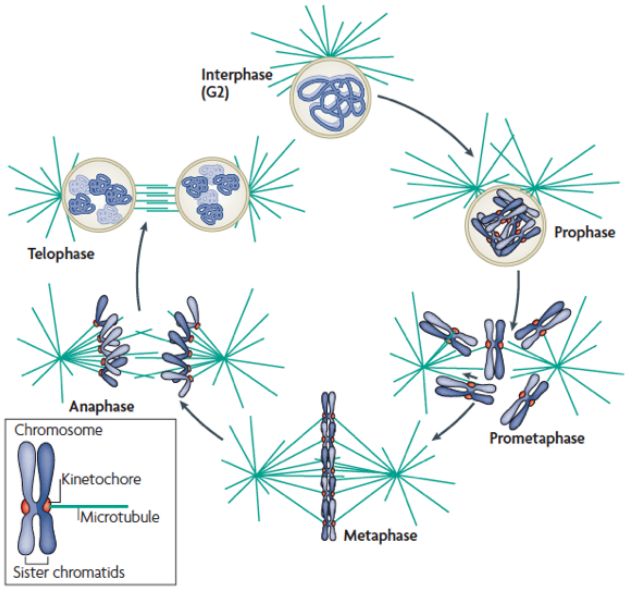

Figure 1-3. The overview of mitosis

Mitosis comprises five phases including prophase, prometaphase, metaphase, anaphase and telophase. Chromatids are condensed and nuclear envelope breaks down during prophase. The microtubule-

kinetochore interaction starts being built in the period of prometaphase. In metaphase, all chromosomes are aligned on the equator of the mitotic spindle, which achieve the biorientated kinetochore-microtubule attachments. Once the biorientation is generated, chromosomes are segregated towards two poles so called anaphase. Separated chromosomes are surrounded by the new-formed nuclear envelope in telophase. Figure is adapted from Cheeseman and Desai, 2008.

1.6 The overview of organizations and functions of kinetochore

The kinetochore is the multisubunit complex that generates load-bearing attachments between sister chromatids and spindle microtubules in mitosis and meiosis (Musacchio and Desai, 2017). The vertebrate kinetochores can be simply divided into different layers as seen in electron micrographs including the inner layer and the outer layer. The inner layer is known as the CCAN (constitutive centromere associated network), functioning in the connection between the centromere and the outer kinetochore (Cheeseman and Desai, 2008; McClelland et al., 2007; Musacchio and Desai, 2017; Pesenti et al., 2016). The outer kinetochore KMN network is composed of three different complexes assembling from the two-subunit Knl1 complex, the four-subunit Mis12 complex and the four-subunit Ndc80 complex. This network is assembled in prophase and disassembled during late ana-/telophase (Cheeseman and Desai, 2008). The functions of KMN network are to build the stable kinetochore-microtubule attachment and the recruitment of the spindle assembly checkpoint (SAC) complex, which is majorly regulated by Aurora B kinase (further discussed in 1.7).

The Ndc80 complex is thought to be the major platform for microtubule-kinetochore attachment, consisting of Ndc80 (also known as Hec1), Nurf2, Spc24 and Spc25, forming a long coiled-coil with globular domains at both ends (Ciferri et al., 2005; Wei et al., 2005). Noteworthy, the RNAi depletion of Ndc80 complex results in a K-fiber-null-phenotype, indicating that the Ndc80 complex is the major component to build microtubule-kinetochore attachments. Additionally, a highly basic and disordered ~80-residues of the N-terminal Ndc80 have been implicated in microtubule binding (Alushin et al., 2010). Phosphorylations on this N-terminal peptide by Aurora B kinase affect Ndc80 to bind microtubules (discuss in detail in 1.7). Interestingly, the internal loop of Ndc80 has been shown to interact with Cis1 (ch-TOG orthologous in fission yeast) that recruits Cis1 to kinetochores (Hsu and Toda, 2011), and this interaction can be also found in human and budding yeast (Miller et al., 2016). The Ndc80 loop mutant, which retains forming the Ndc80 complex and localizes at kinetochores, fails to interact with Cis1, leading to the defective kinetochore-microtubule attachment. In addition to the microtubule binding by Ndc80 *per se*, this result suggests that

Ndc80 cooperates with ch-TOG in regulating kinetochore-microtubule attachment as well (Hsu and Toda, 2011). Thus, Ndc80 complex comprises two microtubule-binding surfaces: the N-terminal region directly binds microtubule lattice and the internal loop indirectly interacts with plus end of microtubules through ch-TOG.

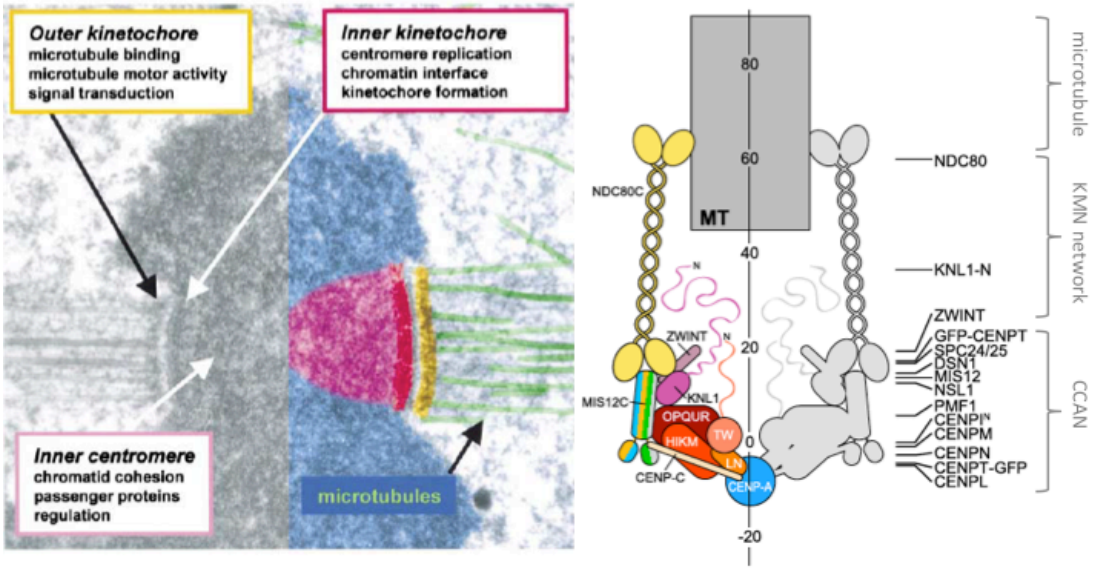

Figure 1-4. The overview of human kinetochore

Left; the electron micrographs of chromosomes and kinetochores. Centromere region in pink, inner kinetochore in red, outer kinetochore in yellow and microtubules in green. Figure is adapted from Cleveland et al., 2003. Right; the schematic cartoon of kinetochore-microtubule attachment based on the known structure and features of kinetochore proteins. The kinetochore comprises the inner kinetochore (constitutive centromere associated network, CCAN) and the outer kinetochore (KMN network). Figure is modified from Petrovic et al., 2016.

1.7 The proper Kinetochore-Microtubule attachment

To segregate chromosomes equally, cells must build the proper kinetochore-microtubule attachment by which accurate copies of genetic materials are delivered to two daughter cells. When improper chromosome segregation happens due to erroneous kinetochore-microtubule attachment, cells have a high risk to acquire the incorrect number of chromosomes (known as aneuploidy) that might lead to carcinogenesis in the end. Kinetochore-microtubule attachments can be simply divided into four different types as shown below.

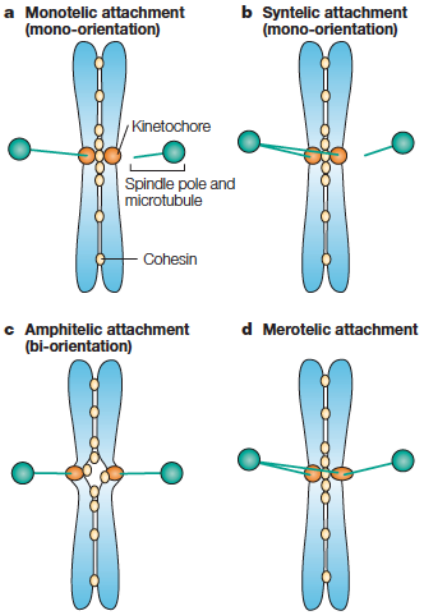

Figure 1-5. Types of the kinetochore-microtubule attachment

(A) Monotelic attachment is a transient state in which only one kinetochore is bound to microtubules from one pole. There are two types of erroneous kinetochore attachments (B)(D). (B) Syntelic attachment is that both kinetochores connect with microtubules from the same pole. (C) Amphitelic attachment: sister kinetochores are attached to microtubules from opposite poles. (D) Merotelic attachment is that a single kinetochore interacts with microtubules emanating from both poles. Figure is adapted from Tanaka et al., 2005

The initial capture of microtubules by kinetochores is asynchronous and stochastic (Magidson et al., 2011; Rieder, 1981). Consequently, erroneous attachments including monotelic, syntelic and merotelic attachments are often observed in early mitosis. However, monotelic attachments and unattached kinetochores arrest cells before anaphase onset that prevent chromosome segregation due to the activation of SAC signaling. Once SAC is activated, Mps1, Mad1, Mad2, Bub1, BubR1 and Bub3 are recruited to the unattached kinetochores, leading to the formation of mitotic checkpoint complex (MCC) (Lara-Gonzalez et al., 2012.) The MCC, a complex including Cdc20, Mad2, Bub3 and BubR1, prevents premature chromosome segregation through inhibiting the anaphase promoting complex (APC/C). Once all sister chromosomes display amphitelic attachments, the SAC is satisfied and disassembles Cdc20 from MCC. Cdc20 as a co-activator then associates and activates APC/C that degrades both cyclin B1 and securin (Lara-Gonzalez et al., 2012; Musacchio and Desai, 2017). On one hand, the degradation of cyclin B1 inactivates Cdk1, allowing subsequent exit from mitosis; on the other hand, the degradation of securin liberates separase to cleave cohesin between two sister chromatids that separates sister chromatids and allows anaphase onset. Syntelic

attachments rarely persist in human cell because the error correction by Aurora B kinase can efficiently adjust this mal-attachment. However, merotelic attachments are more common and dangerous because both kinetochores are attached by microtubules and therefore cells evade the SAC (Cimini et al., 2004; Cimini et al., 2006). As a consequence, anaphase can continue prior correcting them in which chromosomes show a delayed movement. These chromosomes are defined as lagging chromosomes and perhaps cause aneuploidy. Thus, these mal-attachments have to be corrected to amphitelic attachments by the error correction machinery. The error correction highly relies on the dynamic disassociation of microtubules from mal-attachments. Thus a balance between stable kinetochore-microtubule attachments and the efficient error correction is required to form proper bi-oriented attachments.

For correcting erroneous attachments, the detachment of microtubules from chromosomes seems to be the rate-limiting step (Li and Nicklas, 1995; Nicklas and Ward, 1994). Aurora B kinase, which localizes on inner centromeres and is enriched at misaligned chromosome, is one of key players in destabilizing kinetochore-microtubule attachments during the error correction (Cimini et al., 2006). Ndc80 is thought to be the major component to mediate kinetochore-microtubule attachments, which can be phosphorylated up to 9 sites by Aurora B kinase. The Aurora B phosphorylation neutralizes the positive charge of Ndc80 that disrupts the electrostatic interaction between Ndc80 and microtubules (Cheeseman and Desai, 2008; Cheeseman et al., 2013; Ciferri et al., 2008; DeLuca et al., 2006; DeLuca et al., 2011). When bi-oriented attachments are achieved, sister chromosomes are being pulled away from centromeres and towards opposite spindle poles to generate tension. This tension enlarges a distance between centromeres and outer kinetochores where Aurora B activity gradually decreases from centromere towards the outer kinetochore (Lampson and Cheeseman, 2011; Liu et al., 2009; Wang et al., 2011). Thus, once bi-oriented attachments are achieved and tensions are higher, Ndc80 is away from centromere and escapes from Aurora B phosphorylation and is more dephosphorylated by phosphatases on kinetochores, leading to stabilization of kinetochore-microtubule attachment. Consistent with this idea of tension, syntelic attachments that the tensions are not generated can be efficiently corrected Aurora B kinase (Hauf et al., 2003). Conversely, active Aurora B kinase has been shown to enrich at merotelic attachment even though the tension is sufficient, and might perform the error correction (Knowlton et al., 2006). The model of how Aurora B repairs these mal-attachments is shown below.

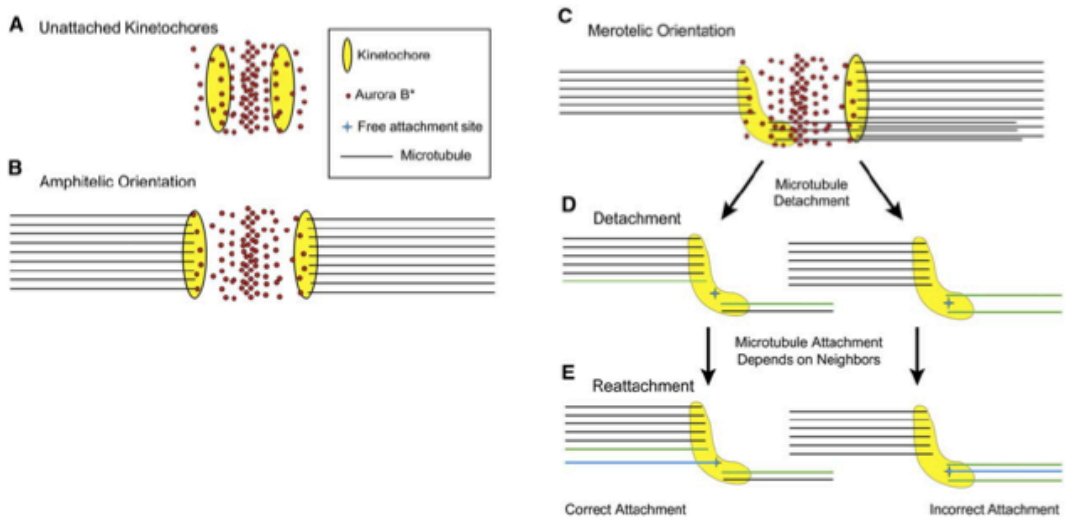

Figure 1-6. Aurora B corrects the merotelic attachment

Aurora B activity is higher in inner centromere. (A) In early prometaphase, there is no tension between unattached sister kinetochores. As a result, the turnover of kinetochore-microtubule attachment is fast. (B) Once amphitelic attachment is built, two sister kinetochores are pulled towards opposite poles and are away from the Aurora B enriched region. The kinetochore-microtubule attachments become more stable. (C) When merotelic attachment happens, the incorrect attachment sites are relatively close to the higher Aurora B gradient. Thus, Aurora B kinase destabilizes the error attachments and leaves empty sites on kinetochores shown in D (blue cross). As illustrated in E, the possibility of new microtubule reattachments (blue microtubule) is generated. The new and stochastic attachment (blue microtubule) can be formed in the correct way (E, left) or incorrect way (E, right). Figure is adapted from Cimini et al., 2006.

MCAK is a potent microtubule depolymerase that accumulates at centrosomes and kinetochores (Knowlton et al., 2006; Lan et al., 2004; Parra et al., 2006). Loss of MCAK activity, for instance MCAK depletion or MCAK mutation, has been shown to cause persistently hyper-stable kinetochore-microtubule attachments (Bakhoum et al., 2009a; Bakhoum et al., 2009b; Maney et al., 1998). The persistent mal-attachments at kinetochores lead to lagging chromosomes, chromosome missegregation and chromosomal instability (CIN) (Bakhoum et al., 2009a; Bakhoum et al., 2009b; Ertych et al., 2014). Consistent with this idea, excess MCAK, which destabilizes microtubules, significantly reduces mal-attachments and chromosome missegregation in high CIN cell lines (Bakhoum et al., 2009a; Bakhoum et al., 2009b). Thus, the regulation of MCAK in controlling microtubule stability might be an additional way to repair mal-attachments.

1.8 Clathrin heavy chain (CHC)

The best-known role of clathrin is its functions in membrane trafficking. In fact, clathrin is unable to bind membranes by itself. However, through the interaction with different adapter proteins on membranes, clathrin can be recruited at the cell membrane or the trans Golgi network to generate clathrin-coated vesicles (CCVs) that are involved in endocytosis or cargo transport (Brodsky, 2012). Two CHC isoforms, CHC17 and CHC22, have been identified in human and are named by their encoding chromosomes. CHC17 is expressed and functions in endocytosis and intracellular transport. Most vertebrates have the second isoform, CHC22, which shares 85% sequence identity with CHC17 and plays a very defined step in retrograde transport from endosome to the trans-Golgi network. Notably, CHC22 lacks the QLMLT motif for Hsc70 binding, therefore the CHC22 cage is not efficiently uncoated by the Hsc70-auxilin complex (Dannhauser et al., 2017). In addition, CHC22 does not substitute for CHC17 in endocytosis because CHC22 is not recruited to the plasma membrane by specific adaptor proteins such as AP2 (Dannhauser et al., 2017). In this study, we focused on CHC17, and abbreviated CHC17 as CHC.

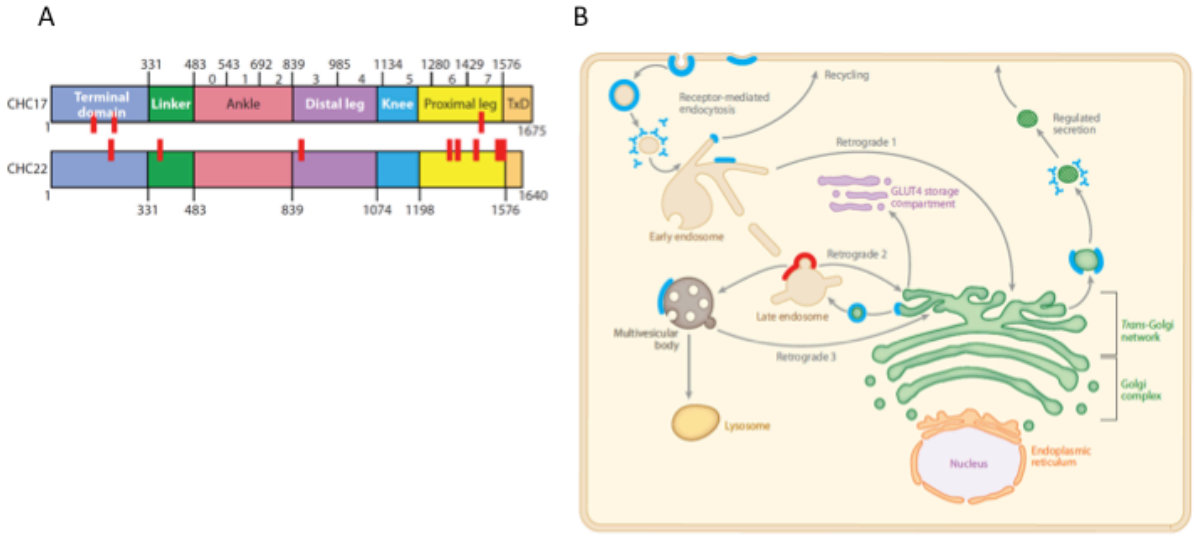

Figure 1-7. Roles of CHC17 and CHC22 in membrane trafficking

(A) Schematic domain organization of clathrin heavy chain. The amino acid boundaries are indicated for functional domains in CHC17 and CHC22. Red boxes show the conserved differences between CHC17 and CHC22; however, two proteins have 85% identity in sequences. (B) Functions of CHCs (CHC 17 in blue and CHC22 in red) in membrane trafficking. In general, proteins are synthesized in the endoplasmic reticulum, and are passed through the Golgi network undergoing post-translational modifications. Afterwards, proteins leave from trans-Golgi network (TGN) and are packed as vesicles. These vesicles are further transported to the cell membranes or endosomes. In membrane traffic pathways, CHC17 is restricted in endocytosis, being involved in transporting from the TGN to

endosomes. CHC22 is involved in retrograde transport where it is in charge in transporting vesicles from the endosome back to the TGN, which retrieves the cargo or protein components. Figure is adapted from (Brodsky, 2012).

1.9 The CHC structure and triskelion

Three CHC form a trimer by its C-terminus known as a triskelion. The N-terminal region of CHC (1-330) folds into a β-propeller with seven-blades containing four well-defined binding sites, which interact with most clathrin adaptor proteins (Figure 1D) (ter Haar et al., 1998). The site 1 is located between blades 1 and 2 and binds a LϕXϕ[D/E] ("clathrin box") motif (ter Haar et al., 2000). The site 2 accommodates a "W-box" motif (PWXXW), located in the center of the β-propeller (Miele et al., 2004). A groove between blades 4 and 5 constitutes the third site that binds a ϕϕGXL motif that is similar to the clathrin-box (Kang et al., 2009). Recently a fourth site has been proposed by mutational analysis and is probably located between blades 6 and 7. However, the corresponding motif that binds to the site 4 is still unclear (Willox and Royle, 2012). More recently, it has been proposed that these peptide-motif interactions should not be considered exclusive. These short peptide sequences may retain some ability to interact with different CHC TD sites, as has been determined by crystallization analysis (Muenzner et al., 2017).

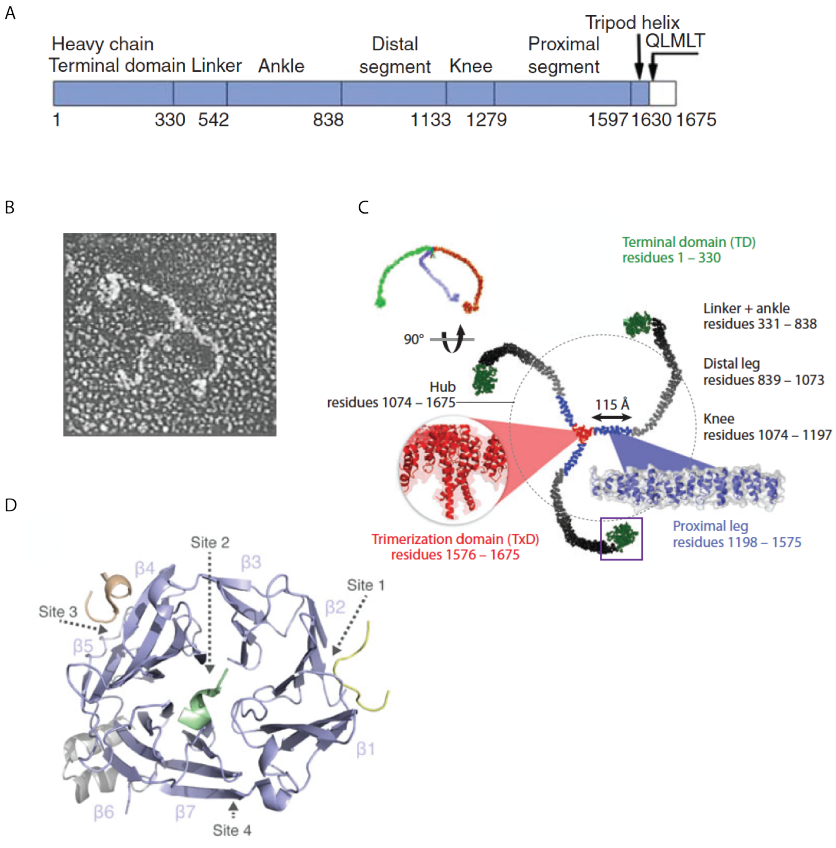

Figure 1-8. The structure of CHC

(A) Domain organization of CHC. (B) The electron micrograph of the CHC triskelion. (C) Low resolution of the structure of the CHC triskelion. The terminal domain (1-330) in green, the ankle domain (542-838) in black and the trimerization domain (1576-1675) in red. The N-terminal domain is circled with purple line and enlarged in D. (D) The β-propeller of CHC N-terminus. Four distinct binding sites are indicated as site 1, site 2, site 3 and site 4, respectively. Figures are modified from Brodsky, 2012; Kirchhausen et al., 2014; Royle, 2012.

1.10 Roles of clathrin heavy chain 17 (CHC) during mitosis

1.10.1 CHC specifically localizes on K-fibers in metaphase

The first evidence showing the spindle localization of CHC was in 1985 when Maro et al. used antibodies against CHC on mouse meiotic spindle (Maro et al., 1985). Much later, the spindle localization of CHC was further confirmed by immunofluorescence using several antibodies in various cell lines in metaphase (Okamoto et al., 2000). More recently, immunofluorescence indicated that CHC is localized at K-fibers and there is no detectable signal at astral, interpolar and midzone microtubules when cells go through mitosis (Royle et al., 2005). The specific K-fiber localization of CHC was further confirmed by immunogold and electron microscopy (Booth et al., 2011; Royle et al., 2005). These observations gave us a hint that CHC specifically localize at spindles/K-fibers and might play unique functions during mitosis.

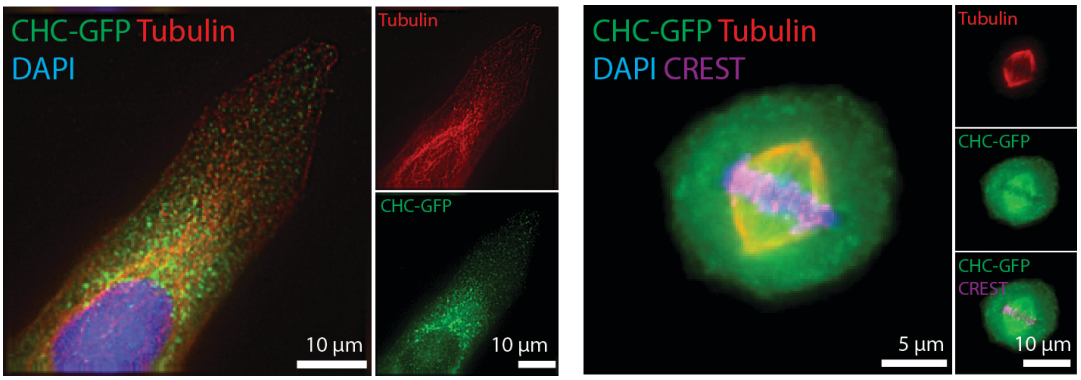

Figure 1-9. The cellular localization of CHC in interphase and metaphase

U2OS expressing CHC-GFP was fixed and stained with indicating antibodies. Left; in interphase CHC showed the vesicle-like patterns and some vesicles located along microtubules. Right; large portions of CHC were recruited to mitotic spindles, which are distinct from the vesicle-like particles in interphase.

1.10.2 Mitotic functions of CHC are distinct from interphase

The mitotic functions of CHC are apparently distinct from its roles in vesicle formation and membrane trafficking. CHC that localizes on spindle does not appear associated with membranes, and most CHC accessory proteins involved in CCVs formation have not been found to localize on spindles yet. Furthermore, the spaces within K-fibers are too narrow to accommodate clathrin-coated vesicles, suggesting that CHC may not tend to form cages, but possibly remain as individual triskelia on spindles. To support the idea that CHC stays as the triskelion instead of forming a cage on spindles in mitosis, GAK-depletion experiments were designed. The function of GAK is to disassemble CCVs that releases free CHC triskelia from vesicles. Therefore, the GAK depletion leads to the accumulation of clathrin cages in both interphase and mitosis, which reduces free CHC triskelia in cells. Interestingly, the spindle localization of CHC is significantly reduced following GAK depletion even though the total amount of CHC proteins in cells is unchanged, which arrests cells in prometaphase or leads to misaligned chromosomes (Shimizu et al., 2009; Tanenbaum et al., 2010). These data suggested that CHC prefers to stay as a triskelion rather than a cage to perform its mitotic functions, which is distinct from its cage formation for endocytosis during interphase. To further distinguish roles of CHC between interphase and mitosis in terms of its conformation and functions, several mutations were designed and examined. A truncated mutant CHC lacking the trimerization domain can not rescue the endocytosis defects in CHC depleted cells during interphase. Surprisingly, this mutant still localizes to mitotic spindles but is unable to restore the mitotic defects including mitotic index and misaligned chromosomes (Royle and Lagnado, 2006). Additionally, a small version of CHC triskelion, which can form a trimer but the CHC legs are much shorter, can fully rescue the mitotic defects but not endocytosis (Royle and Lagnado, 2006). These results suggested that the trimerization of CHC is required for both endocytosis and the mitotic functions but not its spindle localization. Additionally, even thought the trimer is formed, legs of the trimer have to be long enough to form the lattice/cage for endocytosis. Conversely, this length is not important for CHC in mitosis, suggesting that this small triskelion containing the TD, ankle and trimerization domain is enough for its mitotic functions (Royle and Lagnado, 2006).

Clathrin has recently emerged as an unexpected player to control mitotic microtubule stability. Loss of microtubule-kinetochore attachment is often observed following CHC depletion. As a consequence, CHC knockdown results in chromosome misalignment in metaphase-like cells, and chromosomes that are aligned on the metaphase plate are much thicker than control cells. Furthermore, the interkinetochore distance of equatorial

chromosomes is significantly shorter at metaphase following CHC depletion, suggesting that CHC depletion leads to less microtubule stability during mitosis (Royle et al., 2005). However, the mechanisms of how CHC stabilizes microtubules remain unclear yet. It becomes clear that CHC indeed localizes to spindles and regulates spindle integrity during mitosis. During interphase, CHC does not seem to directly bind microtubules on its own but it can decorate microtubules by interacting with an adaptor protein in interphase (Cleghorn et al., 2015). However, most CHC-binding proteins that are required for recruiting CHC in interphase do not localize at spindle during mitosis. It suggests that there must be novel interacting proteins to recruit CHC to spindles. Surprisingly, a CHC22 variant that lacks residues 457-507 forms a trimer and shares high sequence identity with CHC17, but it is unable to localize at spindles during mitosis. Interestingly, a chimeric CHC22 construct, CHC 17(1-728)-CHC22 (729-1640), replaced CHC22 (1-728) with CHC17 N-terminus is sufficient to confer spindle binding to CHC22. In contrast, the chimeric CHC22 variant only containing CHC17 TD (1-330) can not localize at spindles, suggesting that CHC17 331-728 has its unique interacting partner to bring CHC to spindles (Hood and Royle, 2009).

1.10.3 The CHC-TACC3 complex

CHC is recruited to spindles and maintains the spindle integrity during mitosis. In fact, CHC is not a microtubule binding protein, suggesting that CHC needs its interacting proteins for the spindle localization. To identify CHC's interactors in mitosis, Hubner et al. used mass spectrometer and found that CHC forms a complex with TACC3 (Hubner et al., 2010). TACC3 has been shown to play crucial roles in maintaining proper K-fiber integrity. Additionally, it is a well-studied substrate of Aurora A (Kinoshita et al., 2005) (discuss Aurora A in 1.14). Using *in vitro* purified proteins Lin et al. further confirmed a direct interaction between CHC (331-542) and TACC3 (522-577), where the S558 phosphorylation on TACC3 by aurora A is crucial for the interaction (Lin et al., 2010). Furthermore, depletion of either CHC or TACC3 results in similar mitotic defects, suggesting that these two proteins might regulate the spindle integrity via a common pathway (Lin et al., 2010). Similar results were also seen in *Xenopus* where the interaction between xTACC3 (*Xenopus* TACC3) and CHC is also dependent on Aurora A phosphorylation (Fu et al., 2010). Moreover, xTACC3 fails to localize at spindles in CHC depleted oocytes, suggesting that xTACC3 indeed needs to interact with CHC to localize on spindles (Fu et al., 2010). Similarly, like CHC, the purified D-TACC3 (*Drosophila* TACC) protein is unable to bind microtubules by itself *in vitro*; however, D-TACC significantly increases the microtubule binding while incubating

with *Drosophila* embryo extracts, suggesting that there must be some TACC3-interacting proteins for its microtubule binding (Gergely et al., 2000a; Gergely et al., 2000b). Altogether, the interaction between CHC and TACC3 is mediated by Aurora A, and the spindle localization of these proteins are to some extent dependent on each other. Consistent with this idea, when Aurora A activity is inhibited by MLN8054, non-phosphorylated TACC3 disassociates with CHC and also delocalizes from spindles (Hubner et al., 2010). These results suggested that the CHC-TACC3 interaction is able to bind microtubules and thereby brings this complex to spindles. However, whether the CHC-pTACC3 (phospho-TACC3) complex directly binds microtubules is still debated. Purified proteins of CHC (1-574) and TACC3 (519-838) incubated with aurora A seem to have very low affinity to bind microtubules by *in vitro* flow cell assays (Hood et al., 2013). On the contrary, GST-CHC and MBP-phosphorylated TACC3 can not co-pellet with purified microtubules *in vitro* (Lin et al., 2010). It remains unclear if the CHC-pTACC3 complex *per se* is sufficient to bind microtubules or whether the affinity between them is high enough to promote a stable microtubule interaction. Further experiments are needed to test whether the CHC-pTACC3 complex directly binds microtubules.

Immunofluorescence analysis indicated that CHC is specifically localized on K-fibers in mitosis (Royle et al., 2005). Furthermore, CHC-depleted cells lead to the mitotic delay as a result of defects in chromosome congression, less stable K-fibers and microtubule-kinetochore attachments, suggesting that CHC has its unique functions in mitosis (Lin et al., 2010; Royle et al., 2005). It is not clear if these defects in CHC depletion are because of the loss of the CHC-TACC3 complex *per se*, or an additional effect due to the loss of other CHC interacting proteins. Since CHC mediates vesicles trafficking together with its interacting proteins in interphase, it leads us to ask whether any of them are also involved in the CHC-mediated mitotic functions. Importantly, it remains unknown how the CHC TD that is critical for interacting with its adaptor proteins may contribute to the CHC's function in mitosis. One hint is that mutation on the site 1 of CHC TD results in a mitotic delay even though this mutant is able to interact with TACC3 and localize on spindle, suggesting that CHC might recruit downstream proteins for its mitotic functions (Hood et al., 2013). Furthermore, a small molecule inhibitor, Pitstop2, that was designed to target the CHC TD, also induces a mitotic delay and disrupts spindle formation in mitosis, without perturbing clathrin localization on spindles (Smith et al., 2013). These results strongly indicated that the CHC TD may recruit its downstream proteins that are required for the spindle integrity. However, most CHC adaptors

are membrane bound or membrane associated proteins. To date, proteins that are recruited to spindles by the CHC TD are not well characterized.

1.11 TACC3 in mitosis

The human TACC family is comprised of three members: TACC1, TACC2 and TACC3, all of which contain a conserved TACC coiled-coil domain. Even though they all associate with microtubules, each TACC protein has a distinct localization pattern in cells. In general, TACC2 primarily presents on centrosomes throughout the cell cycle whereas TACC1 and TACC3 only localize on centrosomes during mitosis (Gergely, 2002). Moreover, TACC3 is associated with mitotic spindles during mitosis and interacts directly with ch-TOG and forms a one-to-one complex (Kinoshita et al., 2005). This interaction does not depend on the Aurora A phosphorylation (Thakur et al., 2014). Interestingly, interacting with TACC3 is required for ch-TOG to localize to spindles but not kinetochores and centrosomes (Gergely et al., 2003; Gutierrez-Caballero et al., 2015). ch-TOG is a microtubule polymerase and acts as a +TIP, which adds tubulin dimer on the ends of microtubules and stimulates microtubule growth rates (Brouhard et al., 2008; Widlund et al., 2011). In cooperation with TACC3, the TACC3-ch-TOG complex strongly antagonizes MCAK activity (Kinoshita et al., 2005). Interestingly, TACC3 depletion leads to shorter astral microtubules, suggesting that TACC3 is required for the microtubule nucleation on centrosomes (Singh et al., 2014). However, this could also be because ch-TOG can not sufficiently antagonize MCAK activity without TACC3 on centrosomes that leads to shorter astral microtubules. Interestingly, GTSE1 delocalizes from centrosomes following TACC3 depletion, suggesting that under these conditions GTSE1 is unable to inhibit MCAK activity, thus resulting in shorter astral microtubules (Bendre et al., 2016; Hubner et al., 2010). In addition to the centrosomal localization of the TACC3-ch-TOG complex, TACC3 also shows the tip-tracking activity in cells due to the interaction with ch-TOG, suggesting that this complex might have additional functions in regulating microtubule dynamics on the microtubule ends (Gutierrez-Caballero et al., 2015).

Furthermore, TACC3 interacts with CHC that permits these two proteins to localize on the spindles. Interestingly, overexpression of TACC3 shows more electron-dense matrixes so called mesh or bridges that increases microtubule interconnectivity within K-fibers (discussed in next section) (Nixon et al., 2015). TACC3 overexpression also increases the amounts of microtubules that are associated with K-fibers, but it does not increase K-fiber microtubules *per se*. The extra microtubules that appear after TACC3 overexpression are gone after a cold treatment, suggesting that they are not K-fibers (Nixon et al., 2015). Additionally, TACC3

overexpression indeed increases microtubule "bridge/mesh" interconnectivity within K-fibers, indicating that it recruits more CHC and ch-TOG onto the K-fibers and forms more bridges/mesh to stabilize microtubules (Nixon et al., 2015). Additionally, more TACC3-ch-TOG complexes on spindles might also increase more microtubule nucleation by ch-TOG, which increase the amounts of microtubules on spindles.

1.12 Inter-microtubule bridges/mesh

Recently, the CHC-TACC3-ch-TOG complex has been proposed to form the bridges/mesh within K-fiber that cross-links microtubules and thereby stabilizes K-fibers (Booth et al., 2011; Hood et al., 2013; Nixon et al., 2015). The first evidence to support this hypothesis was to label CHC using immunogold and to visualize the gold particles by the electron microscopy, showing that the majority of CHC localizes between paired-microtubules in metaphase. CHC also appears to often localize on a stick-like bridge that interconnects parallel microtubules within K-fibers (Booth et al., 2011; Royle et al., 2005). Evidence supporting the idea that CHC bridges microtubules to stabilize K-fibers is that following CHC depletion, that most of shorter bridges are disappear, and k-fibers are thinner due to the loss of microtubules (Booth et al., 2011). The simplest explanation of the bridge hypothesis is that CHC stabilizes K-fiber by using its triskelion together with TACC3 to physiologically crosslink microtubules. Therefore, removal of TACC3 from spindles has similar phenotype as compared with CHC depletion, showing that most shorter inner-microtubule bridges are gone (Booth et al., 2011; Cheeseman et al., 2013). These results suggest that the CHC-TACC3 complex can physiologically crosslink and stabilize parallel microtubules by using CHC trimerization. Interestingly, the non-trimerized CHC is unable to rescue the mitotic delay following CHC depletion even though this mutant still localizes on spindles (Royle and Lagnado, 2006), which further support the bridge hypothesis of the CHC triskelion. To test if the CHC-TACC3 complex can physiologically crosslink microtubules *in vitro*, the purified proteins including CHC, TACC3, ch-TOG and GTSE1 were phosphorylated by Aurora A kinase and mix with microtubules. Bundles of microtubules could be formed in the presence of these proteins mixture. Additionally, pairs of microtubules are connected by "bridge-like" shorter electron dense connector (Nixon et al., 2015). However, a trimeric CHC plus three molecules of TACC3 would allow for bridging between three microtubules and could lead to less parallel movement of microtubules compared with that formed by biopolar linker. Therefore, whether each CHC arm in the triskelion is able to bind one microtubule needs further investigation. In addition, after mutation of the site 1/Clathrin Box motif in CHC,

nether its trimerization nor the spindle localization is perturbed. This mutant, in theory, should be able to form the inner-bridges within K-fibers; however, it still causes a mitotic delay (Hood et al., 2013). Therefore, CHC might have distinct functions independent of its bridge functions. One reasonable possibility is that CHC should recruit its downstream effectors in regulating spindle integrity. Using mass spectrometer analysis GTSE1 has been found as the novel CHC interactor in mitosis, and the spindle localization of GTSE1 depends on CHC (Hubner et al., 2010). It leads us to hypothesize if GTSE1 could act as the downstream effector in the CHC-mediated mitotic functions.

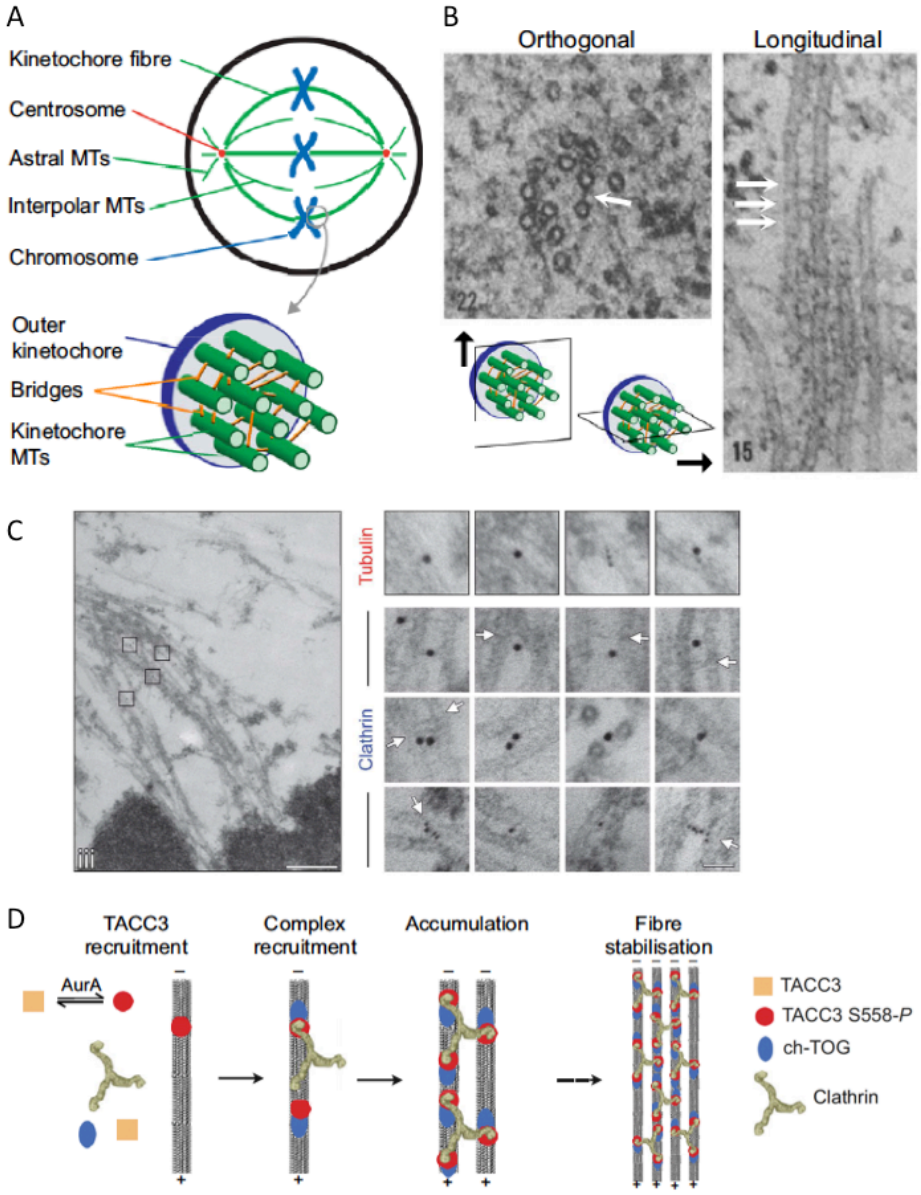

Figure 1-10. The roles of CHC in bridging paired microtubules on mitotic spindles

(A) A cartoon illustrating that the mitotic spindle organization and different kinds microtubules on spindles. (B) Electron micrographs of intra-k-fiber bridges in the mitotic spindle. Left: an orthogonal section and microtubules appear as circles; right: a longitudinal section and microtubules are ling stripes. Bridges are the electron-dense connections between microtubules labeled by arrows. (C) left: A mitotic spindle purified from Hela cell visualizing by electron microscopy following immunogold labeling; Right: enlarged view form left boxes labeled with indicated antibodies. Arrows indicate the site of bridges. (D) The bridge hypothesis. Initially, Aurora A phosphorylates TACC3 which allows TACC3 to bind CHC. The CHC-TACC3-chTG complex interacts with microtubule and crosslinks microtubule through the triskelion of CHC. Figures are modified from Booth et al., 2011; Royle, 2012.

1.13 G2 and S-phase expressed 1 (GTSE1)

GTSE1 is predicted as an intrinsically disordered protein and only exists in vertebrates. It directly binds EB1 and shows the tip-tracking activity during interphase (Scolz et al., 2012). Schneider's laboratory initially screened genes whose protein levels can be up-regulated by p53 in mouse, and they found B99 that mainly associates with microtubules in interphase (Utrera et al., 1998). However, the B99/GTSE1 protein level is only induced by p53 in mouse but not in human (Monte et al., 2003). Additionally, the same laboratory further characterized B99 and found that it decreases in G1, peaking in G2 /M-phase, and is highly phosphorylated during mitosis. Due to its expression profile in the cell cycle, they renamed B99 as G2 and S-phase express 1 (GTSE1) (Collavin et al., 2000). In fact, GTSE1 has a KEN motif in its C-terminus, which is identified as the substrate of APC/Cdh1; therefore its protein is degraded by APC/Cdh1 in late mitosis and is absent in G1 (Pfleger and Kirschner, 2000). Surprisingly, p53 binds not only GTSE1 promoter but also GTSE1 proteins. After DNA damage, GTSE1 is phosphorylated by PLK1 at residue 435, enhancing its translocation from the cytoplasm to the nucleus, shuttling out p53 to the nucleus, and mediates p53 degradation (Liu et al., 2010).

1.13.1 GTSE1 in cancer

GTSE1 has recently been associated with multiple potential roles in cancers. Interestingly, its expression level is positively correlated with tumor size, venous invasion, advanced tumor stage, and short overall survival in breast cancer (Scolz et al., 2012) and hepatocellular carcinoma (Guo et al., 2016), but probably not in lung cancer (Tian et al., 2011). Similarly, GTSE1's mRNA and protein levels are relatively low in two low invasive MCF-7 and MCF10A lines in comparison with three highly invasive lines including MDA-MB-231, MDA-MB-468 and MDA-MB-157. Furthermore, modulating GTSE1 protein affects cell

migration in both breast and hepatocyte cells (Guo et al., 2016; Scolz et al., 2012). For instance, ectopic overexpression of GTSE1 in MCF-7 cells enhances the cell mobility whereas GTSE1 depletion reduces the migratory ability in MDA-MB-231. Moreover, GTSE1 is found to directly bind EB1 through its two SKIP (Ser-Lys-Iso-Pro)-like motifs. This interaction not only accumulates GTSE1 at microtubule plus-ends but also requires for GTSE1-induced cell migration. Mutating SKIP motifs on GTSE1 abolishes it interaction with EB1 in which GTSE1 is unable to enrich on the +TIP and also fails to induce focal adhesion disassembly (Scolz et al., 2012). More recently, GTSE1 has been reported to facilitate epithelial-to-mesenchymal transition (EMT) modulation in hepatocellular carcinoma (Wu et al., 2017). EMT mediates tumor cells to depart from the primary tumor due to the loss of the cell-cell adhesion, which gains the migratory and invasive properties of tumor cells. Interestingly, by analyzing the mRNA levels of 28 types of cancers from the TCGA database, GTSE1 is approximately 100 times higher in cancer tissues than non-tumor tissues (Wu et al., 2017). Additionally, GTSE1 mRNA and protein levels are significantly up-regulated in hepatocellular carcinoma tissues compared with relative adjacent tissues (Guo et al., 2016). High expression of GTSE1 in hepatocellular carcinoma is correlated to the levels of Snail and N-cadherin that have been identified as the marker of EMT (Wu et al., 2017). Therefore, high level of GTSE1 might induce EMT that increases cell migration and invasion.

1.13.2 Roles of GTSE1 in mitosis

GTSE1 is identified as a MAP and enriches on microtubule growing ends by the interaction with EB1 throughout interphase. In fact, GTSE1 is highly phosphorylated during mitosis by which GTSE1 loses the microtubule binding and the microtubule plus end tracking until anaphase onset (Scolz et al., 2012). Thus, GTSE1 might have distinct functions during mitosis independent of its roles in interphase. By mass spectrometry analysis GTSE1 has been found to interact with CHC and TACC3 in mitosis (Hubner et al., 2010). Interestingly, GTSE1 delocalizes from the mitotic spindles in either CHC depletion or TACC3 depletion, suggesting that the CHC-TACC3 complex is required for GTSE1 to localize at the spindles (Cheeseman et al., 2013; Hubner et al., 2010). Several LIDL (Leu-Ile-Asp-Leu) motifs, which are well-known motifs to bind to the CHC TD, are localized in GTSE1 C-terminus; therefore GTSE1 might potentially interact with CHC. Altogether, these findings strongly suggested that GTSE1 is involved in the CHC-TACC3-mediated mitotic functions. However, it is unclear whether GTSE1 interacts directly with CHC or TACC3 by which GTSE1 is recruited

to the spindles, or how GTSE1 participates in the CHC-TACC3 complex to stabilize microtubules.

Previously, our lab found that GTSE1 is a novel microtubule-stabilizing protein in mitosis to control chromosome alignment and segregation. GTSE1 mainly localizes to K-fibers and spindle poles, and loss of GTSE1 from cells leads to the global destabilization of microtubules. Additionally, we further found that the mechanism by which GTSE1 stabilizes microtubules is through the inhibition of MCAK-depolymerizing activity (Bendre et al., 2016). MCAK mainly localizes to the centromeres, centrosomes, midbody and microtubule plus tips during mitosis, and plays a crucial role in assembling a bipolar spindle, correcting improper kinetochore-microtubule attachments, facilitating accurate chromosome segregation (Domnitz et al., 2012; Lan et al., 2004; Wordeman and Mitchison, 1995). Through an interaction with MCAK, GTSE1 inhibits MCAK activity, which is crucial for regulating MCAK-induced microtubule depolymerization. Consequently, GTSE1 depletion results in the excess MCAK depolymerization activity, which leads to short astral microtubules, less inner spindle microtubules, less K-fibers and improper kinetochore-microtubule attachments. Notably, these mitotic defects can be restored by co-depleting GTSE1 and MCAK, suggesting that GTSE1 indeed inhibits MCAK activity *in vivo* during mitosis (Bendre et al., 2016). Interestingly, GTSE1 seems to regulate the MCAK activity at kinetochores in order to achieve proper kinetochore-microtubule attachments. It raises questions whether the K-fiber localization of GTSE1 is sufficient to bring GTSE1 onto kinetochores or GTSE1 is able to localize at kinetochore *per se* through a direct interaction with kinetochore proteins. However, we could not detect GTSE1 at kinetochores yet by immunofluorescence. It might due to that the kinetochore localization of GTSE1 is very dynamic or there is very little portion of GTSE1 at kinetochores. To test if GTSE1 localizes at kinetochores, further experiments are needed.

Hyper-stable kinetochore-microtubule attachments were found in several cancer cell lines and lead to chromosome instability (CIN) (Bakhoum et al., 2009a; Bakhoum et al., 2009b; Ertych et al., 2014). Interestingly, an increase of MCAK expression could restore hyper-stable kinetochore-microtubule attachments and decreases CIN (Bakhoum et al., 2009a; Bakhoum et al., 2009b). Notably, GTSE1 levels are relatively higher in CIN cell lines, suggesting that high GTSE1 expression leads to MCAK inactivation and causes chromosome missegregation. Additionally, the defect in chromosome missegregation can be reduced following GTSE1 depletion in CIN cell lines. Similarly, up-regulation of GTSE1 in HCT116, a chromosomally stable line, for many generations induces CIN (Bendre et al., 2016). In summary, GTSE1

plays several roles in carcinogenesis. First, up-regulated GTSE1 results in hyper-stable KT-MT attachments due to the inhibition of MCAK in mitosis, which frequently leads to CIN. Additionally, higher GTSE1 level also induces EMT, which increases higher cell migration and invasion during interphase for the following tumor progression. Therefore, GTSE1 expression should be precisely controlled in cells. Due to the fact that GTSE1 is highly expressed in several cancers, it might have high potential as a marker for cancer diagnosed and a target for cancer therapy.

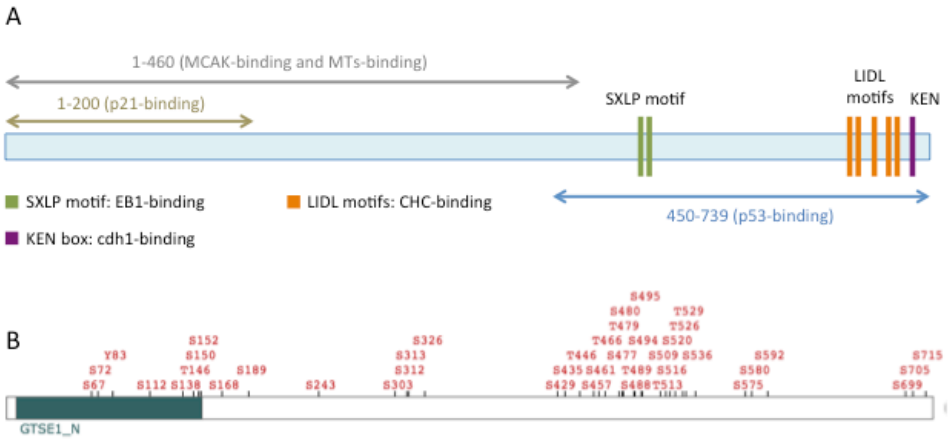

Figure 1-11. The functional domains and phosphorylation sites on GTSE1

(A) Schematic domains based on the validated interaction. The N-terminal region of GTSE1 interacts with p21, MCAK and microtubules. Two SXLP motifs in the middle are required for the EB1-binding. The C-terminal terminus of GTSE1 interacts with p53 and cdh1 as well through the KEN box. There are several LIDL motifs on the very C-terminal tail, which are putative CHC-binding motifs. BD: binding-domain. (B) All phosphorylated sites with more than five references are listed on GTSE1, which are validated by mass spectrometry (https://www.phosphosite.org/).

1.14 Aurora A kinase in cancers

Aurora kinases belong to serine/threonine kinases that consist of three members in mammalian cells termed as Aurora A, B and C. Both Aurora A and B are cell cycle regulated proteins and are detectable in somatic cells during mitosis. Aurora A and B share 70% homology in their catalytic domains (D'Assoro et al., 2015). However, their cellular localizations are distinct during mitosis. Aurora A mainly localizes on centrosomes, spindle poles and transiently along spindle microtubules, which is important in centrosome maturation, mitotic entry and spindle assembly (Barr and Gergely, 2007; Bird and Hyman, 2008; Dutertre et al., 2002; Marumoto et al., 2005). In contrast, Aurora B that interacts with chromosomal passenger complex is primarily presented to the inner centromere from

prophase until metaphase, and moves to the spindle midzone and midbody during late mitosis and cytokinesis. Aurora B is mainly involved in chromatin modification, microtubule-kinetochore attachment, spindle checkpoint and cytokinesis (Ruchaud et al., 2007; Vader et al., 2006). In fact, both kinases can share the same substrates such as CENP-A, Survivin and p53 (Carmena et al., 2009). Recently, a single amino acid change on Aurora A has been shown to convert into Aurora B-like kinase in terms of the cellular localization and interacting partners, suggesting that the different functions between them could be due to the localization (Fu et al., 2009; Hans et al., 2009). Interestingly, Aurora A kinase is highly expressed in aneuploid tumors. The effects of Aurora A in tumorigenesis have been applied in centrosome duplication and mitosis. Accurate centrosome numbers are important to maintain the normal bipolar spindle responsible for the accurate chromosome segregation. Therefore, centrosome amplification is thought to form multipolar spindles and causes aneuploidy and cancer (Raff and Basto, 2017). Aurora A is known to phosphorylate several proteins on centrosomes that are required for centrosome maturation (Barr and Gergely, 2007; Wang et al., 2014). However, excess Aurora A in cultured cells causes cytokinesis failure that accumulates centrosomes and leads to centrosome amplification (Meraldi et al., 2002). PLK1 activity is known to regulate centrosome duplication and mitotic entry (Liu and Erikson, 2002; Macurek et al., 2008). Additionally, Aurora A can also phosphorylate and activate PLK1, which increases PLK1-induced centrosome amplification. Recently, higher Aurora A level has been reported to increase the plus end assembly rate of microtubules that causes hyper-stable microtubule-kinetochore attachments and CIN (Ertych et al., 2014). Even through the TACC3 phosphorylation level is higher in their system, the mechanisms by which Aurora A induces microtubule stability remain unclear.

2. Objective

CHC has emerged as an unexpected player to localize to mitotic spindles that controls spindle integrity and chromosome segregation. Thus, CHC depletion leads to mitotic defects including fewer microtubules within k-fibers and misaligned chromosomes (Booth et al., 2011; Hood et al., 2013; Royle et al., 2005). Importantly, these mitotic roles of CHC have been established to be independent of its role in endocytosis and membrane trafficking (Royle, 2012; Royle, 2013; Royle et al., 2005; Royle and Lagnado, 2006). Recently, the CHC-TACC3-ch-TOG complex has been proposed to stabilize K-fibers by forming bridges between microtubules within K-fibers (Cheeseman et al., 2013; Nixon et al., 2015). A mutant of the CHC TD, which loses its interacting proteins, localizes on spindles and presumably forms triskelion; however, this mutant still causes some mitotic defects. It strongly suggests that CHC might have distinct roles independent of its bridging functions (Hood et al., 2013). Interestingly, GTSE1 was previously identified as a novel CHC-interacting protein from mitotic cell lysates by mass spectrometric analysis (Hubner et al., 2010). Noteworthy, GTSE1 contains several Lue-Ile-Asp (LID) motifs that are implicated in interacting with the CHC TD. Additionally, depleting CHC in cells delocalizes GTSE1 from mitotic spindles, suggesting that GTSE1 is recruited by CHC and acts downstream of CHC. Furthermore, GTSE1 depletion phenocopies CHC depletion in cells, showing loss of microtubule stability and misaligned chromosome, implying that these two proteins might function together in the same pathway. Previously, our laboratory identified GTSE1 as a new microtubule-stabilizing protein by inhibiting MCAK activity (Bendre et al., 2016). MCAK is a potent microtubule-depolymerase and also localizes at kinetochores to regulate kinetochore-microtubule attachments. GTSE1 depletion results in more active MCAK that induces the detachment of microtubules from kinetochores. It raises an interesting question whether GTSE1 physiologically interacts with kinetochore under certain conditions in order to regulate MCAK activity. Altogether, the main goal is to understand mechanisms of how CHC functions in maintaining spindle integrity. One hypothesis is that CHC stabilizes microtubules by directly recruiting GTSE1 to inhibit MCAK. However, the recruitment of GTSE1 on kinetochores seems to be independent of CHC. Another question is to check if GTSE1 directly interacts with kinetochore, presumably outer kinetochore. During my PhD, I aimed to address following questions.

Questions:

(1) Does CHC directly interact with GTSE1?
-Where is/are the interacting surface(s) on CHC and GTSE1?
-How does CHC structurally interact with GTSE by using X-ray crystallography?
-How does CHC interaction with GTSE1 determine GTSE1 subcellular localization?
-Does the CHC-GTSE1 complex specifically localize at K-fibers?

(2) What does GTSE1 interaction with, and recruitment by, CHC on the spindle contribute to microtubule stability?

(3) How does the interaction between CHC and GTSE1 impact chromosome alignment and segregation?

(4) Whether GTSE1 forms an interacting network together with CHC-TACC3-ch-TOG-MCAK, which supports the hypothesis that CHC stabilizes K-fiber by directly recruiting GTSE1 to inhibit MCAK?

(5) Does the GTSE1 colocalize with MCAK on kinetochores to inhibit MCAK activity?
-How is GTSE1 recruited to kinetochores? What is/are the binding partner(s) of GTSE1 on kinetochore? Does this interaction depend on phosphorylations?

3. Results

CHC has been reported to maintain spindle integrity by intra-microtubule bridging within K-fiber. A mutation of the CHC TD, which loses its adaptor-like interacting proteins, localizes on spindles and affects neither its trimerization nor the TACC3 binding. However, it still causes some mitotic defects, suggesting that this N-terminal domain of CHC has its distinct functions independent of the triskelion that bridges microtubules (Hood et al., 2013). Furthermore, Pitstop2, an inhibitor that competes with other proteins to bind the CHC TD, does not affect CHC localization to spindles, but it induces misaligned chromosomes and a mitotic delay (Smith et al., 2013). These results highly suggested that the N-terminal domain of CHC has its unique functions in mitosis. Since this domain has been shown to interact with many adaptor proteins and most of them are not found on spindles yet, we reason that CHC TD might recruit a novel player to regulate spindle integrity. GTSE1 was found to interact with CHC by mass spectrometry and delocalized from spindles following CHC depletion, suggesting that CHC recruits GTSE1 to spindles (Hubner et al., 2010). Our lab previously identified that GTSE1 is a novel microtubule-stabilizing protein by inhibiting MCAK activity in mitosis. Additionally, GTSE1 depletion leads to less inner spindle intensity and misaligned chromosomes. These mitotic defects are very similar in CHC depletion, indicating that GTSE1 and CHC should function in the same pathway. Thus, one mechanism of how the CHC TD stabilizes microtubules is by recruiting GTSE1 to inhibiting MCAK. However, it remains unclear if the CHC-GTSE1 interaction is through a direct binding or an indirect effect. Thus, we first aimed to address the interaction between GTSE1 and CHC.

3.1 GTSE1 specifically interacts with two sites on the CHC TD.

To confirm the interaction results from mass spectrometry, we first performed immunoprecipitation (IP). The mitotic cell lysate was prepared by nocodazole synchronization after 14 hour, and IPs were conducted using either anti-GTSE1, anti-CHC or anti-myc antibodies. As expected, GTSE1 can be detected in complexes precipitated by CHC antibodies and vice versa, indicating that GTSE1 indeed formed a complex with CHC (Figure 3-1A). To further address if this is a direct interaction, an *in vitro* pull-down assay was performed. Both full-length GTSE1 and full-length CHC proteins were expressed and purified from insect cells. As shown in Figure 3-1B, GST-CHC can pull down GTSE1

detected by western blot. Because there are only CHC and GTSE1 proteins in the reaction, this result revealed that CHC directly interacts with GTSE1.

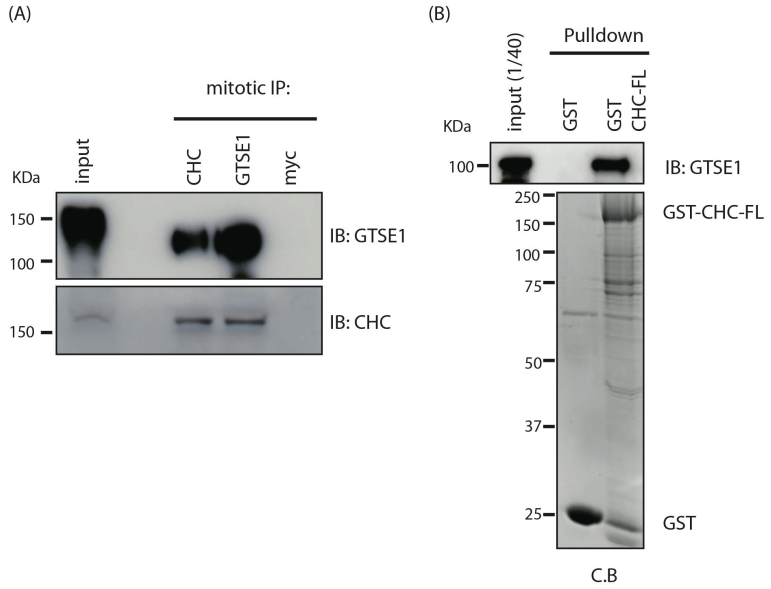

Figure 3-1. GTSE1 interacts directly with CHC

(A) IPs indicating that CHC and GTSE1 form a stable complex during mitosis. IPs were performed using either anti-CHC, anti-GTSE1 or anti-myc (IgG) antibodies. (B) *In vitro* pulldown showing that GTSE1 interacts directly with CHC. GTSE1 proteins were incubated with GST or GST-CHC full-length proteins to perform the pulldown assay.

We next examined if GTSE1 can bind the CHC TD, supporting the idea that GTSE1 is recruited by the CHC TD to regulate the spindle integrity. To test that, serial GST-tagged CHC proteins purified from bacteria were incubated with GTSE1-EGFP FL proteins. Interestingly, only the N-terminal domain of CHC (1-330) can sufficiently pull down GTSE1, indicating that GTSE1 indeed binds to the β-propeller where CHC accommodates most of its adaptor proteins in interphase (Figure 3-2A). To date, four distinct binding sites on the CHC β-propeller have been identified that mediate the interaction with their corresponding motifs in clathrin adaptor proteins (Willox and Royle, 2012). Pitstop 2, a small molecule inhibitor, mainly binds the site 1 of the CHC β-propeller by which Pitstop 2 prevents proteins containing clathrin box motifs (LΦXΦD/E) to bind (von Kleist et al., 2011). Because GTSE1 contains several LIDL motifs (Figure 3-4), it could potentially bind to the CHC TD site 1. To test this hypothesis, we pre-incubated GST-CHC (1-330) with 30 μM Pitstop 2 or DMSO for half hour and examined the interaction by pulldown assays. Interestingly, Pitstop 2 significantly reduced the interaction between CHC and GTSE1, indicating that the site 1 of the CHC β-propeller is important for the binding (Figure 3-2B). To further confirm this result, we individually mutated each of three established adaptor-binding sites on CHC. The detail of

mutations is listed in Figure 3-2C. We next examined the interaction between GTSE1 and CHC mutants (Figure 3-2D and E). As expected, the site 1 mutant (S1M) strongly impaired the interaction, which is consistent with Pitstop 2 that prevents the GTSE1 binding. Surprisingly, the site 3 mutant (S3M) also significantly reduced the interaction, indicating that GTSE1 also binds to the CHC TD site 3. However, mutation of the site 2 (S2M) has no effect or very little effect. In fact, we could not find any PWXXW motifs, a well-known site 2-binding motif on GTSE1 (Miele et al., 2004).

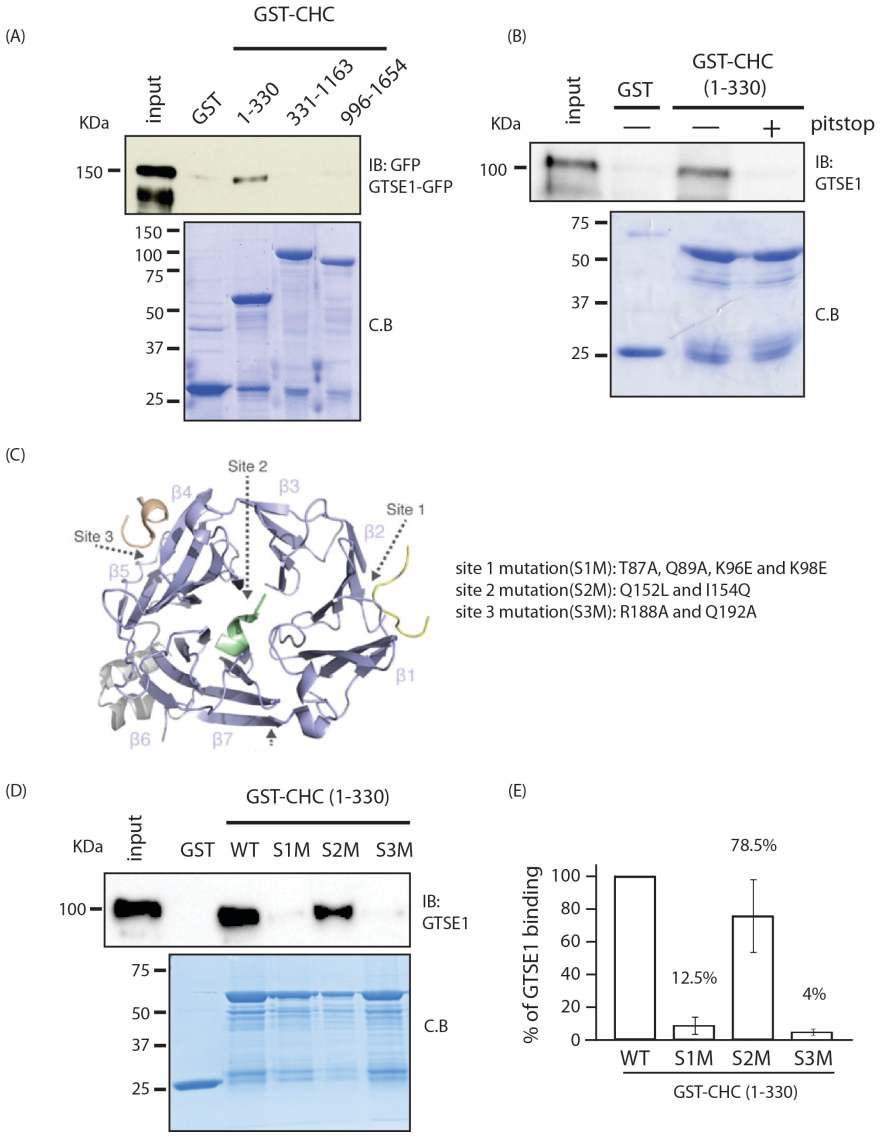

Figure 3-2. The site 1 and 3 of CHC TD interact with GTSE1

(A) Western blot indicating that GTSE1 directly interacts with the CHC TD. GTSE1-EGFP proteins were incubated with GST or various GST-tagged CHC proteins to perform pulldowns and analyzed by western blot. (B) Pitstop 2 competes the interaction between GTSE1 and CHC. Western blot to detect GTSE1 after the pulldown using GST-tagged CHC (1-330) proteins in the presence or the absence of Pitstop 2. (C) Structural model of CHC (1-330) with the seven-bladed β-propeller. Three interaction

sites on CHC TD are indicated by arrowheads. Mutations that abolish each binding site on CHC were shown on the list. The figure is adapted from Royle, 2012. (D) GTSE1 binds both the site 1 and the site 3 on the CHC TD. GTSE1 proteins were incubated with GST-CHC (1-330) WT or mutants and performed pulldowns. (E) Quantification of three independent pulldown assays from D. All interactions were normalized to the WT.

3-2 GTSE1 utilizes its LID motifs to bind the CHC TD.

Next, we aimed to identify the CHC-binding region on GTSE1. Different truncated fragments of GTSE1 proteins with 6xHis tag were purified from bacteria. To test the interaction, we used GST pulldown assays. GST-CHC (1-364) proteins are immobilized on GSH beads and incubated with various GTSE1 proteins. As shown in Figure 3-3A, GST-CHC (1-364) can pull down two C-terminal fragments of GTSE1 including GTSE1 (463-739) and GTSE1-C (639-739) but not the N-terminus (1-460), indicating that a fragment containing last hundred residues (GTSE1-C, 639-739) is sufficient to bind CHC. Because we found two sites on the CHC TD that interact with GTSE1, we hypothesized that GTSE1-C (639-739) should contain two distinct binding-regions corresponding to these two binding sites on CHC. To further identify these CHC-binding regions, three smaller GTSE1 fragments with GST-tags (C1, C2 and C3) were purified from bacteria and tested the interaction. As shown in Figure 3-3C, both two individual fragments, GST-C1 (651-687) and GST-C3 (693-739), can pull down CHC, indicating that these two distinct surfaces directly interact with CHC. Because GTSE1-C, a longer fragment, contains these two distinct binding regions, we reasoned that it should bind tighter than two short fragments. As expected, GTSE1-C showed a stronger interaction than either GTSE1-C1 or GTSE1-C3 (Figure 3-3C). Here, we found two distinct regions on GTSE1 that are required for the interaction with CHC. This finding is consistent with the results where two sites on the CHC TD are required for the interaction with GTSE1 (Figure 3-2D). The overall interactions were summarized in Figure 3-3D.

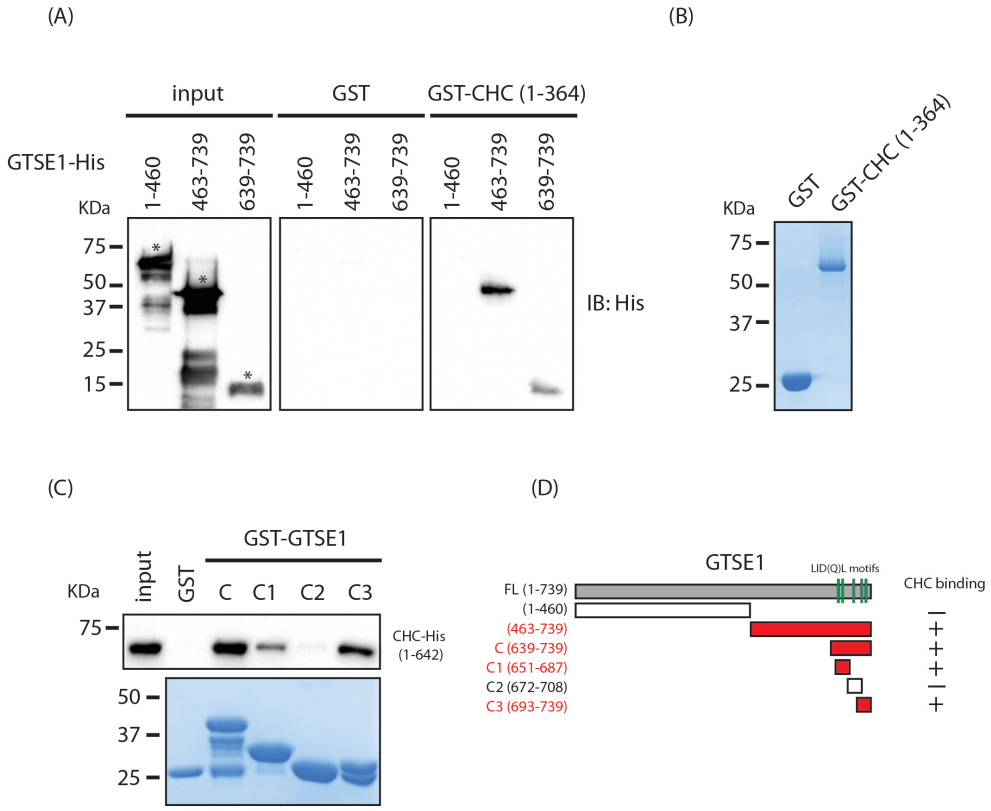

Figure 3-3. Two distinct fragments of GTSE1 interact with CHC

(A) Various GTSE1 proteins were performed pulldown assays using GST or GST-CHC (1-364). (B) Equal amount of GST and GST-CHC (1-364) proteins was shown on a SDS-gel stained with coomassie blue. (C) CHC (1-642)-His proteins were incubated with various GTSE1 proteins tagged with GST and analyzed by western blot. (D) The summary of CHC-binding regions in GTSE1. Positive-interacting fragments were marked with the cross and labeled in red.

To further identify motifs on GTSE1 C1 and C3 that bind the CHC TD, we next aligned GTSE1 proteins sequences among human (H. sapiens), mouse (M. musculus), cow (B. taurus), rat (H. Glaber) and frog (X. tropicalis). Notably, we found that five LID(Q)L motifs on the very C-terminal region are very conserved in all spices (639-739 in human). This LΦXΦ[D/E] (Leu-[Leu/Ile/Val]-any residue-[Leu/Ile /Val/Phe]-[Asp/Glu])-like motif is well-known to bind the CHC TD, implying that these five LID(Q)L motifs might mediate the interaction between GTSE1 and CHC. Consistent with our pulldown results, we confirmed that a GTSE1 fragment containing all five LID(Q)L motifs interacts with the CHC TD (Figure 3-3C and D, GTSE1-C). Because GTSE1 has more than one LID(Q)L motif, it raises a question of how GTSE1 uses them to bind CHC. To distinguish each motif, we named these five LID(Q)L motifs as Box A to E (Figure 3-4).

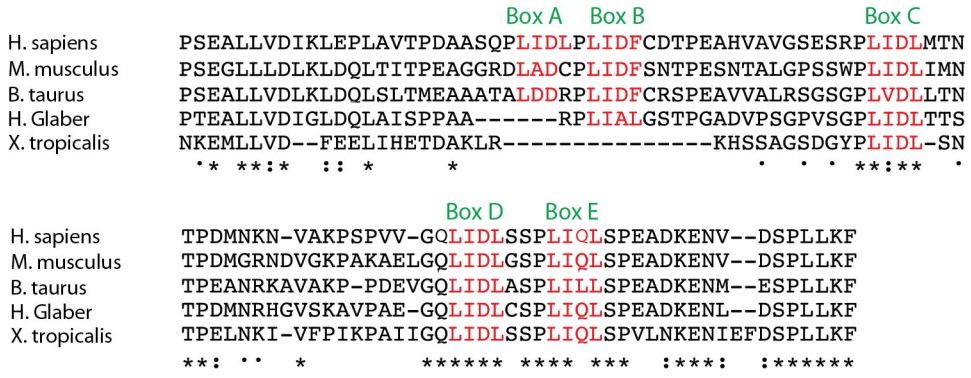

Figure 3-4. Five putative CHC-binding motifs on GTSE1

Five putative CHC-binding motifs, LID(Q)L, on GTSE1 are highly conserved among different spices. According to the order of these motifs, they are named as Box A to E.

To further identify which LID(Q)L motif on GTSE1 contributes the interaction, we aimed to mutate this motif and examined its interaction with CHC. Thus, we decided to substitute the first three residues as triple alanine (AAA) on the LID(Q)L motif. These Mutants that we generated are illustrated in detail in Figure 3-5B. To examine the interaction, we first performed the yeast-two hybrid assays. The CHC TD (1-330) with a Gal4 activation domain (AD) was co-transformed with either GTSE1 (463-739) wild-type (WT) or different mutants into yeast. Cells were then serial diluted and grown on either a histidine positive (+His) or a selecting plate (histidine negative, -His) for 3 days shown in Figure 3-5A. Yeast were grown a similar amount on a +His plate, indicating the number of cells were very similar among different groups. However, as compared with wild type, yeast containing LID(Q) mutants showed quite different growth phenotypes on the selecting plate (–His), suggesting that some of these mutants impair the interaction with CHC. Neither the Box A mutant (A-m) nor the Box E mutant (E-m) had strong effects on the interaction. Notably, mutation of the Box B or D had very sick growth phenotypes, suggesting that these two motifs predominantly bind to CHC. Interestingly, the ACDE-m, multiple mutations on GTSE1 (all putative LID(Q) sites were mutated except the Box B), totally lost its interaction. This observation strongly suggests that GTSE1 uses more than one LID(Q)L motif to interact with CHC. Consistent with our previous pull-down experiments, two distinct fragments containing multiple LID(Q)L motifs are required for the binding (Figure 3-3D and E). Altogether, here we showed that each motif contributes to the binding even though some of them might have predominant interactions and mutations on the first three residues of LID(Q)L are sufficient to disrupt the binding.

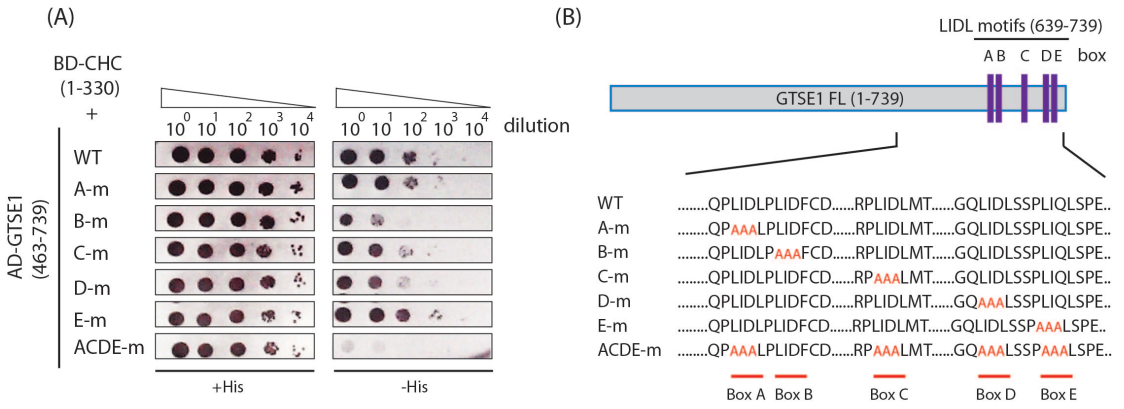

Figure 3-5. Multiple LID motifs of GTSE1 contribute their interaction with CHC

To identify which LID(Q)L motif is required for the CHC binding, several mutants were examined the interaction using the yeast two-hybrid assy. (A) The growth phenotypes of yeast was plated on a either growth plate (+His) or selecting plate (-His). (B) The detail of mutations on GTSE1 designed and used in the yeast two-hybrid assay from A. (WT: wild-type, A-m: Box A mutant, B-m: Box B mutant, C-m: Box C mutant, D-m: Box D mutant, E-m: Box E mutant and ACDE-m: Box ACDE mutant)

To further identify which exact LID motifs interact with CHC, we next used shorter fragments of GTSE1 and performed pulldowns. Due to the fact that only GTSE1-C1 and GTSE1-C3 but not GTSE1-C2 bind to CHC, we then mutated LID Boxes on both GTSE1-C1 (Box A and B) and GTSE1-C3 (Box D and E), and tested their interaction. Interestingly, triple alanine substitution of the Box A, B or AB on GTSE1-C1 strongly reduced the interaction, suggesting that these two LID motifs are required for the CHC-binding (Figure 3-6A, B and C). Since the Box B is more conserved among different spices (Figure 3-4) and its mutation has a stronger reduction than the Box A mutant (Figure 3-6A and B), we postulated that the Box B might be the dominant binding-motif on GTSE1-C1. This result is in consistent with the yeast-two-hybrid where the Box B mutant has strongest influence for the binding (Figure 3-5A). Next, we examined which motifs on GTSE1-C3 are required for the interaction. To mutate the Box D, three different triple-alanine replacements were introduced (LIDL to AAAL, LIDL to LAAA or LIDL to AADA, Figure 3-6 D, E and F). All three mutations on the Box D significantly perturbed the CHC-binding. However, mutating the Box E had very minor effect. Taken together, substitutions of the first three residues to triple alanine on LIDL motif seem to disrupt its interaction with CHC as we showed in the yeast-two-hybrid assay. Here we identified two distinct motifs of GTSE1 in which LIDLPLIDLF (the Box A and B) on GTSE1-C1 and LIDL (the Box D) on GTSE1-C3 interact directly with the CHC TD.

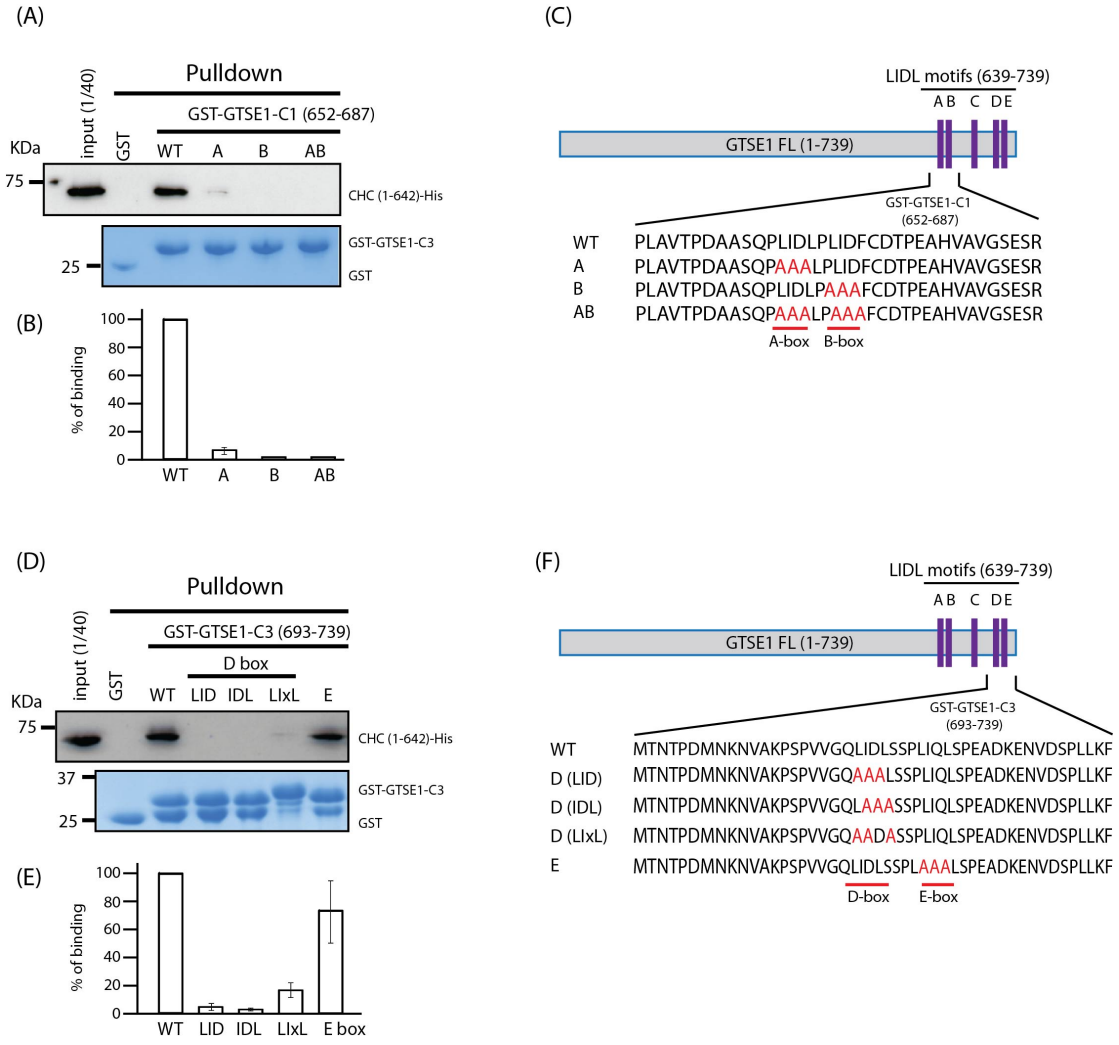

Figure 3-6. Several LIDL Boxes on GTSE1 are required for the interaction with CHC

(A) Both the Box A and the Box B are required for the interaction. Pull-down analysis of CHC (1-642)-His using GTSE1-C1 WT and mutants. (B) Quantification of three independent experiments from A. Interactions were normalized to the WT. (C) Peptide sequences of GTSE1-C1 WT and mutants used in A. (D) The Box D is required for the interaction. The pulldown analysis of CHC (1-642)-His using GTSE1-C3 WT and mutants. (E) Quantification of three independent experiments from D. Interactions were normalized to the WT. (F) Peptide sequences of GTSE1-C1 WT and mutants used in D.

3.3 A proposed model of the CHC-GTSE1 interaction

Here we revealed that GTSE1 uses several LIDL motifs (A, B and D) to bind two sites on the CHC TD (site 1 and site 3). Due to the fact that the shorter GTSE1 fragments (C1 and C3) reduced almost half the interaction in comparison to the longer one (Figure 3-3C), suggesting

that these short fragments selectively bound only one site on CHC and thereby reduce the interaction. However, the exact CHC-GTSE1 binding model is unrevealed. For instance, GTSE1-C1 fragment might bind to the either site 1 or the site 3, and it will be the same case for GTSE1-C3 fragment. To examine that, we used the site 1 mutant (S1M) or the site 3 mutant (S3M) of CHC and performed the pulldown analysis in combination with GTSE1-C1 and C3 fragments. The idea is that; for example, if GTSE1-C1 specifically binds the CHC site 1, the S1M but not the S3M should abolish the interaction. Thus, using these mutants of CHC could inform the binding model of the CHC-GTSE1 complex. As shown in Figure 3-7, the input of GTSE1 and CHC were relatively similar in each condition, and GST alone did not interact with any CHC proteins. Notably, the S1M did not interact with GST-GTSE1-C1 but the S3M can. These results indicated that GTSE1-C1 (Box A and Box B) specifically interacts with the CHC site 1. Therefore, mutation of the CHC site 1 abolished the binding. Similarly, GTSE1-C3 specifically binds to the CHC sites 3, as only the S3M abolished the interaction with GST-GTSE1-C3.

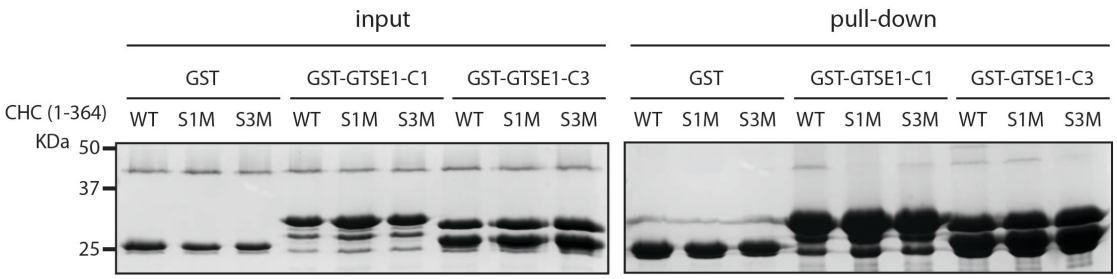

Figure 3-7. LIDL Boxes of GTSE1 specifically bind to different sites on the CHC TD

GST, GST-GTSE1-C1 or GST-GTSE1-C1 proteins were incubated with CHC WT or mutants. Pulldown assays showing that the S1M (site 1 mutant) on CHC abolished the interaction with GST-GTSE1-C1. Additionally, the S3M (site 3 mutant) can not bind to GST-GTSE1-C3. These results indicated that GTSE1-C1 selectively binds to the CHC site 1, and similarly GTSE1-C3 specifically interacts with the CHC site 3.

Here we elucidated that GTSE1 uses its Boxes AB and D to bind the CHC TD site 1 and site 3, respectively. Interestingly, the site 1 and 3 are on the opposite sides of the CHC TD which creates a certain distance between them. If one molecule of GTSE1 is able to interact with both sites at the same time, a loop between the Box A and D has to be long enough to fit this distance. In fact, there are 38 amino acids between these two boxes on GTSE1, which is theoretically long enough to bridge the two interactions together, based on modeling of

GTSE1 peptides on the CHC TD structure (Dr. Ingrid Vetter, personal communication). We postulated that once the loop is shortened, GTSE1 would only be able to bind one site on the CHC TD at a time. Therefore, the loop deletion mutant should have a weaker interaction than the full-length. To test this hypothesis in which the loop is important for the interaction between GTSE1 and CHC, we deleted the loop on GTSE1 (del(675-705)). Here we used GTSE-C containing all LID motifs as the template to generate different mutants and examined their interaction Figure 3-8A and B. Consistent with our previous results, mutations on either Boxes AB (AB-M) or Box D (D-M) significantly reduced its interaction with CHC. As expected, mutating all 5 LID motifs (5xLID) totally abolished the interaction. The loop deletion mutation, del(675-705), also significantly impaired the binding (Figure 3-8A). Although this loop does not interact with CHC *pre se*, it does provide a distance to bridge two interactions together and therefore stabilize the interaction. However, we can not distinguish the stoichiometry of the interaction by pulldowns. Since this loop is long enough to bridge two interactions, it remains a question if one molecule of GTSE1 can intramolecularly bind two sites on the CHC TD or it can bridge two molecules of CHC TDs together (Figure 3-8C).

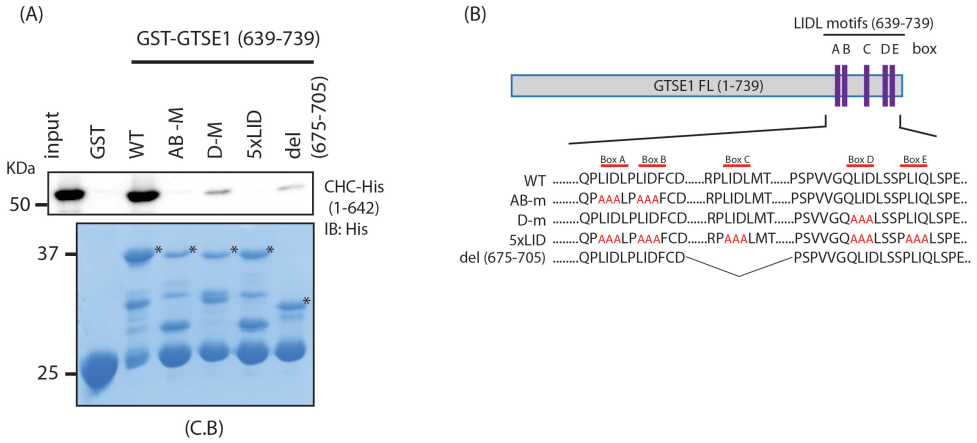

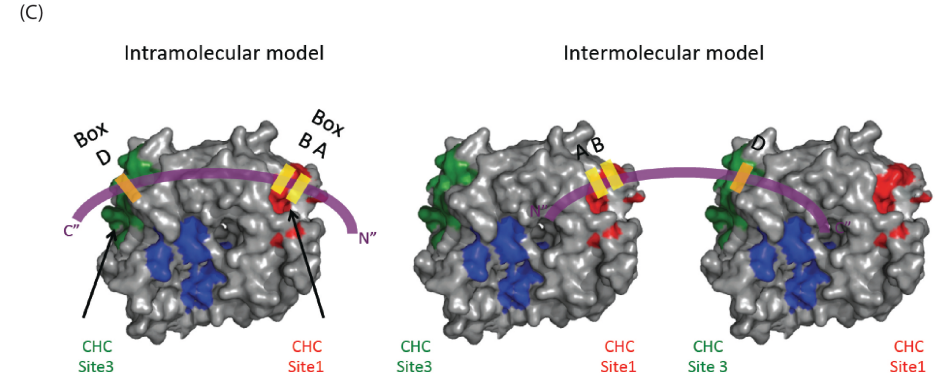

Figure 3-8. A proposed model of the CHC-GTSE1 complex

(A) Pulldown assays showing that several LIDL motifs and a "loop" are required their interaction with CHC. The WT and different mutants of GST-GTSE1 (639-739) were incubated with CHC (1-642)-His proteins. (B) A scheme illustrated mutants that were used in A. (C) Two proposed models illustrating how GTSE1 binds CHC. Left; GTSE1 might bind to two sites on one CHC TD or right; GTSE1 can bridge two molecules of CHC TDs. The site 1 and 3 on CHC TD are labeled in red and green and the GTSE1 peptides is in purple.

3.4 The CHC-GTSE1 interaction is independent of the phosphorylation.

Here we showed that GTSE1 interacts with CHC. Due to the fact that GTSE1 is highly phosphorylated and shows a molecular weight shit during mitosis (Figure 3-9A), it leads us to ask if the phosphorylation of GTSE1 alters its interaction with CHC. Our lab has identified that Aurora A, B and Cdk1 kinases are able to phosphorylate GTSE1 *in vitro* (Divya Sighn, unpublish data). Therefore, we first used these kinases to phosphorylate GTSE1 and compared the interaction before and after the phosphorylation. GTSE1 was phosphorylated by kinases confirmed by ProQ Diamond staining (Figure 3-9C), and the equal loading was examined by CB staining (Figure 3-9B). To test the interaction, 1 μM GST-GTSE1 proteins were incubated with 1 μM CHC (1-642) for an hr at 4 degree and following added GSH beads for 1 more hr incubation. GSH beads were washed 3 times with GST-binding buffer and analyzed by a SDS-page. Here, we did not see any remarkable differences of the CHC-GTSE1 interaction before or after phosphorylation (Figure 3-9D). Furthermore, we did detect the interaction from all pulldown assays where CHC and GTSE1 proteins were purified from bacteria and not phosphorylated. In addition, we can easily detect the interaction from asynchronized cell lysates by IP in which the majority of GTSE1 is non-phosphorylated or not full phosphorylated (Figure 3-9E). These results are consistent with the idea that the phosphorylation on GTSE1 might not change the binding intensity to CHC. However, we do not know yet if the phosphorylation of GTSE1 changes its stoichiometry of the interaction with CHC. Further experiments are needed to perform in order to test this idea.

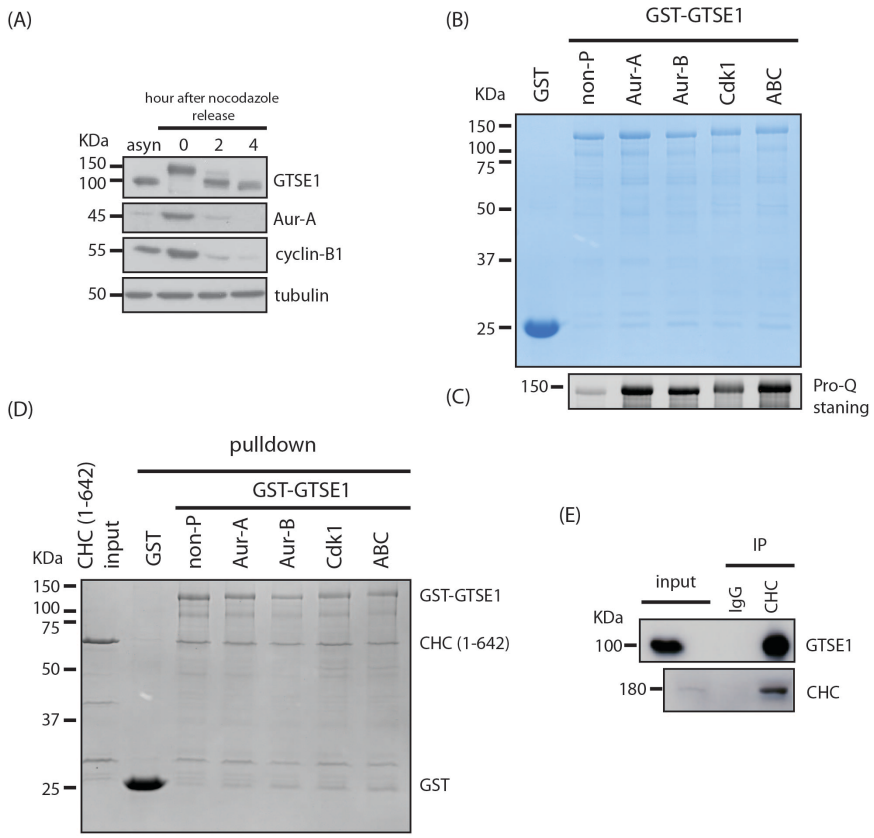

Figure 3-9. Phosphorylation of GTSE1 does not alter its interaction with CHC

(A) GTSE1 is highly phosphorylated in mitosis. U2OS cells were synchronized with nocodazole for 18 hour and released from nocodazole in the culture medium. Cell lysates were prepared at the indicated time point and analyzed by western blot using indicated antibodies. asyn: asynchronized cell lysates (B) GST-GTSE1 proteins were *in vitro* phosphorylated by either Aurora A (Aur-A), Aurora B (Aur-B), Cdk 1 or Aurora A plus Aurora B plus Cdk1 kinases (ABC). Proteins were analyzed by a SDS-page and stained with coomassie blue. Non-phosphorylated GST-GTSE1 proteins is labeled as Non-P (C) ProQ staining showing that GTSE1 proteins were phosphorylated after incubating with kinases *in vitro* from B. (D) CHC (1-642) proteins were pulled down by non-phosphorylated or phosphorylated GST-GTSE1 proteins. (E) IPs indicating that GTSE1 interacts with CHC in cycling cells. IPs were performed using anti-CHC and anti-myc (IgG) antibodies.

3.5 X-ray crystallography of the CHC-GTSE1 complex

Although we have characterized the interaction between CHC and GTSE1 in detail, we could not provide the binding model of how these LIDL motifs of GTSE1 interact with their corresponding binding sites on CHC on the molecular level. In order to gain insight into this interaction at the atomic resolution by means of X-ray crystallography, we attempted to crystallize the complex using the vapor diffusion method with the sitting-drop implementation.

To prepare the CHC-GTSE1 complex for crystallization trials, we subcloned CHC (1-364) and GTSE1 peptide (662-726) containing all 5 LIDL motifs into pGEX-6p-1 vector shown in Figure 3-10. In this construct, the GTSE1 peptide was fused after a GST tag following a PreScission protease cleavage site, and CHC has no additional tag. Because the ribosome-binding site (RBS) is located between GST-GTSE1 and CHC, this construct allows two individual proteins to be translated at the same time from the same mRNA transcript that facilitates equimolar expression of both proteins.

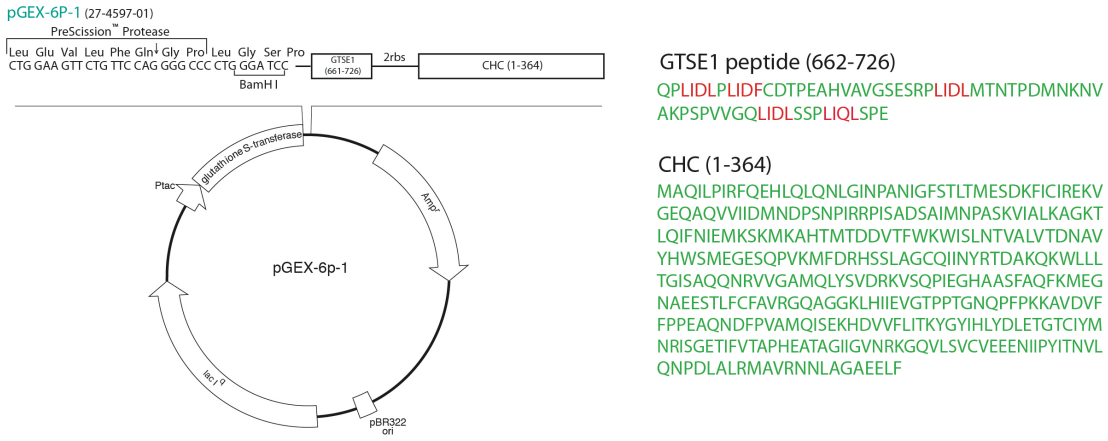

Figure 3-10. The construct of GTSE-GTSE1-CHC complex

Left; The pGEX-6p-1 vector containing GTSE1 and CHC was used for the protein expression in bacteria. GTSE1 (661-726) was first subcloned following the GST tag with a PreScission Protease cleavage site, and CHC (1-364) without any tag was then cloned into the vector after a ribosome-binding site (2rbs). Right; the exact amino acids of each gene are shown in green letters. The five LIDL motifs on the GTSE1 peptide are labeled in red.

This construct was transformed into E. *coli* BL21 (DE3) cells for protein expression. To get the stable CHC-GTSE1 complex, the idea is if the short GTSE1 peptide has high affinity to CHC we can efficiently co-purify CHC while purifying GST-GTSE. To check the stable CHC-GST-GTSE1 complex was formed, the bacteria lysate was first purified by GST affinity column, and proteins was following subject to size-exclusion chromatography using a Superdex 75(16/600) column. As shown in Figure 3-11A and B, GST-GTSE1 and CHC were eluted at same fractionations, suggesting that two proteins have an affinity high enough to form a stable complex. To cleave GST tags form the complexes, protein fractionations from 1 to 4 (Figure 3-11B) were pooled and incubated with GST-PreScission protease at 4°C

overnight. As the final purification step to remove GST and GST-PreScission protease, the cleaved GTSE1-CHC complex was again subject to the Superdex 75 (16/600) column attached a GST column and equilibrated in a buffer containing 20 mM Tris pH 7.0 and 50 mM NaCl by which GST-tagged proteins were trapped in the GST column and CHC-GTSE1 complexes without GST tags were presented in the flowthrough (Figure 3-11C). We collected the fractionations and analyzed by the SDS-page. Here, we can only detect CHC proteins from CHC-GTSE1 complexes after the gel filtration. Because the molecular weight of GTSE1 peptide is very small (~12 Kd) and contains very less basic amino acids, this peptide is not detectable using the coomassie blue staining on a SDS-page (Figure 3-11D). At the first purification step, we showed that GST-GTSE1 forms a very stable complex with CHC following the gel filtration (Figure 3-11A and B), we assumed that GTSE1 without GST tag should also bind CHC. The CHC-GTSE1 complexes were concentrated to 30 mg/ml for the crystallization trail.

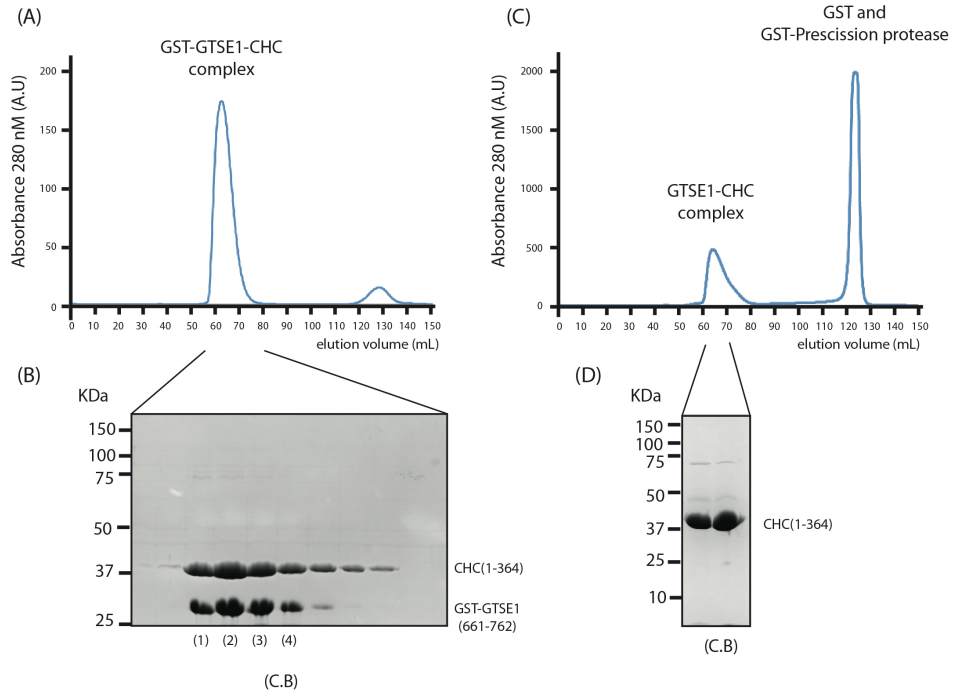

Figure 3-11. Protein purification of the CHC-GTSE1 complex

To check if the affinity of GST-GTSE1-CHC complex is high enough while purification, the proteins after the GST affinity purification were subject to a Superdex 75(16/600) column (A and B). The GST-GTSE1 and CHC proteins were eluted at same fractionations evidenced by the chromatography (A) and the SDS-pages (B), indicating that GST-GTSE1and CHC form a stable complex. To remove the GST tag from the GTSE1-CHC complex, the GST-GTSE1-CHC complex was treated with GST-PreScission protease. To get rid of the GST and GST-tagged proteins including the PreScission protease, the protein mixtures were separated by the Superdex 75(16/600) column attached with an

additional GST affinity column. The chromatography was shown in C, and the GTSE1-CHC complex was analyzed by the SDS-page in D.

To crystalize the complex, proteins were screened against a broad range of commercial crystallization conditions at 20°C in sitting drop 96-well plates. Box-shaped crystals grew in several conditions containing middle-chain to long-chain of PEGs (4000 and 8000). Crystals formation usually occurred within hour to few days. Due to the predicted flexibility of the GTSE1 peptide, crystallization trials were also set up in the presence of trypsin using *in-situ* proteolysis approach. Crystals were isolated in a very thin liquid film from the crystallization drop and flash-cooled without additional cryo-protection. The best crystals, GTSE1-CHC-2, diffracted better than 2.4 Å resolution on a rotating anode using an image plate detector in house. High resolution data were collected at X10SA beamline at Swiss Light Source of PSI (Villigen, Switzerland). Shapes of crystals were shown in the middle panel in Figure 3-12, and crystallization conditions were summarized in Table 3-1. All diffracted crystals are belonged to space group $P4_3$ and contain one molecule of the GTSE1 peptide and CHC in the asymmetric unit.

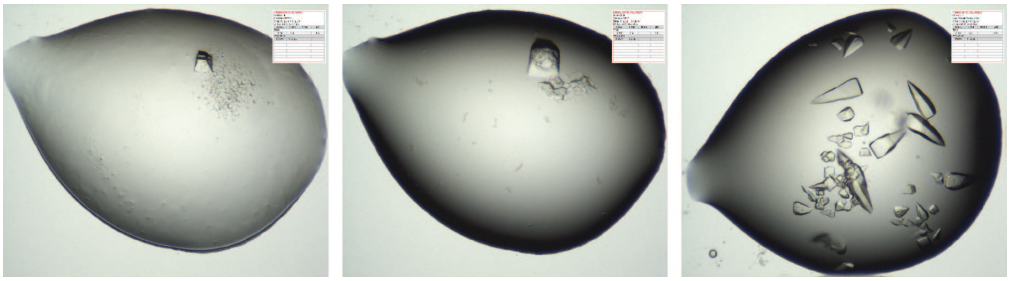

Figure 3-12. Crystals of the CHC-GTSE1 complex

The CHC-GTSE1 complex was crystalized in several different conditions. The left crystal was in the condition of 0.1 M Tris pH 8.5 and 8% PEG 8000 after 56 hour; the middle one is the same crystal as left one after 104 hour; the right condition was in 0.1 M Tris pH 8.5, 8% PEG 8000 and 75ng/ml trypsin after 36 hour. Figure is provided by Dr. Arthur Porfetye.

Table 3-1. Crystallization conditions of the CHC-GTSE1 complex

Cystal name	Resolution	Space group	Salt	Buffer	Precipitant	Condition
GTSE1/CHC -2	< 2.4Å	$P4_3$	/	0.1 M Tris pH 8.5	8% PEG 8000	PEG2 H6
GTSE1/CHC-3	< 2.4Å	$P4_3$	/	0.1M Tris pH 8.5 75 ng/ml Trypsin	8% PEG 8000	PEG2 H6
GTSE1/CHC-6	< 2.3Å	$P4_3$	0.1 M NaAc 0.05 M MgAc	/	10% PEG 8000	PEG2 H9
GTSE1/CHC-11	2.5Å	$P4_3$	0.1 M MgAc	0.1M Tris pH 7.5	12% PEG 8000	ProComplex E8
GTSE1/CHC-9	no diffraction		/	0.1M imidazole pH 8.0	10% PEG 8000	Core4 C7

The diffraction data set of the GTSE1/CHC-2 crystal was indexed, integrated and processed using the XDS package. The structure of CHC 1-364 was solved by molecular replacement using PHASER of the CCP4i suite based on a model of CHC 1-357 (PDB 4G55). The structure was refined in iterative cycles using refmac5 and coot, the statistic are shown in Figure 3-13D. After a few cycles of refinement, strong consecutive electron density is unambiguously fitted to the GTSE1 peptide (Figure 3-13 A, B and C) in which the Box D (LIDL) binding to the site 3 (Figure 3-13C) and the Box E (LIQL) bound to the site 1 of the CHC symmetry neighbor (Figure 3-13B). Interestingly, a weaker peptide-like electron density potentially fitting a few amino acids is visible in this crystal, which was found above the CHC site 2 (data not shown). Even though the exact sequences of GTSE1 could not be assigned into the electron density above this site, it is much different from the published amphiphysin peptide (PWDLW) that binds to the site 2 (Miele et al., 2004). It suggested that GTSE1 could potentially bind to the site 2 of CHC; however, this weak electron density could also be an artifact on the crystallization. Additionally, the mutation on the site 2 of CHC (S2M) does not affect the GTSE1-binding (Figure 3-2D), indicating that GTSE1 might not interact with this site. In summary, in our crystal this GTSE1 peptide (Box D) can interact with the site 3 and it can extend and cross over the site 2 on the same CHC TD. Perhaps, the GTSE1 peptide could further extend in which GTSE1 binds the site 1 by the Box A and B. However, we can not observe the electron density from these Boxes in the crystal.

(A)

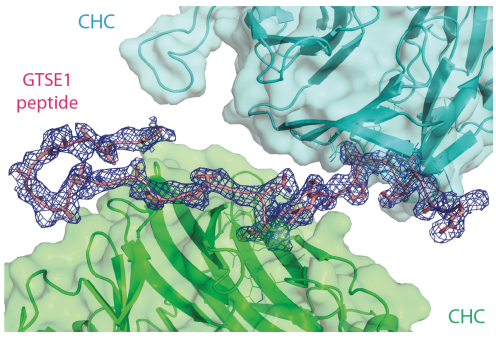

(B)

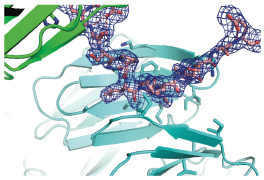

(C)

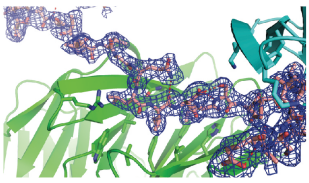

(D)

	Clathrin-GTSE1 (crystal 2)
Data collection	
Space group	$P4_3$
Cell dimensions	
a, b, c (Å)	53.59, 53.59, 156.95
α, β, γ (°)	90.0, 90.0, 90.0
Wave length (Å)	0.99993
Resolution (Å)	44.25 – 1.99 (2.11-1.99)
Monomers / au	1
CC $^1/_2$	99.9 (37.8)
I / σ(I)	11.75 (0.65)
Completeness (%)	95.1 (95.1)
Redundancy	12.93 (12.64)
Refinement	
Resolution (Å)	44.25-1.99 (2.05-1.99)
Number of Reflexes	26567(1992)
R_{work}	25.05 (36.1)
R_{free}	28.15 (41.2)
Number of Atoms	
Protein	2771
Ligand/Ions	14
Water	76
B-factor	
Protein	56.01
Ligand	78.82
Water	50.40
RMSD	
Bond length (Å)	0.008
Bond angle (°)	1.360
Ramachandran	0.27 / 1.9 / 97.83
Clash score	4.6
Rotamer outlier (%)	1.5
RSRZ outlier (%)	5.9
Molprobity score	1.48

Figure 3-13. Electron density of GTSE1 peptide on the CHC TD

(A) The overview of the unambiguous electron density of GTSE peptide bound to the CHC TD. (B) The electron density of GTSE1 on the site 1 of CHC TD. (C) The electron density of GTSE1 on the site 3 of CHC TD. (D) Crystallographic data and refinement statistics. Figures are provided by Dr. Arthur Porfetye.

Unambiguous electron density corresponding to the N-terminal part of GTSE1 peptide (662-699) could not be observed in this crystal structure. Residues 700-725 of GTSE1 were fitted into the final crystal structure, in which one molecule of GTSE1 bridges two CHC TDs (Figure 3-14A). The GTSE1 Box D (694-697) interacts with the CHC site 3 in the crystal (Figure 3-14B) that is consistent with our pulldown results. The key residues contributing the interaction in the Box D (LIDL) are L694, I695 and L697, which insert into hydrophobic pockets made by residues of CHC R188, Q192, L183, F216, F218 and H229. Interestingly, Arrestin2L was first reported to bind the CHC TD site 3 using a LLGXL motif (Arrestin motif) in which three leucines are buried into these hydrophobic packets as GTSE1 does. However, the binding mode of Arrestin2L is different in which the directionality of Arrestin2L peptide is reverse compared to GTSE1. Even through the glycine of Arrestin motif has no direct interaction with CHC, it might make this peptide very flexible and tends to bend this peptide in order to fit three leucines spatially into these pockets; therefore, alanine replacement of this glycine totally abolished the interaction (Kang et al., 2009). To date, GTSE1 is the second protein that specifically binds the canonical site 3 on CHC solved by X-ray crystallography. Remarkably, the sequence of the Box D on GTSE1 is distinct from the arrestin motif. Instead of bending the arrestin motif by glycine, GTSE1 used the side chain of Q712 to form the intra-hydrogen bond to I695. This intramolecular hydrogen bond might curves the peptide, which makes itself more feasible bind to the CHC site 3.

Unexpectedly, we observed that the GTSE1 Box E (LIQL) bound the site 1 on the symmetric CHC neighbor (Figure 3-14C). This result controverts our findings from pulldowns (Figure 3-6D) and yeast two-hybrid assays (Figure 3-5A) in which the Box E mutation did not significantly perturb the interaction with CHC, indicating that this motif should not interact with the CHC TD. Nevertheless, three hydrophobic amino acids (L, I and L) on the Box E inserted into hydrophobic pockets formed by blades 1 and 2, fitting into the known canonical model on the CHC TD site 1. Since all diffracted crystals that we have gotten are belonged to the same space group ($P4_3$), so far we can not check if this interaction is reproducible in a different crystal packing. In fact that there are only 3 residues between the Box D and E, it is hard to believe that GTSE1 is able to physiologically bridge two CHC TDs using these two

boxes. Based on to our pulldown assay and the crystal packing, we postulated that the Box E might be an artificial binding due to this specific crystal packing. As a consequence, the Box E unexpectedly occupied the site 1 on the symmetry neighbor CHC TD, and it might further block the Box A or B to interact with the site 1. Additionally, an explanation why the crystal structure differs from pulldown results in which we did not detect these Boxes to bind CHC is that the peptide for crystallization is too short. This peptide only contains two residues before the Box A that is ten residues shorter than GTSE1-C1 used for pulldowns. Thus, if these amino acids preceding Box A contribute to the binding and help discriminate between the different binding boxes, the affinity to the CHC TD of the shorter peptide might be reduced.

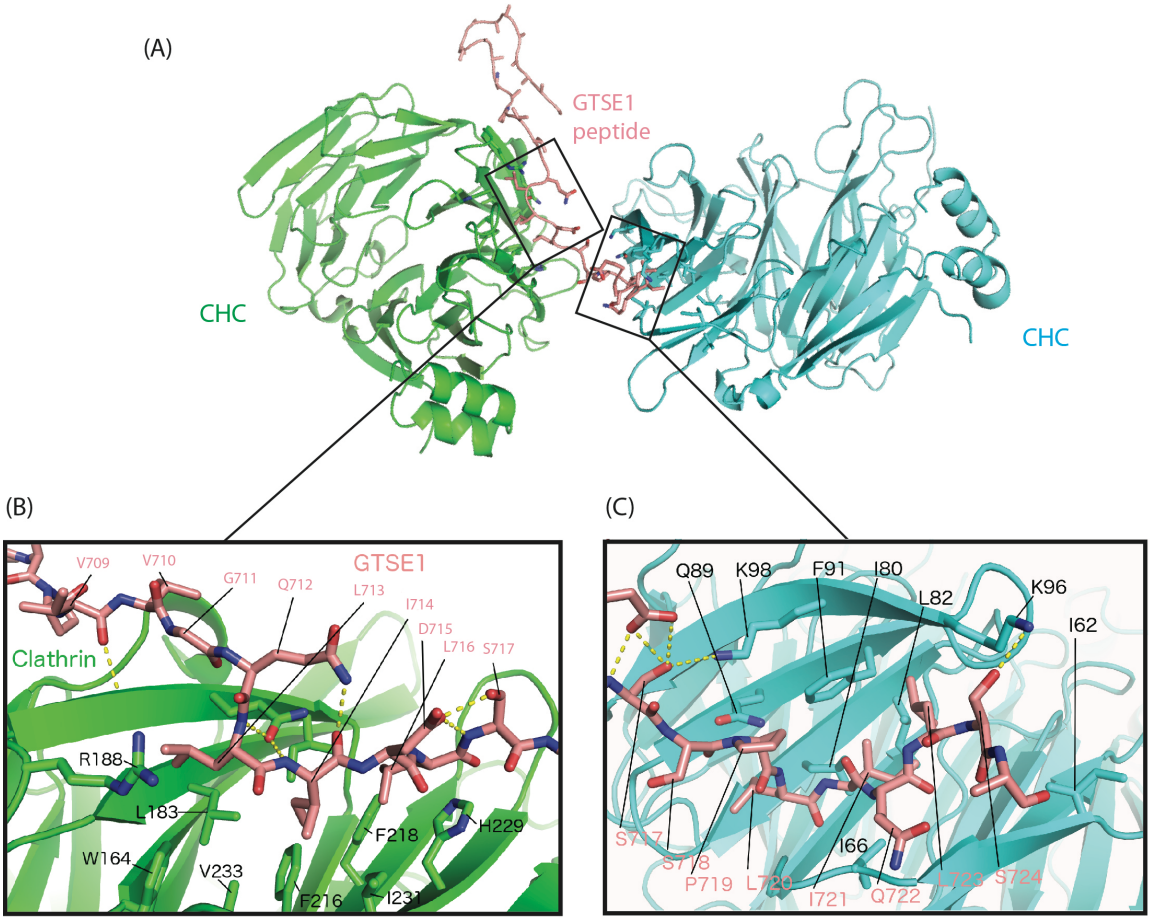

Figure 3-14. Crystal structure of the CHC-GTSE1 complex

(A) The overview of the crystal structure. GTSE1 peptide (residues 700-725, pink) binds to one CHC (green) and bridges to another neighbor molecule of CHC (cyan). (B) Detailed view of the interface between the CHC TD site 3 and GTSE1 Box D. GTSE1 L694, I695 and L697 interact with hydrophobic pockets made by residues of CHC R188, Q192, L183, F216, F218 and H229. (C) The interaction between the CHC site 1 and GTSE1 Box E in detail. GTSE1 L720 fits into a small hydrophobic pocket. GTSE1 I721 and L723 fit into a large second hydrophobic pocket of CHC I66, I80, L82, I93 and F91. Figures are provided by Dr. Arthur Porfetye.

3.6 Characterizing functions of the CHC-GTSE1 interaction in cells

Here, we revealed that GTSE1 interacts with CHC using its LID motifs by different biochemical approaches, and further gained insight into this interaction by X-ray crystallography. Additionally, we also showed that different combinations of LID mutations gradually affected their binding to CHC. Next, we aimed to address if this interaction between GTSE1 and CHC has its biological relevant and functions in cells. Thus, we used a bacteria artificial chromosome (BAC) to express the transgene in cells. Because BACs contain regulatory elements from the genome, the gene expression is relatively equal to the endogenous level. To generate GTSE1 mutant in which we would assure abolishment of the interaction with CHC, we decided to substitute all 5 LID motifs to 5 times triple alanine and referred it as 5xLID mutant in our study. To examine functions of transgenes without a disturbance from the endogenous background, GTSE1-WT and GTSE1-5xLID were made resistant to GTSE1 siRNA and tagged with GFP. U2OS cells were transfected with these BACs, and clonal cells stably expressing GTSE1-WT or GTSE1-5xLID mutant were isolated. We first checked if the GTSE1-5xLID mutant also abolishes its interaction with CHC in cells. To test that, we prepared the unsynchronized cell lysates from both GTSE1-WT and GTSE1-5xLID lines and used anti-CHC antibodies to perform IPs. As expected, CHC can efficiently pull down endogenous GTSE1 proteins in both WT and 5xLID lines. However, CHC can only interact with the WT transgene but not the 5xLID mutant, indicating that this mutant indeed abolishes the interaction with CHC *in vivo* (Figure 3-15A). Because these transgenes are siRNA resistant and unaffected following GTSE1 depletion, we next characterized the cellular localization of them after GTSE1 depletion. It is worth to mention that these transgenes' levels are comparably equal to the endogenous GTSE1 in the control depletion, and the WT and the 5xLID mutant transgene also showed similar protein expression (Figure 3-15B). Cells were fixed by 4% PFA/PIPES buffer and stained with anti-GFP antibodies to label the GTSE1 transgene. GTSE1 is higher expressed in G2 phase and mitosis we then selected the G2 phase to represent interphase. As is shown in Figure 3-15C, GTSE1-5xLID showed a similar cellular localization as GTSE1-WT during certain cell cycle phases. Both of them were accumulated on centrosomes/ poles in interphase and late mitosis. Remarkably, their localizations in metaphase are very different. GTSE1-WT can be easily observed on the mitotic spindle and poles in metaphase. However, GTSE1-5xLID was hard to detect or just very little on spindles and defused in the cytoplasm. Due to the high cytosolic background in GTSE1-5xLID, it is very difficult to distinguish whether this mutant is able to present on the

poles in metaphase. Altogether, here we showed that GTSE1 5xLID mutant abolishes the interaction with CHC *in vitro* (Figure 3-8A) and *in vivo* and thereby this mutant does not localize on mitotic spindles in metaphase, revealing that this interaction is required for GTSE1 to localize at spindles. Due to the fact that we only observed the different cellular localization of 5xLID mutant in metaphase in which it delocalizes from spindles, it highly suggested that this mutant might have some mitotic defects. We thereby investigated and characterized the phenotypes of GTSE1-5xLID mutant during mitosis.

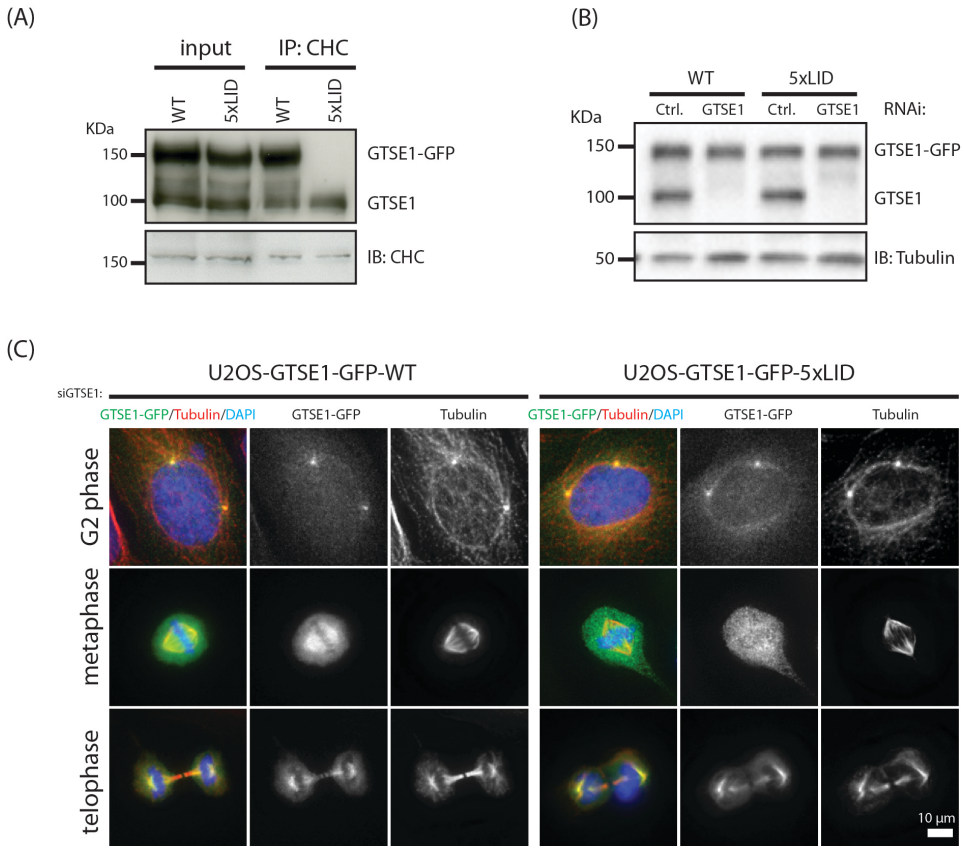

Figure 3-15. The GTSE1-5xLID does not bind CHC and delocalizes from spindles

(A) IPs indicating that the 5xLID mutant does not bind CHC *in vivo*. IPs were performed using anti-CHC antibodies. (B) Western blot showing that these transgenes are siRNA resistant following GTSE1 depletion. Figure is provided by Dr. Arnaud Rondelet. (C) The 5xLID mutant delocalized from spindles in metaphase. IFs showing that the localization of GTSE1-WT and 5xLID mutant in different cell cycle stages. Images were taken by DeltaVision with a Z-optical spacing of 0.2 µm, subsequently deconvolved and analyzed using the SoftWoRx 5.0.

Here we showed that the CHC-GTSE1 interaction is required for GTSE1 to localize on spindles in metaphase; therefore the 5xLID mutant does not interact with CHC and

delocalizes from spindles. This result strongly suggested that CHC might recruit GTSE1 to the spindles. A direct experiment to test this hypothesis is to check the cellular localization following CHC depletion. To avoid the GTSE endogenous background, we visualized the localization of transgenes following GTSE1 siRNA in combination with CHC depletion. As expected, the WT GTSE1 transgene localized on spindle in the control condition (Figure 3-16A (i)). Notably, it delocalized from mitotic spindles following CHC depletion, indicating that CHC indeed recruits GTSE1 to mitotic spindles (Figure 3-16A (ii)). In consistence with this idea, the 5xLID mutant does not present or only very little on spindles. Interestingly, abnormal shapes of spindles are often observed in this mutant (Figure 3-16A (iii)). These results revealed that the spindle recruitment of GTSE1 is dependent on CHC. Since the 5xLID mutant is unable to bind CHC, the CHC-GTSE1 interaction is specifically to recruit GTSE1 to spindle microtubules. However, it is hard to detect if GTSE1 still localized on poles following CHC depletion due to the high cytosolic background by the IF. Next, we examined the dependency of CHC and TACC3 after GTSE1 siRNA. Both CHC and TACC3 were unaffected and remained to localize on spindles following GTSE1 depletion shown in Figure 3-16B (ii), suggesting that GTSE1 functions downstream of the CHC-TACC3 complex which is consistent with previous findings (Bendre et al., 2016; Cheeseman et al., 2013; Hubner et al., 2010). Taken together, here we showed that GTSE1 directly interacts with CHC and GTSE1 is recruited by CHC as a downstream effector to regulate the spindle integrity.

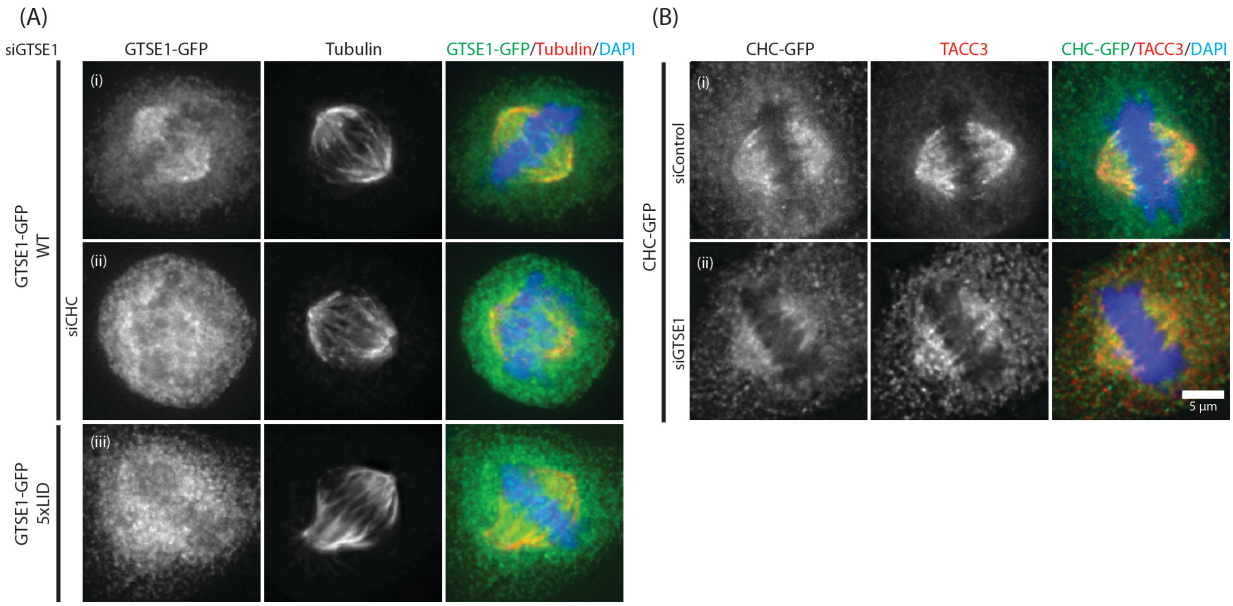

Figure 3-16. CHC recruits GTSE1 to the mitotic spindle

(A) The interaction with CHC is required for GTSE1 to localized on spindles. U2OS cells expressing GTSE1-WT-GFP were depleted by GTSE1 siRNA (i) or GTSE1 plus CHC siRNA (ii). IF showing that GTSE1-WT transgene delocalized from spindles following CHC depletion (ii). U2OS cells expressing GTSE1-5xLID-GFP were treated with GTSE1 siRNA and this mutant was undetectable or hard to detect on spindles (iii). (B) The spindle localization of the CHC-TACC3 complex was not affected following GTSE1 depletion. U2OS cells expressing CHC-GFP were treated with GTSE1 siRNA. IF showing that the localization of CHC and TACC3 has no visually changes following GTSE1 depletion (ii) in comparison to control siRNA (i). Images were taken by DeltaVision with a Z-optical spacing of 0.2 μm, subsequently deconvolved and analyzed using the SoftWoRx 5.0.

3.7 The CHC-GTSE1 complex specifically presents on K-fibers

Here we revealed that the CHC-GTSE1 complex presented on the mitotic spindle. CHC has been shown to specifically localize to K-fibers by IF staining and immunogold electron microscopy (Booth et al., 2011; Royle et al., 2005). Since the spindle localization of GTSE1 is dependent on CHC, we reason that the majority of GTSE1 should localize to K-fibers because of their direct interaction. A good way to examine this idea is to deplete Hec1. Hec1 is one subunit of Ndc80 complex, which is identified to mediate kinetochore-microtubule attachment. Thus, following Hec1 deletion the bipolar spindle can still be formed, but chromosomes are unable to congress due to loss of K-fibers. We first examined the cellular localization of CHC following Hec1 depletion in U2OS expressing CHC-GFP. In control-depleted cells, CHC is easily seen on mitotic spindles in metaphase (Figure 3-17A (i)). After depleted Hec1, cells showed typical defects in which chromosomes can not congress on the metaphase plate (Figure 3-17A (ii-iv)). As expected, we could not observe the detectable signal of CHC on spindles. Due to the fact that Hec1 depletion leads to the K-fiber null phenotype and CHC is no longer on spindles, we thereby confirmed that CHC might specifically present on K-fibers. Next, we checked the GTSE1-GFP signal after Hec1 depletion. In control-depleted cells, GTSE1 was localized on spindles and spindle poles (Figure 3-17B (i)). Interestingly, the majority of GTSE1 delocalized from spindles following Hec1 depletion, suggesting that a large portion of GTSE1 does bind K-fibers (Figure 3-17B (ii-iv)). Additionally, we very often observed that GTSE1 accumulated on poles (Figure 3-17B (iii-v)) and few cells did show the weak spindle localization (Figure 3-17B (v)) following Hec1 depletion. Although GTSE1 is a microtubule-binding protein, it is highly phosphorylated during mitosis (Figure 3-9A) and the majority of GTSE1 does not tend to bind microtubules (Scolz et al., 2012). Thus, its K-fiber localization is highly dependent on CHC, which is also confirmed by the fact that the 5xLID mutant, loss of CHC-binding, does

not present on K-fibers (data not shown). Altogether, these results indicated that CHC recruits GTSE1 to K-fibers. However, we do see that GTSE1 localizes on poles following CHC depletion in live cells (Hubner et al., 2010) and Hec1 depletion. It strongly suggests that the pole localization of GTSE1 is independent of CHC. The pole/centrosomal localization of GTSE1 is presumably due to its intrinsic microtubule-binding ability under unphosphorylated status, or GTSE1 might potentially interact with centrosomal proteins.

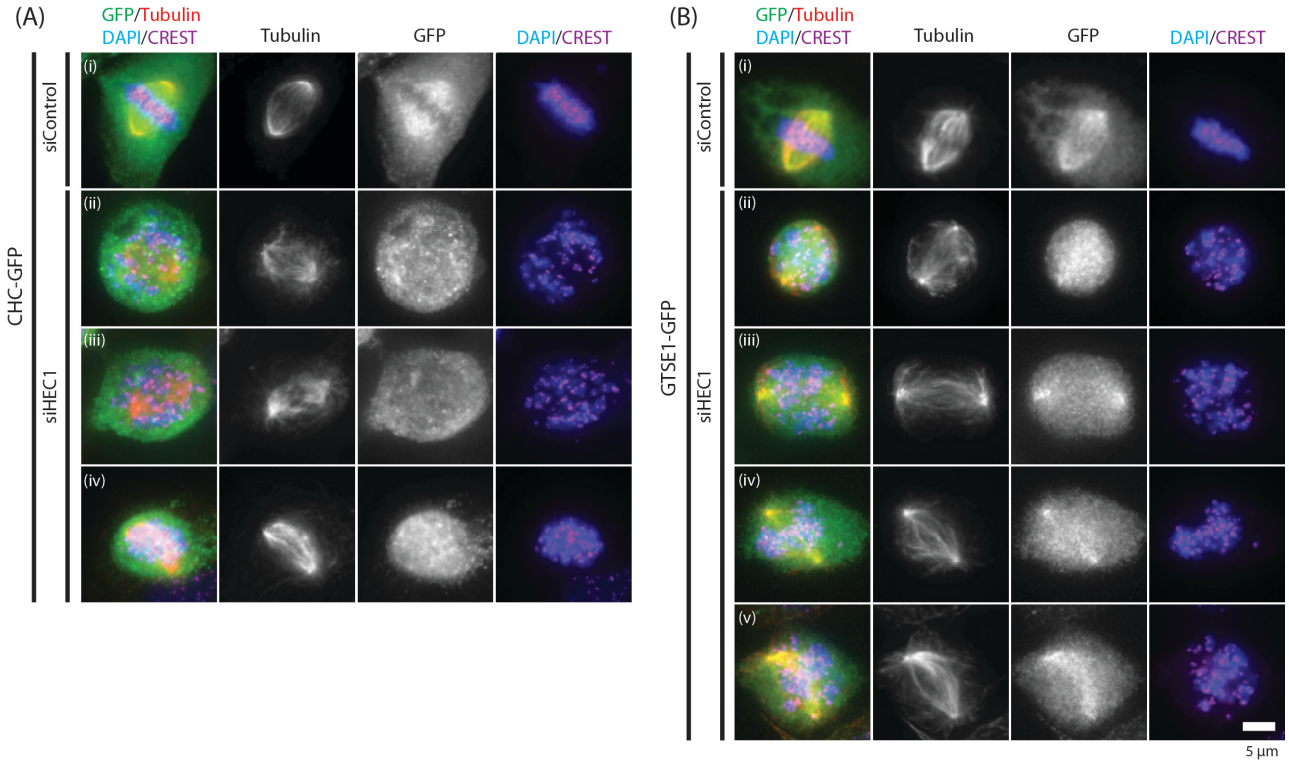

Figure 3-17. The CHC-GTSE1 complex specifically localizes on K-fibers

(A) CHC presents on K-fibers and it loses the localization following Hec1 depletion. U2OS cells expressing CHC-GFP were treated with Control siRNA (i) or Hec1 siRNA (ii-iv). (B) The majority of GTSE1 is bound to K-fibers in metaphase. U2OS cells expressing GTSE1-GFP were treated with Control siRNA (i) or Hec1 siRNA (ii-v). The major phenotypes following Hec1 depletion were ii and iii where GTSE1 accumulates on two poles and defuses from poles. Little amount of GTSE1 can be found at spindles after Hec1 depletion in few cells (v). Images were taken by DeltaVision with a Z-optical spacing of 0.2 µm, subsequently deconvolved and analyzed using the SoftWoRx 5.0.

3.8 GTSE1 binds the outer kinetochore and colocalizes with MCAK on kinetochores.

Here we showed that the CHC-GTSE1 complex localizes on K-fibers. We previously identified that GTSE1 is a novel microtubule-stabilizing protein by inhibiting MCAK. MCAK is recruited by Sgo2 to kinetochores where MCAK depolymerizes microtubules and regulates

microtubule-kinetochore attachment (Huang et al., 2007). Interestingly, GTSE1 depeltion also leads to slight defects in microtubule-kinetochore attachment even if chromosomes are fully congressed and correctly alignmed at the metaphase plate (Bendre et al., 2016). This result implied that GTSE1 might presumably localize on kinetochore to inhibit the MCAK-depolymerizing activity. Although GTSE1 is presented on K-fibers, we do not know yet if the K-fiber localization is able to bring itself to kinetochores, or GTSE1 is able to localized on kinetochores independent of K-fibers. However, we could not clearly detect GTSE1 on kinetochores by IF so far. It may be because the portion of GTSE1 on kinetochore is very little and even very dynamic. Thus, to answer if GTSE1 localizes to kinetochores, the best way is to test whether GTSE1 is able to interact with kinetochore proteins. In fact, MCAK localizes on the outer kinetochore or corona. In order to inhibit MCAK activity, GTSE1 has to be physiologically close and interact with MCAK. We therefore hypothesized that GTSE1 might localize at outer kinetochore through interacting with protein complexes on outer kinetochore. Additionally, GTSE1 is highly phosphorylated during mitosis. Thus, we reasoned that this interaction might depend on the phosphorylation. To examine the interaction, here we used the KMNZ complex containing 10 proteins, which almost cover all components on the outer kinetochore (Cheeseman and Desai, 2008; Musacchio and Desai, 2017; Pesenti et al., 2016). We first phosphorylated GST-GTSE1 by different kinases, and checked the interaction with the KMNZ complex. Because the interaction is very weak we can not detect any kinetochore proteins that were pulled down by the coomassie staining (data not shown). We next used western blot to detect the interaction. Each subunit of the KMNZ complex forms a very stable network, meaning that if one protein from this complex is pulled down the whole KMNZ complex can be detected. Thus, we used anti-His or anti-Hec1 antibodies to detect samples from pulldowns. As shown in Figure 3-18A, GTSE1 can pull down the outer kinechore once GTSE1 is phosphorylated by either Aurora A or Aurora B kinase. Interestingly, the non-phosphorylated GTSE1 or phosphorylated by cdk1 can not bind the outer kinetochore. Next, we exmained whether the 5xLID mutant is able to interact with the outer kinetochore. We then independently performed the second pull down assays and detected by anti-Hec1 antibodies. As indicated in Figure 3-18B, the non-phosphorylated GTSE1 can not bind the KMNZ complex as expected. Once GTSE1 got phosphorylated by Aurora B, both WT and 5xLID can interact with the outer kinetochore. Interestingly, we found the phosphorylation by Aurora A or B kinase is required for GTSE1 to interact with kinetochores. This is not surprising because these two kinases regonize similar motifs. In fact, lpl1, the only Aurora kinase in yearst, shares functions and substrates with Aurora A and

Aurora B. More recently, a single amino acid change coverts Aurora A into Aurora B-like kinase in terms of substrates and celluar localization (Fu et al., 2009; Hans et al., 2009). Thus, these phsophrylation events are more dependent on Aurora kinases' subcellular localizations. Since Aurora B kinase physiologically localizes near kinetochores, we hypothsize that GTSE1 is phosphorylated by Aurora B which induces GTSE1 to bind kinetochores. The 5xLID mutant, which does not bind CHC and delocalizes from spindles/k-fibers, also binds kinetochores. Thus, the kinetochore recruitment of GTSE1 is dependent on Aurora B kinase rather than its K-fiber localization. However, GTSE1 somehow only shows a weak affinity to outer kinetochores.

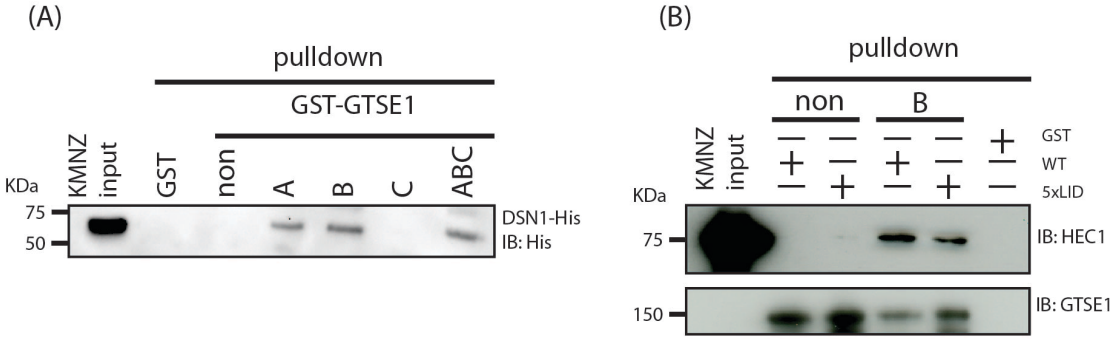

Figure 3-18. GTSE1 interacts with kinetochores in an Aurora B phosphorylation-dependent manner

(A) GTSE1 interacts with the KMNZ complex after Aurora A and Aurora B phosphorylation. 2μM of GST-GTSE1 proteins were phosphorylated by different kinases at 4°C overnight. Non-phosphorylated- or phosphorylated-GST-GTSE1 were immobilized on GSH beads and washed with buffer to remove kinases. These beads were incubated with the KMNZ complex to perform the pulldown assays. A: Aurora kinase A. B: Aurora B kinase. C: cdk1 kinase. ABC: A plus B plus C. (B) Both GTSE1 WT and 5xLID mutant interact with the KMNZ complex after Aurora B phosphorylation.

To further confirm if GTSE1 can interact with MCAK on kinetochore, we decided to use the proximity ligation assay (PLA) that allowed us to detect the interaction *in situ*. We treated cells with 3.3 μM nocodazole overnight and performed the PLA. As shown in Figure 3-19, the PLA signal can be detected in both GTSE1-WT and 5xLID mutant. Interestingly, we found that the PLA signal occasionally overlaps with CREST and is not detected on each kinetochore, suggesting that the GTSE1-MCAK complex is only formed under certain circumstances and could function together on kinetochores. Because we treated cells with nocodazole, the kinetochore localization of this complex is independent of microtubules.

Importantly, using PLA we first identify that GTSE1 can localize on kinetochores and interacts with MCAK. Moreover, the 5xLID mutant still colocalizes with MCAK on kinetochores. Even through the mutant could not bind K-fibers, it could still localize to kinetochores and perhaps controls the proper microtubule-kinetochore attachment by inhibiting MCAK.

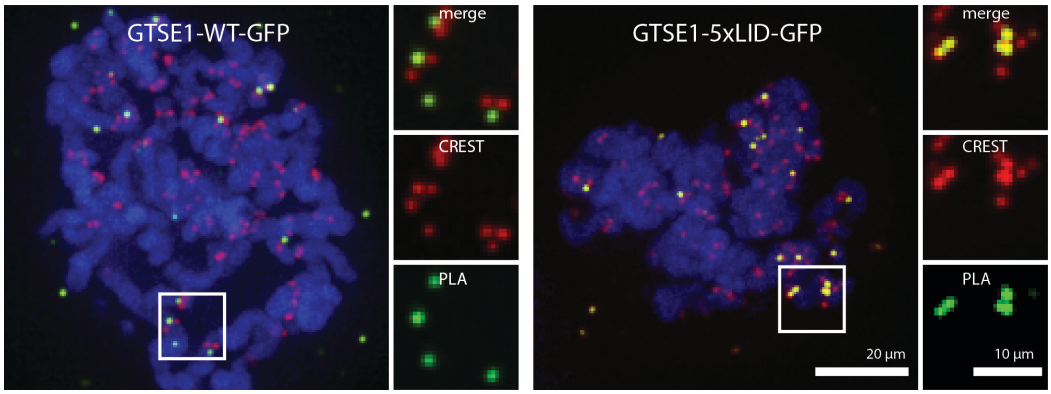

Figure 3-19. GTSE1 interacts with MCAK on kinetochores

Cells were fixed with 4% PFA/PIPES following the nocodazole treatment. GFP and MCAK antibodies were diluted 200 times and performed PLA. The green color represents the GTSE1-MCAK interaction by the PLA signal. Kinetochores were labeled by CREST. Both GTSE1-WT and 5xLID can interact and colocalize with MCAK on kinetochores. Images were taken by DeltaVision with a Z-optical spacing of 0.5 µm, subsequently deconvolved and analyzed using the SoftWoRx 5.0.

3.9 *In vitro* reconstitution of the microtubule-stabilizing complex

CHC has been shown to interact with TACC3 in an Aurora A kinase-dependent manner, which permits this complex to translocate onto mitotic spindles and regulates spindle integrity (Fu et al., 20110; Hubner et al., 20110; Lin et al., 20110). Additionally, the CHC-TACC3 complex functions as a central hub to interact with different proteins. On one hand, TACC3 recruits ch-TOG to spindles (Cheeseman et al., 2013; Gutierrez-Caballero et al., 2015; Thakur et al., 2014); on the other hand, CHC directly recruits GTSE1 onto spindles during mitosis, indicating that the CHC-TACC3 complex can bring another novel microtubule-stabilizing protein, GTSE1, to spindles. The cooperation of ch-TOG and TACC3 is proposed to antagonize MCAK activity *in vitro* although high concentration of ch-TOG alone slightly reduced MCAK activity (Kinoshita et al., 2005). However, this complex does not seem to bind MCAK directly. We previously showed that GTSE1 interacts with MCAK and inhibits MCAK-depolymerizing activity (Bendre et al., 2016). Thus, this large protein complex

containing CHC, TACC3, ch-TOG and GTSE1 can simply stabilize microtubules through regulating the activity of microtubule polymerase (ch-TOG) and deploymerase (MCAK) in addition to its function in bridging microtubules. Here, we defined this protein complex as the microtubule-stabilizing complex and schemed in Figure 3-20.

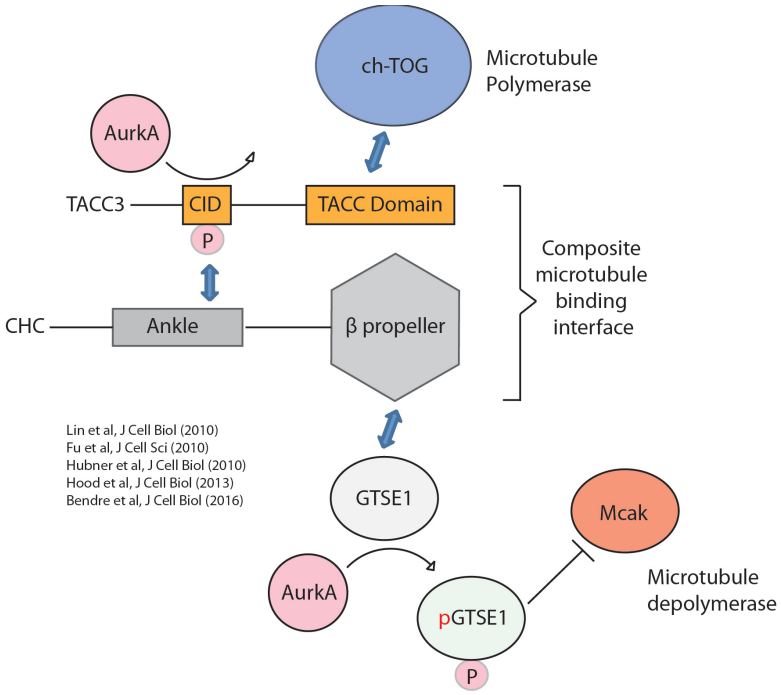

Figure 3-20. A microtubule-stabilizing complex including CHC, TACC3, ch-TOG and GTSE1

TACC3 interacts with CHC in an Aurora A phospho-dependent manner that translocates to spindles. Furthermore, the CHC-TACC3 complex acts as a central hub to recruit GTSE1 and ch-TOG onto spindles. ch-TOG could polymerize microtubules that maintains spindle integrity. Additionally, GTSE1 direct interacts with MCAK and inhibits MCAK-mediated microtubule depolymerization. Figure is provided by Dr. Arnaud Rondelet.

Next, to test if this is a *bona fide* microtubule-stabilizing complex formed only in mitosis, we performed IPs. To get cell lysates from different stages of cell cycle. U2OS cells were arrested in mitosis with nocodazole or in S phase using a single thymidine block. IPs were performed using anti-CHC, anti-TACC3 or anti-GTSE1 in presence of phosphatase inhibitors. As shown in Figure 3-21B, we can detect CHC, TACC3 and GTSE1 in a complex pulled down by CHC, TACC3 or GTSE1 antibodies in mitosis. In contrast, neither the CHC-TACC3 nor the TACC3-GTSE1 complex can be formed, and only the CHC-GTSE1 complex can be found in interphase (Figure 3-21A). TACC3 needs to be phosphorylated by Aurora A, which permits its interaction with CHC. Thus, it is unlikely to see the CHC-TACC3 complex in interphase as expected. Since we do see GTSE1 forming a complex with TACC3 only in

mitosis (Figure 3-21B), suggesting that the TACC3-GTSE1 interaction might depend on the phosphorylation, or it is an indirect interaction through CHC. Therefore, the interaction between GTSE1 and TACC3 needs to be further clarified.

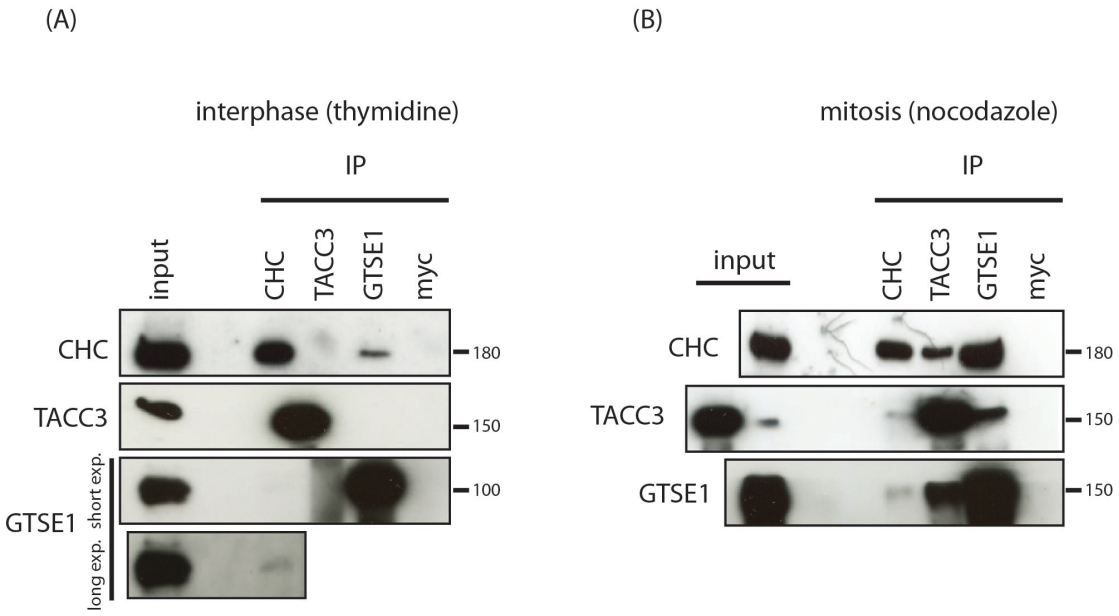

Figure 3-21. CHC, TACC3 and GTSE1 form a complex only in mitosis

(A) IPs indicating that TACC3 does not interact with the CHC-GTSE1 complex in interphase. Cells were arrested in S phase by thymidine block for 30 hour. Cell lysates were prepared and performed IPs using indicated antibodies. (B) IPs showing that CHC, TACC3 and GTSE1 form a stable complex in mitosis. Cells were synchronized in mitosis by adding nocodazole for 18 hour. Cell lysates were prepared and performed IPs using indicated antibodies.

Notably, GTSE1's spindle localization depends on not only CHC but also TACC3. Removing TACC3 from spindles severely impairs GTSE1's spindle localization (Hubner et al., 2010; Cheeseman et al., 2011). Here, we elucidated that GTSE1 indeed forms a complex with TACC3 in mitosis. Delocalizing GTSE1 from spindles following TACC3 depletion raises a question if TACC3 directly recruits GTSE1 to spindles or it is simply due to loss of CHC on spindles. Therefore, we next examined the interaction between TACC3 and GTSE1 by using the recombinant proteins. Because GTSE1 is heavily phosphorylated during mitosis, and TACC3 is phosphorylated by Aurora A as well, it leads us to consider if the interaction is mediated by phosphorylation. To test that, we thereby phosphorylated GTSE1 using different kinases and phosphorylated TACC3 by Aurora A. The phosphorylation of GTSE1 was confirmed by pro-Q staining shown in Figure 3-22A (low panel). Phosphorylated TACC3 was analyzed using anti-pS558 TACC3 antibodies that specific detect against the phosphorylated

serine 558 on TACC3 (Figure 3-22B). However, we could not detect any interaction between TACC3 and GTSE1 *in vitro* after phosphorylation, suggesting that there is no direct interaction, or this interaction is mediated by other kinases (Figure 3-22C). To answer this question, the idea is to do IPs using the mitotic cell lysates of GTSE1-5xLID, because this mutant, in theory, should get fully phosphorylated in cells during mitosis. Since the 5xLID mutant does not bind CHC, we can check the TACC3-GTSE1 interaction independent of CHC. U2OS cells expressing GTSE1-WT or GTSE1-5xLID tagged with GFP were arrested using nocodazole. Mitotic cell lysates were then prepared to perform IPs. As shown in Figure 3-22D, GTSE1-WT could pull down an interacting complex including CHC and TACC3 (line 1). However, GTSE1-5xLID does not bind to CHC and failed to interact with TACC3 (line 2), suggesting that there is no direct interaction between GTSE1 and TACC3. To further confirm this observation, we then added Aurora A kinase inhibitor (MLN8054) in our IPs, which prevented TACC3 phosphorylation by Aurora. The interaction between CHC and TACCs is Aurora A dependent. Thus, the MLN8054 treatment abolished their interaction as expected (line 3). Remarkably, it also eliminated the interaction between TACC3 and GTSE1. In summary, GTSE1 does not bind TACC3; however, through the direct interaction with CHC, GTSE1 can indirectly form a complex together with TACC3 during mitosis.

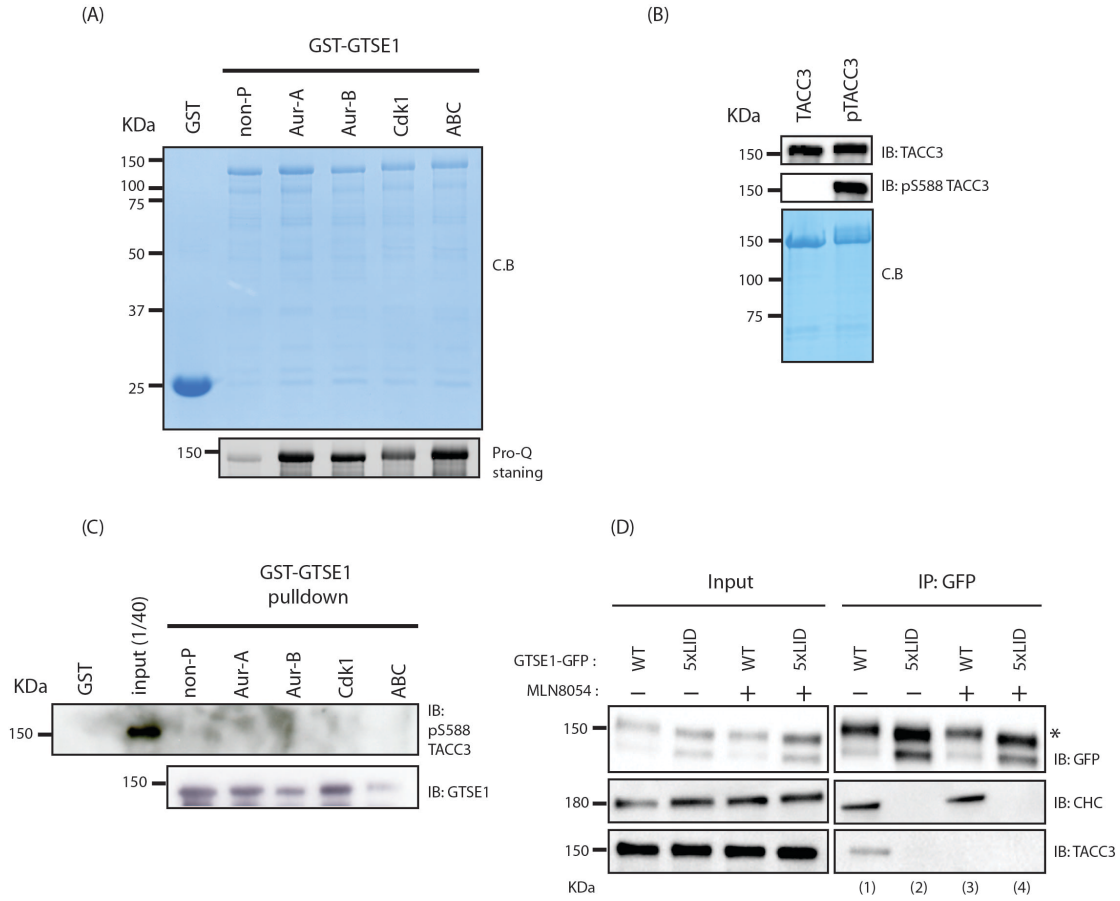

Figure 3-22. GTSE1 does not interact directly with TACC3

(A) GST-GTSE1 proteins were phosphorylated by either Aurora A (Aur-A), Aurora B (Aur-B), Cdk 1 or Aurora A plus Aurora B plus Cdk1 kinases (ABC) *in vitro* and stained with coomassie blue. Non-P: non-phosphorylated proteins. Phosphorylated GTSE1 proteins were confirmed by ProQ staining. (B) *In vitro* phosphorylation of TACC3 by Aurora A kinase, and detected using coomassie staining or western using indicated antibodies. (C) The pulldown analysis examining the interaction between phosphorylated GST-GTSE1 and phosphorylated TACC3 proteins. Western blot was performed using anti-pS558 TACC3 antibodies. (D) *In vivo* IPs by anti-GFP antibodies from cell lines stably expressed GTSE1-WT-GFP or GTSE1- 5xLID-GFP in the presence or absence of aurora A kinase inhibitor (MLN8054). IPs were performed by Dr. Arnaud Rondelet.

We next aimed to reconstitute the whole microtubule-stabilizing complex including CHC, TACC3, ch-TOG and GTSE1 *in vitro.* We thereby checked the pair interactions among these proteins first. The interaction between CHC and TACC3 has been described in detail from previous study (Lin et al., 2010) as well as the interaction between TACC3 and ch-TOG (Gutiérrez-Caballero et al., 2015; Hood et al., 2013; Thakur et al., 2014). We next tried to reproduce these interactions in our hands. Because phosphorylated TACC3 allows itself to bind CHC, we then phosphorylated TACC3 by Aurora A. As shown in Figure 3-23A, the full-length phosphorylated TACC3 can be pulled down by both GST-CHC-FL and GST-CHC (1-642). We could detect very weak interaction between non-phosphorylated TACC3 and CHC. However, it might be due to the high concentration of proteins that forces the interaction in our reactions. Next, we used a shorter fragment of TACC3 containing only the TACC domain (410-838). As expected, the TACC domain following the Aurora A phosphorylation binds to CHC (1-642) as well (Figure 3-23B and C). We can also confirm that a short fragment of ch-TOG (1806-2032) interacts with TACC3 (Figure 3-23D) as shown from the previous study (Hood et al., 2013).

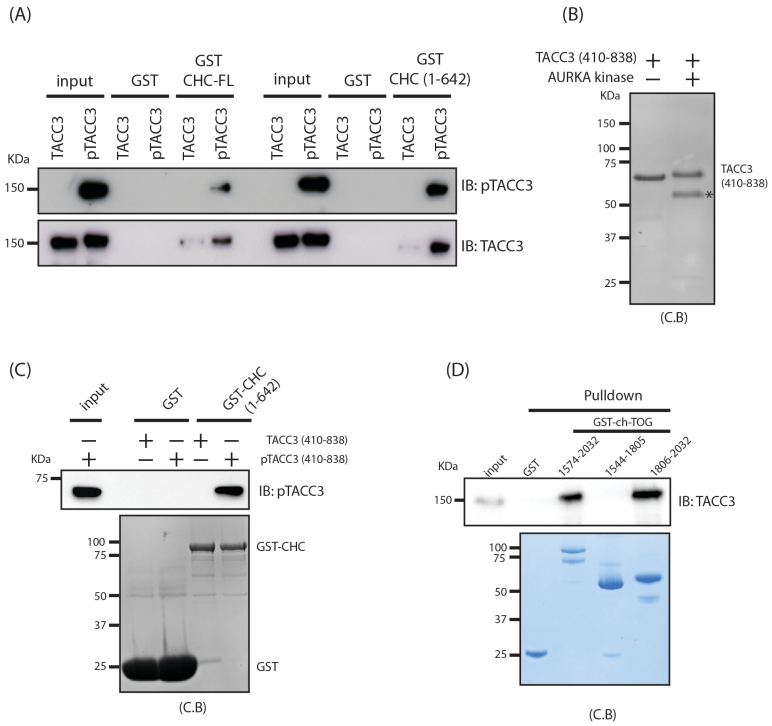

Figure 3-23. TACC3 interacts with both CHC and ch-TOG

CHC directly interacts with TACC3 in (A)(C). (A) GST-CHC-FL and GST-CHC (1-642) can pull down TACC3 following Aurora A phosphorylation. (B) A SDS-gel showing that the TACC domain (410-838) is phosphorylated by Aurora A and induces the molecular weight shift. (C) The phosphorylated TACC domain (410-838) interacts with CHC (1-642). (D) A shortest fragment of ch-TOG (1806-2032) interacts with TACC3 independent of Aurora A phosphorylation.

From previous pulldown experiments, we found that CHC (1-642) interacts with both GTSE1 (639-739) and phosphorylated TACC3, and the phosphorylated TACC3 (410-838) can bind ch-TOG (1806-2032) as well (data not shown). Due to the identified interactions among these proteins as shown in Figure 3-23, we postulated that CHC, TACC3, ch-TOG and GTSE1 can form one integral complex at the one arm of CHC triskelion. Because CHC (1-642) lacks the trimerization domain, it would stay in a monomer in our assays. The idea is that GTSE1 (639-739) can interact with a monomer CHC (1-642). Once TACC3 and ch-TOG were added into the reaction, this CHC-GTSE1 complex can indirectly pull down ch-TOG by the CHC-TACC3 interaction. Therefore, each arm of CHC triskelion enables to recruit all these proteins together. We then tested this hypothesis. As shown in Figure 3-24, we first examined that GTSE1 (639-739) neither binds ch-TOG (1806-203) (line 7) nor the ch-TOG (1806-2032)-pTACC3 (410-838) complex (lines 10 and 11). As expected, GTSE1 can interact with CHC (line 2). The CHC-GTSE1 complex could pull down very little pTACC3 (line 4). Noteworthy, this complex tended to pull down more pTACC3 in the presence of ch-TOG

(line 6) as compared to the line 4, suggesting that ch-TOG might increase the interaction between CHC and pTACC3. However, we do not know yet the mechanism of how ch-TOG enhances pTACC3 to bind CHC. Our results support the mesh hypothesis in which the CHC triskelion has to bridge at least two microtubules, meaning that each CHC of the triskelion must interact with TACC3 to generate a microtubule-binding surface. In conclusion, here we showed that CHC (1-642), as a monomer, can interact with GTSE1 and the pTACC3-ch-TOG complex as well, supporting the idea that each individual arm of the CHC triskelion contains all these proteins in order to bind/bridge microtubules.

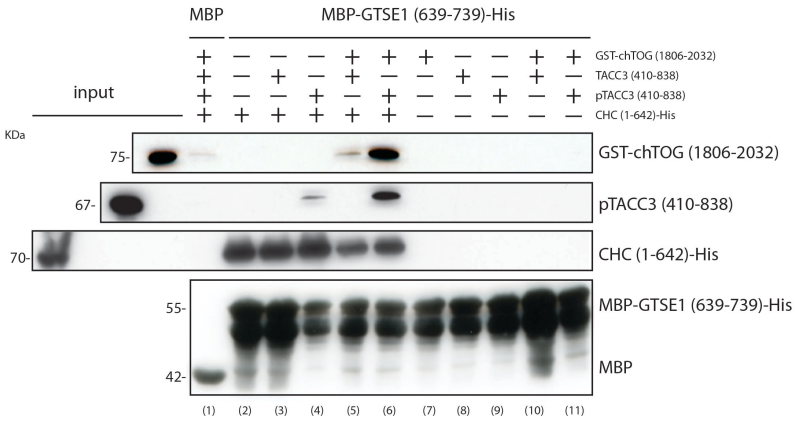

Figure 3-24. CHC interacts with GTSE1 and the TACC3-chTOG complex

MBP-GTSE1 (639-739) was incubated with indicated proteins to perform the pulldown assays. Samples were analyzed by western blot using indicated antibodies.

Even though the CHC triskelion could cross-link microtubules, the CHC TD has its unique roles to stabilize microtubules independent of the bridging functions in mitosis. Here we revealed that the CHC TD directly interacts with GTSE1 (Figure 3-2) and this interaction is required for GTSE1 to localize on mitotic spindles (Figure 3-16). The 5xLID mutant, which is unable to interact with the CHC TD, delocalizes from spindles and causes mitotic defects (Figure 3-16). Our lab previously identified that GTSE1 is a novel microtubule stabilizer by inhibiting MCAK-depolymerizing activity. Thus, one mechanism by which CHC promotes microtubule stability in mitosis is by recruiting GTSE1 to inhibit MCAK. However, CHC itself is unable to bind microtubules. Thus, CHC has to interact with TACC3 to translocate onto spindles in order to regulate spindle integrity. Our model therefore hypothesized that these proteins including CHC, TACC3, ch-TOG, GTSE1 and MCAK should presumably form a large-interacting complex. To test that, we used an *in vitro* pulldown assay in which

we purified CHC FL, TACC3 FL, MACK FL, GST-GTSE1 FL and ch-TOG (1806-2032) proteins. To test the interactions among them, TACC3 and GST-GTSE1 proteins were first phosphorylated by Aurora A kinase. Phospho-GST-GTSE1 proteins were then immobilized on GSH beads as baits to perform the pulldown. As shown in Figure 3-25, GTSE1 could form an interacting complex with all these proteins, supporting the model in which the TACC3-CHC complex recruits GTSE1 to spindles to stabilize microtubules through the inhibition of MCAK.

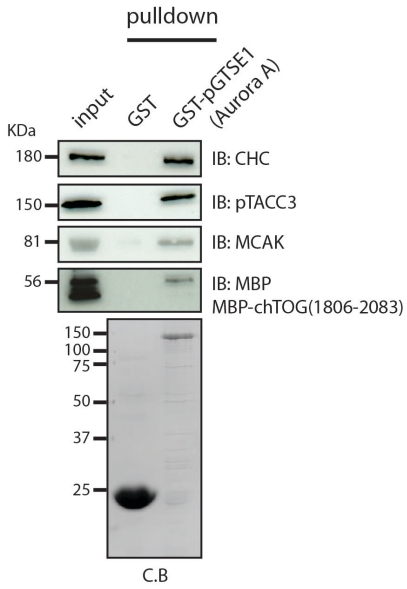

Figure 3-25. The microtubule-stabilizing complex interacts with MCAK

GST-GTSE1-FL can pull down a complex containing CHC-FL, TACC3-FL-, ch-TOG (1806-2032) and MCAK-FL. GST-GTSE1-FL and TACC3 proteins were phosphorylated by Aurora A kinase. GST-GTSE1-FL proteins were immobilized on GSH beads to perform the pull down assay.

The N-terminal region of GTSE1 binds MCAK (Bendre et al., 2016) and its C-terminus interacts with CHC identified from our study, suggesting the CHC-GTSE1-MCAK axis exists in cells. GTSE1 is an intrinsically disordered protein, and some disordered proteins indeed need their interacting partners to stabilize their protein conformation. It raises a question if the CHC binding on GTSE1 could affect GTSE1's interaction with MCAK and vice versa, meaning that there could be either a competition or a synergistic effect among these interactions. Because the GTSE1 5xLID mutant does not interact with CHC, we can compare the GTSE1-MCAK interaction between the GTSE1 WT and mutant in the presence of CHC. This experiment allowed us to address if CHC has any effects on the GTSE1-MCAK interaction. As expected, GTSE1-WT bound CHC (Figure 3-26A line 2) but not GTSE1-5xLID (Figure 3-26A line 3). We next examined whether this mutant effects the interaction

with MCAK. MCAK binds to the N-terminal region of phosphorylated GTSE1; therefore, theoretically, the C-terminal 5xLID mutant should not affect its interaction with MCAK. As shown in line 4 and line 5, MCAK was sufficiently and equally pulled down by both GTSE1-WT and 5xLID, suggesting that the 5xLID mutant has no detectable effect on the MCAK binding. As shown in line 6, GTSE1-WT can efficiently pull down both CHC and MCAK. Interestingly, GTSE1-5xLID remains the same binding capability to MCAK (line 7) in comparison with GTSE1-WT (line 6), indicating that the CHC-GTSE1 interaction does not affect GTSE1 to bind MCAK. To conclude the pulldown experiments, we showed that GTSE1 binds both CHC and MCAK and one pair of interactions has no effect on the other one. The GTSE1 5xLID mutant still binds MACK, which is consistent with the PLA assays where both GTSE1-WT and mutant could bind MCAK on kinetochores (Figure 3-19).

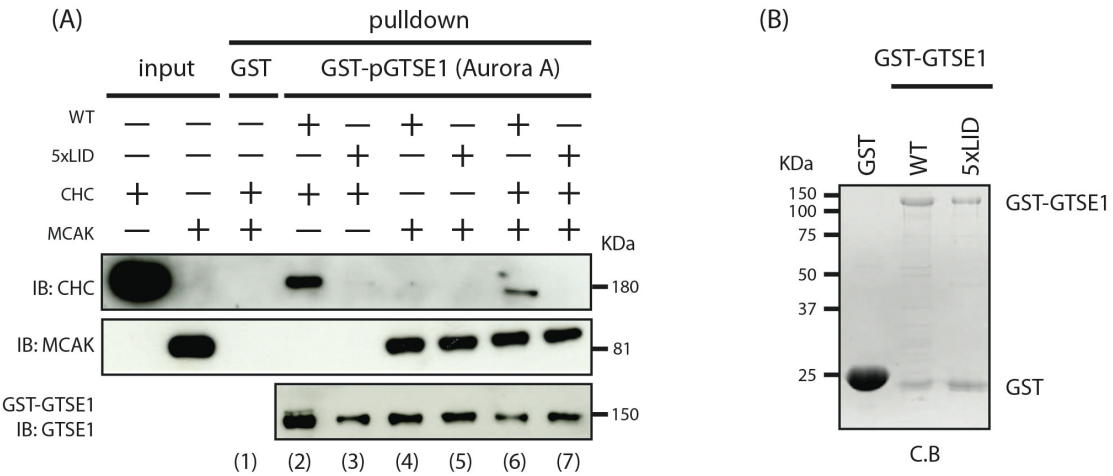

Figure 3-26. GTSE1 interacts with both CHC and MCAK

(A) Pulldown experiments showing the interaction among GTSE1, CHC and MCAK. (B) A-SDS-page showing the quality of GST, GST-GTSE1-WT and 5xLID proteins.

4. Discussion

CHC has been shown to bridge microtubules through forming the triskelion by its C-terminus, which stabilizes microtubules and maintains spindle integrity. However, a mutation on the CHC TD, abolishing the interaction with its adaptor proteins, does not affect its trimerization but causes mitotic defects. Thus, in addition to the bridging function, the CHC TD has its unique roles during mitosis. However, the function of the CHC TD has not been revealed yet. Here we identified GTSE1, a microtubule-stabilizing protein, and acts as a downstream effector of CHC. GTSE1 directly binds the CHC TD through an adaptor-like interaction that recruits GTSE1 to mitotic spindles. GTSE1 might be the first protein that is involved in the CHC TD-mediated microtubule stability in mitosis. As a consequence, the GTSE1 5xLID mutant, which can not bind to CHC and does not localize to spindles, leads to a global microtubule stability defects in spindle integrity, chromosome alignment and timely mitosis. We previously determined that GTSE1 inhibits MCAK activity that is required for the proper microtubule dynamics in mitosis (Bendre et al., 2016). Thus, one mechanism of how the CHC TD controls microtubule stability is through the GTSE1-MCAK axis. To gain insight these interacting networks, we could reconstitute a microtubule-stabilizing complex including CHC, TACC3, ch-TOG and GTSE1 *in vitro*, and this complex can further interact with MCAK. We previously revealed that GTSE1 might be involved in regulating microtubule-kinetochore attachment. In our study, we further confirmed that both GTSE1-WT and 5xLID mutant could weakly interact with kinetochores dependent on Aurora B phosphorylation, and they could occasionally associate with MCAK on kinetochores independent of microtubules. It sheds a light on a novel mechanism in which GTSE1 colocalizes with MCAK and regulates its activity on kinetochores to control the proper microtubule-kinetochore attachment.

4.1 The binding-stoichiometry and crystal structure of the CHC-GTSE1 complex.

In our study, we identified the interacting surfaces in detail on CHC and GTSE1 (Figure 3-2D and 3-3C). It becomes clear that two pairs interactions between them can stabilize the CHC-GTSE1 complex (Figure 3-8A). Therefore, GTSE1-C containing these two-binding domains has the stronger interaction than short fragments including C1 and C3 (Figure 3-3C). Consistent with the idea, some CHC adaptor proteins often use more than one motif to interact with the CHC TD; for instance, amphiphysin and β-arrestin2L (Kang et al., 2009;

Miele et al., 2004). Due to the fact that GTSE1 contains 5 almost identical LID motifs, it raises a question why GTSE1 specifically used two pairs of these motifs to bind CHC. Since GTSE1 can interact with CHC in both interphase and mitosis, does GTSE1 change its stoichiometry to bind CHC during the cell cycle? CHC and GTSE1 might behave differently in interphase and mitosis. The most well known function of CHC in interphase is to form a cage by its triskelion to mediate endocytosis. On the contrary, CHC prefers to maintain the triskelion and localizes on spindle in metaphase. Because high concentration of CHC triskelia can spontaneously pack into a cage, mechanisms may exist to avoid their polymerization to form a cage on the spindle. For example, protein interactors or post-translational modifications may prevent CHC from forming a cage in mitosis. Actually, some CHC adaptors are phosphorylated during mitosis, for instance; AP1 and AP2, which abolish their interactions with CHC (Wilde and Brodsky, 1996). Furthermore, most CHC adaptor proteins are not found to localize to spindles that might not help CHC polymerization (Royle, 2012; Royle, 2013). Additionally, another hypothesis is that free triskelia on spindles might be far away from each other which also prevents the cage formation. Nevertheless, the CHC cage is very different from the free triskelion in terms of the distance between two CHC TDs. CHC triskelia are highly packed in the cage, and therefore this distance between two N-terminal domains (~64 Å) might be shorter than the free triskelion. Additionally, we found a loop between these two CHC-binding domains on GTSE1 is long enough to fit this distance. Thus, due to the fact that CHC favors to polymerize and forms a cage in interphase, we postulated that GTSE1 might bridge two CHC TDs to stimulate the cage formation rather than binding two sites within a triskelion. To support the idea in which GTSE1 is able to bind CHC cages, a short peptide of GTSE1 containing the 5 LID motifs was artificially bound on membrane, which was shown to further recruit CHC onto the membrane and induce CHC-mediated vesicle formation (Wood 2017 JCB). Furthermore, GTSE1 has been shown to trap in the CHC cages following Auxilin depletion (Borner et al., 2012). Although GTSE1 is not known to be an endocytotic protein yet, it is still able to bind and even recruits CHC. To further confirm if GTSE1 is surely presented in the CHC cage *in vitro*, we could co-incubate the CHC cage with GTSE1 full-length protein together and visualize this complex by the electron microscopy, which would also answer the binding stoichiometry of this complex in the cage-stage. Additionally, the CHC triskelion purified *in vitro* can spontaneously polymerize into cages only in the presence of magnesium or calcium ions at low pH (<6.5) (Crowther and Pearse, 1981; Ungewickell and Branton, 1981) and spontaneously disassemble at pH 8.5. However, the CHC cage formation can be enhanced at neutral pH by incubating with its

adaptor proteins; for instance AP1 and AP2 (Keen, 1990). It might be interesting to see if GTSE1 plays roles to enhance the cage formation at neutral pH or stabilize the cage at pH 8.5. In mitosis, GTSE1 is heavily phosphorylated by different kinases. Interestingly, there are several (S/T)P sites close to each LID motifs except the Box A, which are phosphorylated by Cdk1 confirmed in our lab (Divya Singh, unpublished data) and a database of mass spectrometry studies (https://www.phosphosite.org/). It raises a question if these phosphorylations change the way that GTSE1 binds CHC. Although we did not detect remarkable difference of the interaction before and after Cdk1 phosphorylation (Figure 3-9), this experiment did not tell us if the phosphorylation changes the binding stoichiometry, or even induces GTSE1 to bind CHC by using different pairs of LID motifs. An interesting experiment to examine that is to use short fragments including C1 (Box A and B), C2 (Box C) and C3 (Box D and E). Because the Box C (C2 fragment) does not contribute too much for the binding (Figure 3-3C), it will be interesting to see if the C2 fragment alters the interaction before and after the phosphorylation. Additionally, it would be also good to compare the interaction of C1 and C3 before and after the phosphorylation. These experiments might tell us if the phosphorylation of GTSE1 changes different way to bind CHC as compared to the unphosphorylated state. However, to gain insight into the stoichiometry, the best way is to use the AUC (analytic ultracentrifugation). By the measurement using AUC, we can roughly predict the molecular weight of the protein complex. Therefore, this molecular weight can be reflected to the binding ratio of the proteins, which indicates the stoichiometry of the CHC-GTSE1 complex. Additionally, Auxilin, binding to the CHC TD, is known to uncoat the CHC cage by creating a global distortion of the CHC triskelion/cage (Fotin et al., 2004). However, the isoform of Auxilin in somatic cells, GAK, does not present on mitotic spindles, suggesting that it could not uncoat the CHC cage at spindles, and there must be some proteins to help CHC stay in a triskelion. Interestingly, in fact, a GTSE1 short peptide indeed enhances the CHC vesicles formation in cells during interphase (Wood et al., 2017). Since GTSE1 binds CHC in interphase and mitosis, why GTSE1 does not tend to maintain the CHC cage in mitosis? Does the phosphorylation on GTSE1 change the binding stoichiometry to CHC in mitosis, and therefore destabilize the cage? Further experiments have to plan to ask these interesting questions.

In our crystal structure, we unexpectedly found that the Box E can bind to the CHC TD site 1 (Figure 3-14C). This binding in our crystal differs from our biochemical experiments in which the Box E does not contribute the interaction too much (Figure 3-5A and 3-6D). Because we just had one packing form from all diffracted crystals, we could not confirm if

this binding is happened universally in different crystal packings. To examine this possibility, we could try different buffer conditions in the crystallization to get different packing forms. However, it is surprising that we do not see the Box A or B binds to the CHC TD site1. One possible reason is that the peptide that we used is too short from the N-terminus (from the residue 662). This short peptide only contains two amino acids before the Box A, and therefore it might reduce the binding to CHC. In order to compare the result from the pulldown (GTSE1-C1 fragment, N-terminus is from the residue 651, Figure 3-3C), we should use the same length from the N-terminus as we used for the pulldown. The short peptide in the crystal (only two residues before the Box A) might not be sufficient enough to bind the CHC site 1.

4.2 The CHC-GTSE1 complex in interphase

Here, we identify the CHC-GTSE1 interaction in not only mitosis but also interphase. It suggested that this interaction could be also important during interphase. More recently, CHC has been shown to control cell migration. One important stage in cell migration is the focal adhesion disassembly. A focal adhesion is a large protein complex that connects the cell to the extracellular environment. Integrin, a transmembrane protein that acts as a connector between cells and the substrate, is one of these components in focal adhesions (Parsons et al., 2010). Thus, the internalization of integrin is thought to be an important step during focal adhesion disassembly. CHC is known to recycle different integrins by its endocytosis function through which CHC enhances focal adhesion turnover. Therefore, CHC depletion leads to accumulate focal adhesions in cells and reduces cell motility (Chao and Kunz, 2009; Ezratty et al., 2009). In order to recycle these integrins, CHC has to physiologically localize at focal adhesions. Actually, some of CHC's adaptor proteins do localize at focal adhesions; for example Numb, which can further recruit CHC (Nishimura and Kaibuchi, 2007). However, this recruitment is hard to explain how CHC that is far away from focal adhesions can interact with Numb. Thus, CHC has to be transported next to focal adhesions and further be recruited. One possible mechanism to explain how CHC transportation works is by microtubules. Microtubule is shown to transport vesicles by using different cargo proteins. Interestingly, in fact, microtubules are known to target focal adhesions, suggesting that microtubules might bring some essential components to induce focal adhesion turnover while targeting (Ezratty 2005). However, CHC does not bind microtubules by itself, but CHC occasionally colocalizes with microtubules in interphase. Arrestin, which binds both CHC and microtubules, can act as a linker between them; therefore, arrestin knockout leads to an increase of the number and

size of focal adhesions and reduces cell mobility. Notably, CHC also binds much less microtubules by a cosedimentation assay in arrestin knockout cells (Cleghorn et al., 2015). These results well explained how microtubules could bring CHC to specific subcellular localization by CHC-interacting proteins. It raises a question: what if CHC can interact with +TIPs? Because +TIPs are usually accumulated on the plus end of microtubules, it might concentrate CHC on the microtubule tips. In our study, we identify the direct interaction between a +TIP, GTSE1, and CHC. In fact, this interaction is also detected in interphase (Figure 3-21A), and GTSE1 indeed plays roles in regulating cell migration. First, GTSE1 is overly expressed in different cancers and highly invasive cell lines (Scolz et al., 2012). Additionally, increasing GTSE1 level in cells by transfecting cDNA enhances cell migration and reduces the amount of focal adhesions (Figure s5-1F and G), although focal adhesion dynamics in this status have not be checked yet. Similarly, down-regulating GTSE1 expression following siRNA depletion significantly reduces cell mobility due to the accumulation of focal adhesions (Figure s5-1A and D) and a decrease of focal adhesion disassembly rate (Figure s5-1H and I).

Remarkably, we found that GTSE1 targets towards focal adhesions through its EB1-binding during microtubule-mediated targeting (Figure s5-2A). Interestingly, the tip-tracking activity of GTSE1 is essential for its roles in cell migration. A SXXP mutation on GTSE1, which abolishes the interaction with EB1 and does not accumulate on microtubule tips but still binds microtubule lattices, induces neither cell migration nor focal adhesion turnover (Scolz, 2012). This observation suggests that the tip-tracking activity is required for GTSE1-induced cell migration. One explanation is that GTSE1 might bring its interacting proteins to the sites while microtubules/GTSE1 target towards focal adhesions. Since GTSE1 interacts with CHC in interphase, we hypothesize that GTSE1 could “concentrate” CHC on focal adhesions while the microtubule targeting which induces the CHC-mediated focal adhesion disassembly. This might explain why the EB1-binding mutant of GTSE1, which binds microtubules and should not perturb the interaction with CHC, could not mediate the GTSE1-incuded cell migration (Scolz et al., 2012). Because this mutant does not enrich at microtubule tips, it might not “concentrate” CHC while microtubules target towards focal adhesions. Thus, CHC on the microtubule tips seems to be more important than transporting CHC along microtubules in regulating cell migration. The more CHC triskelia are accumulated at focal adhesions by +TIP while microtubule targeting, the more focal adhesions are disassembled. Notably, we also saw that CHC shows the tip tracking while co-overexpressed both CHC and GTSE1 in cells (data not shown). Even though CHC does not show the tip tracking in the endogenous

level, we could not rule out the possibility that only a little endogenous CHC is presented on the tip of microtubules. To confirm this hypothesis, we could isolate the focal adhesion fractionation and compare the amount of CHC between the WT and the SXXP mutant. Additionally, the CHC-GTSE1 interaction is also important to regulate cell migration. We found that the 5xLID mutant could not mediate GTSE-induced cell migration (Figure s5-2B). The possible mechanism is that the CHC-GTSE1 interaction is required for transporting CHC towards focal adhesions and therefore induces focal adhesion disassembly. Thus, it will be interesting to check the amount of CHC at focal adhesions by an IF or by the fractionation, and also examines the focal adhesion dynamics in the 5xLID mutant.

ACF7, another +TIP protein, has been shown in modulating cell migration (Wu et al., 2008; Wu et al., 2011). Interestingly, ACF7 is not only a microtubule-binder but also an actin-interacting protein (Yue et al., 2016). A proposed model of ACF7 in regulating cell migration is that it can physiologically cross-link microtubule and actin, guiding microtubules along actin filaments towards focal adhesions, and induces focal adhesion disassembly. Interestingly, GTSE1 can also bind to F-actin by the pulldown assay, suggesting that it might potentially cross-link actins and microtubules (Figure s5-3). However, GTSE1 does not seem to co-localize with actin filaments in cells by IF, and we did not check yet the organization of the actin network following GTSE1 depletion. Thus, to examine if GTSE1 is a real actin-binding protein, further experiments need to be performed; for example the flow cell assays. Based on observations in which GTSE1 shows accumulation on the tips and interacts with CHC and probably F-actin in interphase, a proposed mechanism is that GTSE1 might involved in guiding microtubules along F-actins to bring CHC to focal adhesions and induces CHC-mediated focal adhesion disassembly.

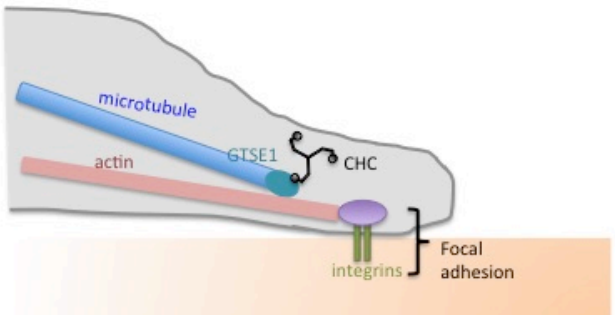

Figure 4-1. A proposed model of how GTSE1 regulates focal adhesion disassembly

GTSE1 guides microtubules to target towards focal adhesions along actin filaments. Additionally, GTSE1 interacts with CHC, which can bring CHC to focal adhesions. CHC can further recycle integrins and mediates focal adhesion disassembly.

4.3 How does the CHC-TACC3 complex specifically bind/stabilize K-fiber?

Neither CHC nor TACC3 binds microtubules by itself. Nevertheless, both of them localize to spindles in mitosis. One hypothesis is that this interacting-complex creates an interacting-surface to bind microtubules. However, it is an open question whether this complex is sufficient to bind microtubules. The two proteins plus Aurora A in the presence of ATP weakly bound to microtubules by a flow cell assay (Hood et al., 2013). On the contrary, this complex after phosphorylation by Aurora A does not seems to bind microtubules by the cosedimentation assay (Lin et al., 2010). Actually, the interaction between CHC and TACC3 recombinant proteins is never too strong in our hands. We can only detect this interaction by western blot as opposed to coomassie staining in pull-down assays. If these two proteins must bind together first and then interact with microtubule, the low affinity of this complex could explain why the microtubule binding is hard to see *in vitro*. Consistent with the idea, an artificial fusion of Clathrin and TACC3 (CLACC) should overcome the problem of their weak interaction (Hood et al., 2013). In fact, this fusion protein indeed localizes on spindle in cells. However, it is hard to distinguish whether this fusion binds microtubules directly or is recruited to spindles by other proteins in cells. Nevertheless, this fusion does not seem to bind microtubules in interphase. Actually, due to the fact that CHC only presents on K-fibers, the CHC-TACC3 might only bind to specific microtubules. Microtubules within K-fibers are undergone several modifications including polyglutamination, acetylation and detyrosination (Janke and Bulinski, 2011). These modifications indeed change the property of microtubules in terms of the binding affinity. For example, Kinesin-1 prefers to bind detyrosinated microtubules rather than tyrosinated microtubules (Reed et al., 2006). Thus, it would not be surprising if CHC only binds K-fibers because of these specific posttranslational modifications. This could be the reason why it is hard to detect the CHC-TACC3 complex binding microtubules *in vitro*. Recently, TACC3 has been shown to recruit a new player, PI3K-C2α, to spindles. Interestingly, this protein can bind both TACC3 and CHC and is required for CHC to localize to spindles. Thus, PI3K-C2α is important to stabilize or bridge the CHC-TACC3 complex together (Gulluni et al., 2017), and therefore further increases the microtubule binding affinity of the CHC-TACC3 complex. In our study, we showed that GTSE1 delocalizes from mitotic spindles following Hec1 depletion (Figure 3-17B). Additionally, GTSE1 is recruited by CHC to spindles (Figure 3-16A). These results strongly suggest that GTSE1 mainly presents on the K-fiber, and the CHC-TACC3 complex is required for this localization. It will be also interesting to see if the CHC-TACC3 complex or the CLACC fusion is able to recruit GTSE1 onto microtubules by the flow cell assay *in vitro*.

However, to choose right modifications of microtubules to bind the CHC-TACC3 complex might be a challenge.

GTSE1 itself is a microtubule binding protein and indeed binds microtubule lattices during interphase. Interestingly, it is highly phosphorylated during mitosis and almost completely loses its microtubule binding (Scolz et al., 2012), and we also comfirmed this results in our hands (Figure S5-4). Therefore, its spindle localization in mitosis is highly dependent on the CHC-TACC3 complex. However, it is still a debate if GTSE1 can not bind microtubule in metaphase due to the phosphorylation. In fact, we did see very little signal of the GTSE1-5xLID-GFP mutant on spindles (Figure 2-16A(iii)), and weak GTSE-WT-GFP staining on microtubules following Hec1 depletion (Figure 2-17B(v)). These data suggested that GTSE1 might not completely lose its entire microtubule binding in mitosis due to the phosphorylation. Actually, the transition between phosphorylation and dephosphorylation might be very dynamic and fast in cells although the major population of GTSE1 in metaphase is highly phosphorylated. Since we do not know yet which phosphorylation sites are corresponding to the microtubule binding, we can not rule out that once GTSE1 is slightly dephosphorylated in mitosis, it could bind microtubules again. This might well explain why GTSE1 is mainly localized on K-fibers and very weakly present on non-k-fiber microtubules in metaphase. However, this weak microtubule binding from the partially phospho-GTSE is not sufficient enough to stabilize spindle integrity by inhibiting MCAK. Thus, the 5xLID mutant, which almost delocalizes from entire spindles, leads to severe mitotic defects including abnormal bipolar spindles and misaligned chromosomes (Figure 3-16A(iii)).

It is interesting why cells use so much energy to phosphorylate GTSE1 and make it not bind microtubules directly in mitosis; however, the CHC-TACC3 complex later brings it back onto spindle microtubules again. It is indeed a matter if GTSE1 binds microtubule directly or indirectly. In fact, unphosphorylated purified-GTSE1 (1-460) proteins can bundle microtubules *in vitro* (Figure S5-5), suggesting that it is not only an intrinsic microtubule binder but also a microtubule stabilizer. Additionally, GTSE1 is more expressed during mitosis than interphase. Therefore, if large amounts of GTSE1 directly bind to microtubules and cause bundles of spindle microtubules, that perhaps affects the formation of normal bipolar spindle during mitosis. Therefore, GTSE1 has to indirectly bind to microtubules by the TACC3-CHC complex and stabilizes microtubules by inhibiting MCAK in mitosis.

4.4 The mitotic defects caused by 5xLID might be distinct from GTSE1 depletion.

In general, GTSE1 is mainly localized at centrosomes, spindle poles, K-fibers and little on kinetochores during mitosis. After GTSE1 depletion, MCAK becomes highly active at these places and destabilizes microtubules. Therefore, GTSE1 depletion leads to defects in astral microtubules, inner spindle intensity and microtubule-kinetochore attachment (Bendre et al., 2016). The GTSE1-5xLID is delocalized from spindles, but appears to retain some localization capacity from GTSE1-WT. It does not localize on K-fibers but it still interacts with kinetochores (Figure 3-18B) and probably localizes at poles. Due to that 5xLID does not present on K-fiber/spindles, this mutant is unable to inhibit MCAK activity and stabilizes spindle microtubules. Thus, we often saw abnormal bipolar spindles and misaligned chromosomes (Figure 3-16A(iii)). To confirm if these defects are due to the less microtubules density in the mutant, we can measure the microtubule intensity in the inner spindle by IF. Furthermore, if these defects are due to the problems of less stable microtubules, we should rescue these defects by adding low dose Taxol to stabilize microtubules. Additionally, we could not clearly detect the pole localization of the mutant because of the high cytosolic background by IF (Figure 3-16A(iii)). Conversely, GTSE1 can be clearly detected at poles following CHC depletion in live cells (Hubner et al., 2010). It suggested that the pole localization of GTSE1 is not dependent on CHC; therefore, the 5xLID mutant is unlikely to totally lose its pole localization. However, we can not rule out that the mutant presents much less at poles than the WT. Interestingly, we did see that astral microtubules are significantly shorter in the 5xLID mutant, indicating that the amount of 5xLID mutant at poles is insufficiently to inhibit MCAK activity (unpublished data). Another possibility is that GTSE1 has to interact with CHC in order to inhibit MCAK. It seems unlikely because GTSE1 alone is enough to do this job (Bendre et al., 2016). However, it will be interesting to see in the help of CHC if GTSE1 could increase the MCAK inhibition *in vitro*.

In fact, the 5xLID mutant still interacts with MCAK *in vitro*, and we could not see any remarkable changes of the interaction as comparing to the WT (Figure 3-26A). This result suggested that the 5xLID mutant might be able to inhibit the MCAK activity as well. Contrary to the *in vitro* result, this mutant binds much weaker *in vivo* confirmed by IPs (unpublished data). Is it simply because it does not present on spindle? Due to the absence of this mutant on spindles, the portion of the GTSE1-MCAK interaction on spindle is gone and therefore the total interactions are less in the mutant by IP. Another hypothesis is that the interaction between GTSE1 and MCAK is mediated by Aurora kinase A. Since the 5xLID mutant is unable to localize on spindles, it might get less phosphorylations by Aurora A that

reduces its interaction with MCAK. However, we did not have any evidences to support that the phosphorylation states are much less on this mutant. Since this mutant still interacts with MCAK and localizes on kinetochores after Aurora B phosphorylation (Figure 3-18 and 19), it should also inhibit MCAK activity on kinetochores. Therefore, this mutant should not have the microtubule-kinetochore attachment problem. To test that, we can deplete endogenous GTSE1 in U2OS-WT and U2OS-5xLID cells. Cells following GTSE1 depletion are then treated with Cdk1 inhibitor and synchronized in metaphase by MG132 for 2 hour. Within these 2 hour, cells should have enough time to align and congress chromosomes on the metaphase plates. If there is a microtubule kinetochore attachment problem, we should see misaligned chromosomes in cells under this setup. We will assume to see the defect in U2OS-WT but not in U2OS-5xLID cells following GTSE1 depletion. Additionally, our lab previously found that up-regulation of MCAK activity following GTSE1 depletion reduces hyper-stable microtubule-kinetochore attachments, which reduces lagging chromosomes in U2OS (Bendre et al., 2016). Since the GTSE1-5xLID mutant still localizes at kinetochores and interacts with MCAK, it should not reduce the hyper-stable microtubule-kinetochore attachments. Thus, it will be interesting to check the lagging chromosomes in U2OS expressing 5xLID mutant.

4.5 How does Aurora A kinase increase microtubule stability?

It has been shown that Aurora A overexpression leads to an increase in microtubule polymerization rates that induces hyper-stabilized microtubules and causes CIN (Ertych et al., 2014). Notably, hyper-stabilized microtubules and CIN can be rescued by partially depleting either TACC3 or ch-TOG, suggesting that this TACC3-ch-TOG complex might be the downstream effector of Aurora A (Ertych et al., 2014). ch-TOG is a microtubule polymerase and enhances microtubule stability by simply polymerizing microtubules. Additionally, the recruitment of ch-TOG onto spindle is dependent on TACC3 (Cheeseman et al., 2013; Gutierrez-Caballero et al., 2015); however, their interaction does not depend on Aurora A. Therefore, overexpression of Aurora A might not directly enhance their interaction. Remarkably, TACC3 is identified as a substrate of Aurora A (Kinoshita et al., 2005). As expected, while Aurora A is overexpressed, an increase in TACC3 phosphorylation is observed in different cell lines (Ertych et al., 2014). TACC3 interacts with CHC in an Aurora A dependent manner, which permits this complex to localize at spindles. Therefore, it highly suggests that more TACC3-CHC complexes are on spindles while increasing Aurora A expression. Even through Aurora A does not directly enhance the interaction between TACC3

and ch-TOG, forming more TACC3-CHC complexes by Aurora A can indirectly recruits more ch-TOG to spindles.

Furthermore, the TACC3-CHC complex can bring GTSE1, another microtubule stabilizer, to spindles. GTSE1 is an intrinsic microtubule binding protein in interphase. Surprisingly, once GTSE1 is phosphorylated by Aurora A, it significantly reduces the microtubule binding (Figure S5-4). Interestingly, the interaction between GTSE1 and MCAK is also mediated by Aurora A. Thus, once GTSE1 is phosphorylated by Aurora A, GTSE1 reduces its microtubule binding and bundling activity. In the meantime, Aurora A permits the TACC3-CHC complex on spindles, which further brings GTSE1 on spindles. The phospho-GTSE1 by Aurora A and then interacts and inhibits the MCAK-depolymerizing activity, by which GTSE1 indirectly stabilizes microtubules on spindles. In conclusion, one mechanism of how Aurora A stabilizes microtubules is to enhance the TACC3-CHC complex onto spindles as a central interacting hub. On one hand, TACC3 can recruit ch-TOG and the TACC3-ch-TOG complex could antagonize the MCAK-depolymerizing activity (Kinoshita et al., 2005). On the other hand, CHC can bring GTSE1 in which GTSE1 can further inhibit the MCAK activity in the Aurora A-dependent manner. Importantly, these interacting-networks are highly dependent on Aurora A kinase.

4.6 Can GTSE1 be a microtubule polymerase?

Proteins interacting with both tubulin dimer and microtubules can stabilize microtubules by different mechanisms. First, they can sit close to microtubule ends by the microtubule-binding activity and add new tubulin dimers, which increase microtubule growth rate; for example, ch-TOG. Additionally, some proteins do not add tubulin dimmers on tips but act as caps on microtubule ends due to the tubulin binding to inhibit catastrophes, which also promotes microtubule growth such as CPAP and CLASP (Al-Bassam et al., 2010; Sharma et al., 2016).

GTSE1 is a microtubule-binding protein (Scolz et al., 2012) and bundles microtubules under the non-phosphorylated state (Figure S5-4). Interestingly, we found that GTSE1 also binds tubulin dimers (Figure S5-6 left), but this activity is inhibited by phosphorylation (Figure S5-6 right). It supports the idea that GTSE1 might not directly increase microtubule stability by binding both tubulin dimers and microtubules during mitosis. Since GTSE1 could bind both microtubules and tubulin dimers in interphase, can GTSE1 be a microtubule polymerase or how can GTSE1 stabilize microtubules? To test if GTSE1 could act as a polymerase, we can incubate tubulin dimers with GTSE1 and see if GTSE1 can induce the microtubule polymerization by the microtubule turbidity assay. Additionally, we can immobilize

microtubule seeds on the flow cells and add tubulin dimers and GTSE1 proteins in solution. By tracing the dynamics of microtubules using the TIRF microscopy, we can quantify the dynamic events of microtubules. Although GTSE1 does not have any TOG domain, a HEAT loop (X-Trp-X-X-Arg-X) is presented on its N-terminal region (Ser-Ser-Trp-Gln-Ala-Lys-Arg-Val). The HEAT loop is well known to bind tubulin dimers, and mutations of Trp and Arg on this loop can totally abolish the binding with tubulin dimers (Slep, 2009). It will be interesting to mutate these two amino acids on GTSE1 and examines the tubulin binding. If this mutant prevents GTSE1 to bind tubulin dimers but not the microtubules, we can further compare the microtubule dynamics between WT and this mutant.

4.7 How does the microtubule-stabilizing complex stabilize/bridge microtubules in mitosis?

Here, we defined that the CHC-TACC3-ch-TOG-GTSE1 complex as a microtubule-stabilizing complex. Actually, both ch-TOG and GTSE1 are microtubule-binding proteins. Even through phospho-GTSE1 significant reduces its microtubule-binding, we can not rule out the partial microtubule binding activity that could slightly bundle and stabilize microtubules. Thus, it will be good to remove the microtubule-binding domain from GTSE1 and ch-TOG as well. In our work, we identified the minimal domain of GTSE1 (639-739) that binds CHC but not microtubules. The ch-TOG fragment (1806-2032) that we used for the pulldown assays does not bind microtubules either. We can also confirm that these short fragments can form a mini-complex by the pulldown (Figure 3-24). Thus, if this mini-complex of TACC3-CHC-GTSE1(fragment)-ch-TOG(fragment) can bind microtubules, this binding is mediated by the TACC3-CHC complex. Recently, this complex has been proposed to bundle microtubules after Aurora A phosphorylation (Nixon et al., 2015). However, it might be simply due to the partially microtubule-bundling activity from GTSE1. It will be interesting to use this mini-complex and see how it stabilizes microtubules i*n vitro*. Additionally, we can also visualize this complex with microtubules under the electron microscopy, which could also gain insight the structure of this microtubule-stabilizing complex.

5. Supplementary Figures

5.1 GTSE-mediated cell migration in interphase

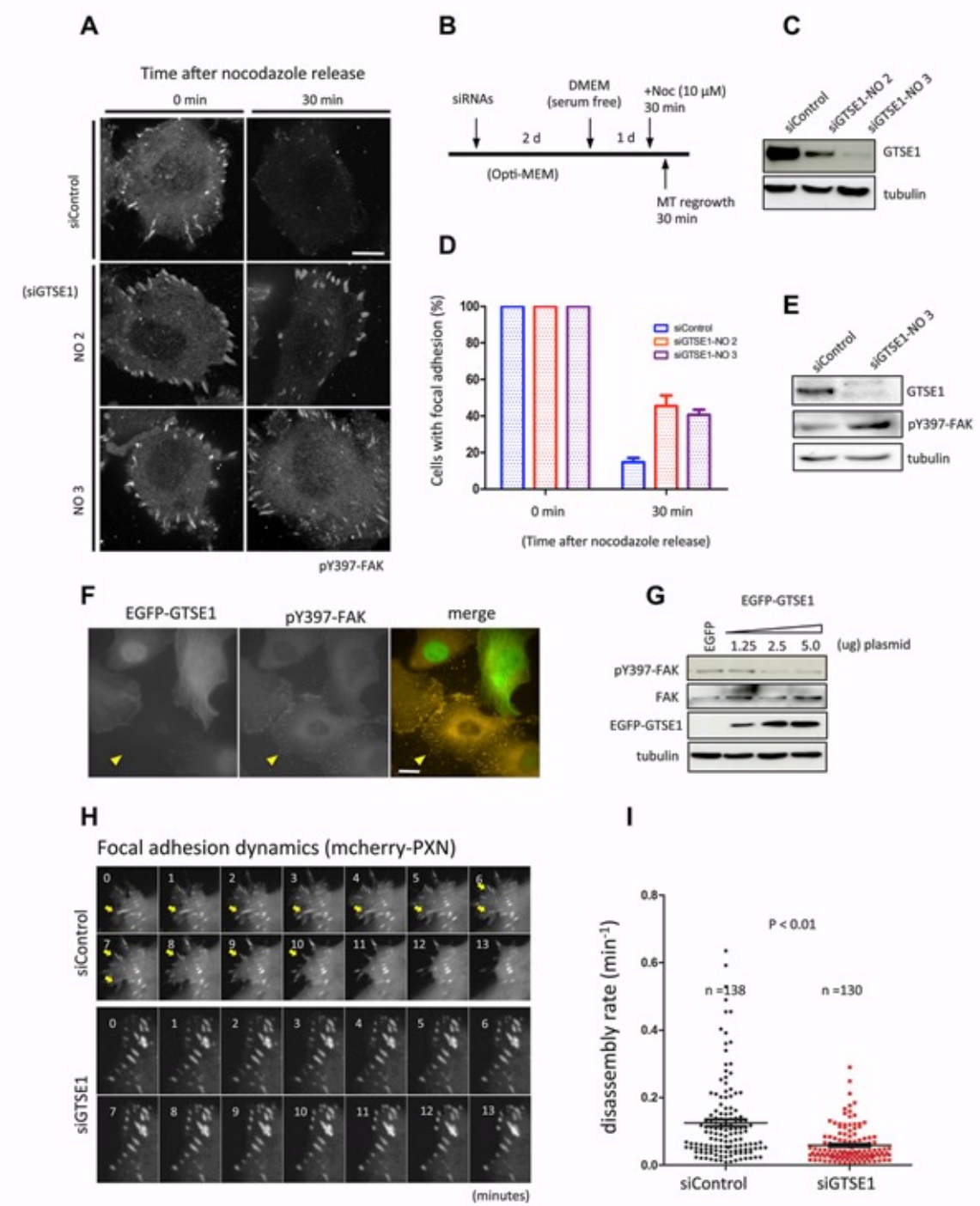

Figure s5-1. GTSE1 is required for focal adhesion disassembly

Microtubule-induced focal adhesion disassembly assay (A)(B)(D). (A) immunofluorescence of pY397- FAK (a marker of focal adhesions) in control siRNA (siControl) and GTSE1-depleted (siGTSE1) HT1080 cells. Imagines were taken at 0 and 30 minute after nocodazole washed out and microtubule regrowth. (B) A protocol shows the method of GTSE1 depletion and microtubule regrowth. (C) Two siRNAs (NO 2 and NO 3) are used against GTSE1. Western blot showed GTSE1 protein level after the depletion in HT1080 cells. (D) Quantitative analysis of focal adhesions in either

siControl or siGTSE1 cells. Cells were scored positive if they retained more than 10 pY397-FAK staining after nocodazole release (n=100 in triplicate). GTSE1 protein level is inversely correlated with focal adhesion amount (E)(F)(G). (E) Depletion of GTSE1 increases the amount of focal adhesions in asynchronized HT1080 cells. Overexpression of GTSE1 reduced the amount of focal adhesions in HT1080 cells shown in (F) and (G). (F) immunofluorescence of pY397-FAK in EGFP-GTSE1 transient transfected HT1080 cells. Yellow arrow showed the dynamics of focal adhesions. (G) Western blot showed pY397 FAK protein levels in either EGFP- or EGFP-GTSE1 transient transfected cells. GTSE1 regulates focal adhesion dynamics (H)(I). (H) Representative time-lapse images of mcherry-paxillin following Control or GTSE1 depletion in HT1080 cells, Yellow arrow shows individual focal adhesion undergoing disassembly. (I) Quantitative analysis of the disassembly rate of focal adhesions. Each dot represents individual focal adhesion. The disassembly rate of focal adhesions is reduced in GTSE1 depleted HT1080 cells (two independent experiments).

5.2 GTSE targets towards focal adhesions, and the CHC-binding is required for GTSE1-induced cell migration.

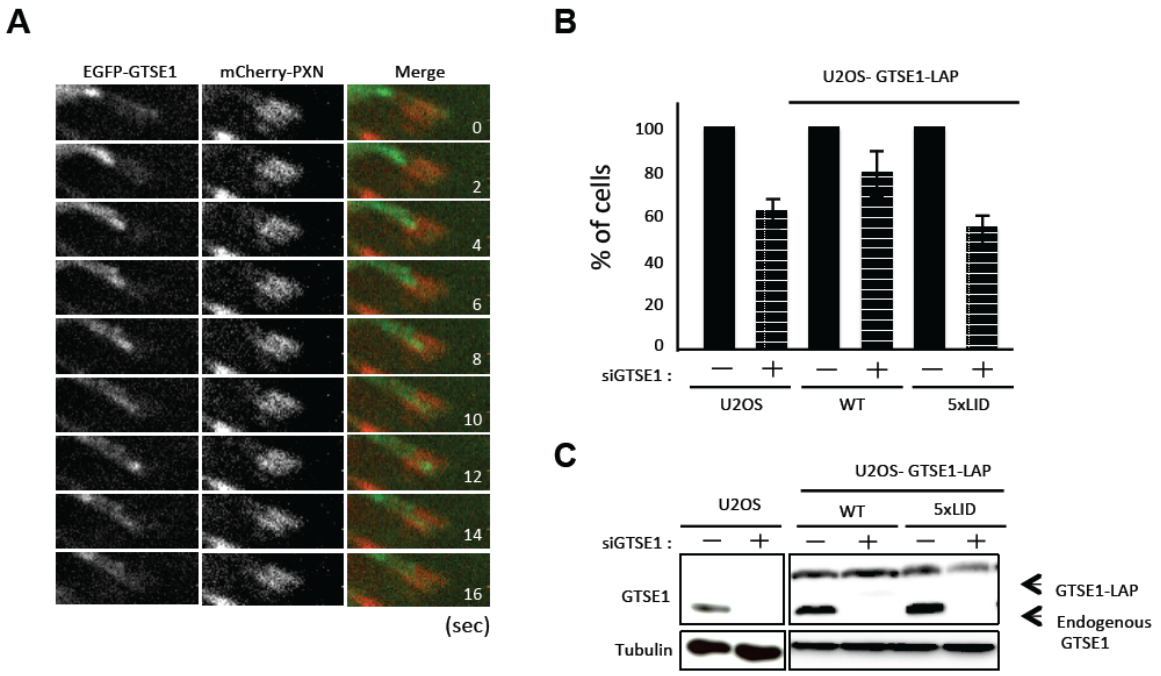

Figure s5-2. GTSE1 targets towards focal adhesions and regulates cell migration through a cooperation with CHC

(A) Time-lapse images of EGFP-GTSE1 showing that GTSE1 targets focal adhesions. mcherry-paxillin was used as a marker for focal adhesions (B) Transwell migration assay in U2OS cells, and U2OS cells stably expressing RNAi-resistant GTSE1-WT-GFP, or RNAi-resistant GTSE1-5xLID-GFP. Cells were treated with or without GTSE1 siRNA for 48 h and seeded on transwell membranes for 16 h. Error bars represent the standard error of the mean from two independent experiments. (C)

Western blots were performed on cells after the same treatment, and blotted with anti-GTSE1 and anti-tubulin.

5.3 GTSE1 binds F-actin

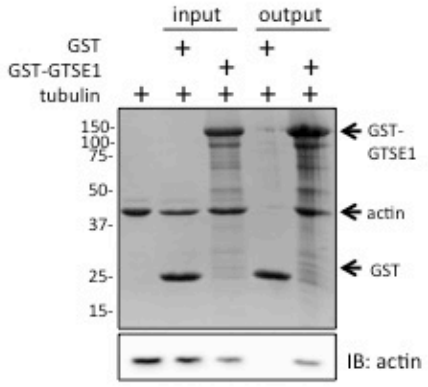

Figure s5-3. GTSE1 binds F-actin

Two μM GST-GTSE1-FL or GST proteins were immobilized on the GSH beads and incubated with 2 μM F-actin in 50 μl F-actin binding-buffer at 4°C for 2 hour. 5 % of each reaction was taken as input. Beads were washed 3 times with F-actin binding buffer and indicated as output. Samples were analyzed by a SDS-page and western blot. GST-GTSE1 could pull down F-actin shown by the SDS-page and western blot against anti-actin antibodies.

5.4 GTSE1 reduces the microtubule-binding after Aurora A phosphorylation

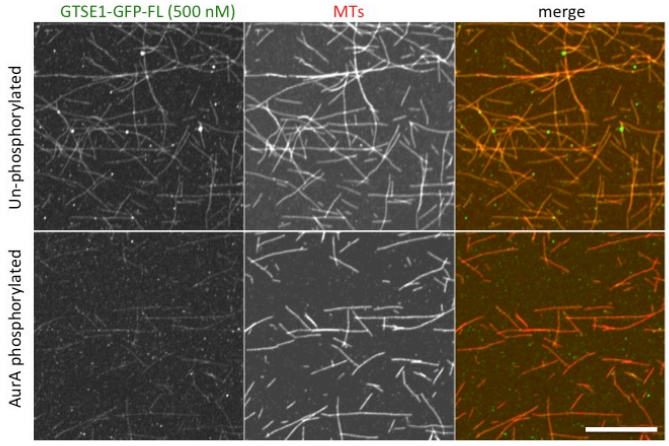

Figure s5-4. GTSE1 reduces its microtubules-binding after Aurora A phosphorylation

GTSE1-GFP-FL proteins were phosphorylated with or without Aurora A kinase and performed the flow cells assay. Upper panel; 500 nM of un-phosphorylated proteins were add into the flow cell and imagined after 10 min. GTSE1-GFP-FL strongly bound to microtubules. However, phospho-GTSE1 significantly reduced its microtubule binding after Aurora A phosphorylation shown in the lower panel.

5.5 GTSE1 (1-460) bundles microtubules

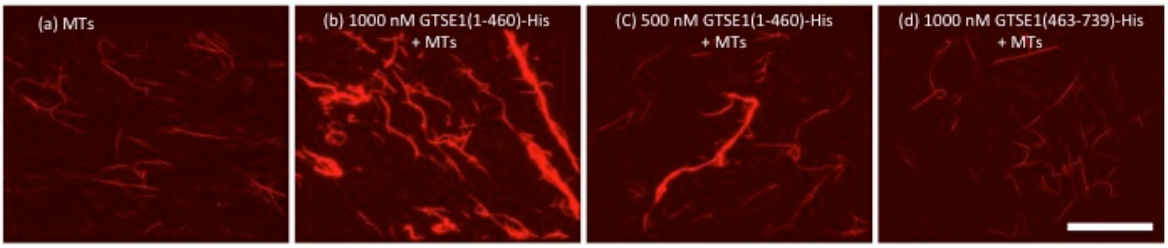

Figure s5-5. GTSE1 (1-460) bundles microtubules

Two nM of Rhodamine-labelled microtubules were incubated with GTSE1 (1-460) or (463-739) at room temperature for 10 min. Reactions were terminated by adding 0.2 % glutaraldehyde and fixed on slides. GTSE1 (1-460) could induce microtubule bundling in different concentrations; however, GTSE1 (463-739) has no effect on microtubule bundling.

5.6 GTSE1 loses tubulin binding after phosphorylation.

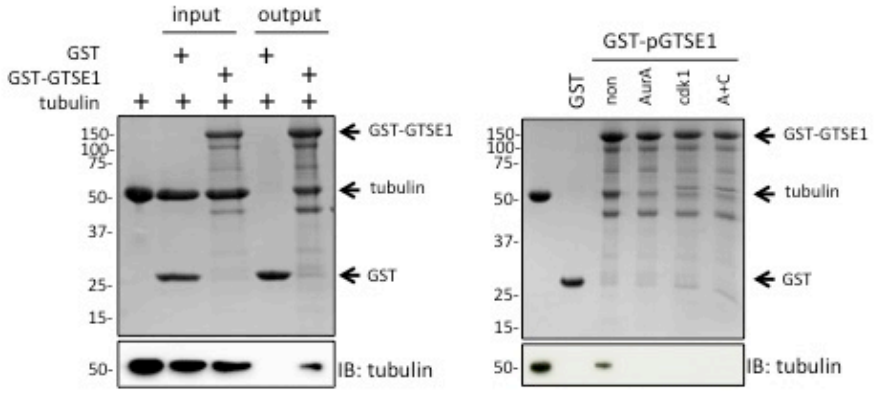

Figure s5-6. GTSE1 significantly reduces the tubulin binding after the phosphorylation

Left; GTSE1 binds tubulin dimer. Two μM GST-GTSE1-FL or GST proteins were immobilized on the GSH beads and incubated with 2 μM tubulin in 50 μl BRB buffer at 4°C for 2 hour. 5 % of each reaction was taken as input. Beads were washed 3 times with BRB buffer and indicated as output. Samples were analyzed by a SDS-page and western blot. GST-GTSE1 could pull down tubulin dimmer indicated by the SDS-page and western blot against anti-tubulin antibodies. Right; Phosphorylated GTSE1 by Aurora A and cdk1 strongly reduces the tubulin binding. 2 μM GST-GTSE1-FL proteins were phosphorylated by either Aurora A (AurA), cdk1 or Aurora A plus cdk1 (A+C). The phosphorylated or non-phosphorylated GTSE1 proteins were incubated with tubulin and performed pulldowns. Pulldowns were analyzed by a SDS-page and western blot.

6. Materials and Methods

6.1 Chemicals and Solutions

Table 6-1. List of chemicals and solutions

Chemical Name	Ingredients	Company
Agarose		Carl Roth GmbH, Karlsruhe, Germany
Ammonium persulfate (APS)		Max-Planck-Institute, Dortmund, Germany
Ampicillin sodium salt		GERBU Biotechnik GmbH; Heidelberg; Germany
Blasticidine		Invitrogen, California, U.S.A
Bradford Solution		Bio-Rad Laboratories GmbH, Munich, Germany
BRB80 Buffer	80 mM Pipes-KOH pH 6.9 1 mM EGTA 1mM $MgCl_2$ 150 mM KCl 10 μM ATP 1 mM TCEP	Sigma-Aldrich GmbH, Steinheim, Germany Thermo Fisher Scientific, Waltham, U.S.A J.T Baker Chemicals, Center Valley, USA Avantor Performance Materials (J.T. Baker), Center Valley, U.S.A. Sigma-Aldrich GmbH, Steinheim, Germany Biosynth AG; Staad; Switzerland
Buffer A	50 mM HEPES pH 7.5 300 mM NaCl 5% Glycerol	Sigma-Aldrich GmbH, Seelze, Germany VWR Chemicals, Darmstadt, Germany GERBU Biotechnik GmbH,

		Heidelberg, Germany
	2 mM TCEP	Biosynth AG; Staad; Switzerland
Cdk1 inhibitor (RO-3306)		Calibiochem
Cell Lysis Buffer	50 mM HEPES pH7.2	Sigma-Aldrich GmbH, Seelze, Germany
	50 mM Na_2HPO_4,	Avantor Performance Materials (J.T. Baker), Center Valley, U.S.A
	150 mM NaCl	VWR Chemicals, Darmstadt, Germany
	10% glycerol	GERBU Biotechnik GmbH, Heidelberg, Germany
	1% Triton X-100	Thermo Fisher Scientific, Waltham, U.S.A
	1 mM EGTA	Thermo Fisher Scientific, Waltham, U.S.A
	1.5 mM $MgCl_2$	J.T Baker Chemicals, Center Valley, USA
CO_2 Independent Medium		Thermo Fisher Scientific (Gibco), Waltham, U.S.A.
Coomassie Brilliant Blue staining solution	10% Acetic acid	Sigma-Aldrich GmbH, Hamburg, Germany
	2.5% Coomassie G250	Serva GmbH, Heidelberg, Germany
Destaining solution for ProQ Diamond staining	20% Acetonitrile	Fisher Scientific, UK
	50 mM Sodium acetate	Sigma-Aldrich GmbH, Steinheim, Germany
Dimethyl sulfoxide (DMSO)		SERVA Electrophoresis GmbH, Heidelberg, Germany
Disodium phosphate(Na_2HPO_4)		Avantor Performance Materials (J.T. Baker), Center Valley, U.S.A.

Dithiothreitol (DTT)		SERVA Electrophoresis GmbH, Heidelberg, Germany
DNA Loading Buffer (6x)	0.4% Orange G 30% Glycerol 10 mM Tris-HCl 25 mM Ethylenediaminetetraacetic acid (EDTA)	Sigma Aldrich, Hamburg, Germany GERBU Biotechnik GmbH, Heidelberg, Germany Carl Roth, Karlsruhe, Germany GERBU Biotechnik GmbH, Heidelberg, Germany
Dulbecco's Modified Eagle's Medium (DMEM)		PAN Biotech, Aidenbach, Germany
Dynabeads Protein G magnetic beads		Invitrogen GmbH, Karlsruhe, Germany
ECL prime Western blotting detection reagent		GE Healthcare, Freiburg, Germany
Effectene transfection reagent		QIAGEN GmbH, Hilden, Germany
Ethanol		Sigma-Aldrich GmbH, Seelze, Germany
Fetal Bovine Serum		Thermo Fisher Scientific (Gibco), Waltham U.S.A.
Fixing solution for ProQ Diamond staining	50% Methanol 10% Acetic acid	Sigma-Aldrich GmbH, Steinheim, Germany Sigma-Aldrich GmbH, Steinheim, Germany
FuGENE® HD Transfection Reagent		Promega GmbH, Mannheim, Germany
GeneRuler 1 kb Plus DNA		Fermentas, Hennigsdorf, Germany
Gentamycin		Sigma-Aldrich GmbH, Seelze, Germany

GSH Amintra Glutathione Resin		Amintra, Cambridge, UK
GST-Binding buffer	25 mM HEPES pH 7.5 300 mM NaCl 1 mM EDTA 5% Glycerol 1% Triton X-100 DNase	Sigma-Aldrich GmbH, Seelze, Germany VWR Chemicals, Darmstadt, Germany GERBU Biotechnik GmbH, Heidelberg, Germany GERBU Biotechnik GmbH, Heidelberg, Germany Thermo Fisher Scientific, Waltham, U.S.A Sigma-Aldrich GmbH, Seelze, Germany
HEPES		Sigma-Aldrich GmbH, Seelze, Germany
Isopropyl β-D-1-thiogalactopyranosid (IPTG)		Carl Roth, Karlsruhe, Germany
Imidazole		Merck Millipore, Darmstadt, Germany
Kanamycin		GERBU Biotechnik GmbH; Heidelberg; Germany
L-Glutamine		Thermo Fisher Scientific, Waltham, U.S.A.
L-Glutathion reduced		Biochemica, Darmstadt, Germany
Laemmli SDS Sample loading buffer (5X)	4% Sodium dodecyl sulfate (SDS) 10% Glycerol 1% 2-Beta mercaptoethanol 0.02% Bromophenol Blue	Sigma-Aldrich GmbH, Steinheim, Germany GERBU Biotechnik GmbH, Heidelberg, Germany Thermo Fisher Scientific, Waltham, U.S.A Sigma Aldrich, Hamburg,

	50 mM Tris-HCl	Germany Carl Roth GmbH, Karlsruhe, Germany
Lipofectamine 2000 Reagent		Invitrogen GmbH, Karlsruhe, Germany
Luria-Bertani medium (LB medium)	1% Peptone 0.5% Yeast extract 0.5% NaCl	Sigma Aldrich, Hamburg, Germany GERBU Biotechnik GmbH, Heidelberg, Germany VWR Chemicals, Darmstadt, Germany
Methanol		Sigma-Aldrich GmbH, Steinheim, Germany
Midori Green DNA Stain		Nippon Genetics Europe GmbH, Düren, Germany
Milk powder		Carl Roth, Karlsruhe, Germany
MLN8054		Sigma-Aldrich GmbH, Seelze, Germany
Nickel-NTA-Superose Beads		GE Healthcare, Freiburg, Germany
BioTrace Nitrocellulose Membrane		Pall Life Sciences, Pensacola, Florida, USA
Nocodazole		Sigma-Aldrich GmbH, Steinheim, Germany
OptiMEM		Invitrogen GmbH, Karlsruhe, Germany
Oligofectamine		Invitrogen GmbH, Karlsruhe, Germany
Paraformaldehyde (PFA, 16%)		Thermo Scientific, Rockford, USA
Penicillin Streptomycin		PAN-Biotech GmbH, Aidenbach, Germany
Phenylmethylsulfonyl-fluorid (PMSF)		Serva Electrophoresis GmbH, Heidelberg, Germany

Phosphate buffered saline (PBS)	137 mM Sodium chloride 2.7 mM Potassium chloride 10 mM Di-Sodium hydrogen phosphate dihydrate 2 mM Potassium dihydrogen-phophate (0.2 g/l)	VWR Chemicals, Darmstadt, Germany J.T.Baker Chemicals, Center Valley, USA Merck Millipore, Darmstadt, Germany AppliChem GmbH, Darmstadt, Germany
Poly-L-Lysin		Sigma Aldrich, Hamburg, Germany
Potassium chloride (KCl)		Avantor Performance Materials (J.T. Baker), Center Valley, U.S.A.
Precision Plus Protein unstained standards		Bio-Rad, Munich, Germany
Precision Plus Protein prestained standards		Bio-Rad, Munich, Germany
ProLong® Gold antifade mounting solution with DAPI		Molecular Probes, Life technology
ProQ Diamond Phosphoproetin gel stain		Invitrogen, Molecular probes, Eugene, Oregon, USA
Protease Inhibitor mix (500X)		Serva GmbH, Heidelberg, Germany
Pull-down buffer	20 mM HEPES pH 6.9 150 mM NaCl 1 mM ATP	Sigma-Aldrich GmbH, Seelze, Germany VWR Chemicals, Darmstadt, Germany Sigma-Aldrich GmbH, Steinheim, Germany
Sf-900 III medium		Thermo Fisher Scientific Gibco, Waltham, U.S.A.

SDS PAGE electrophoresis buffer	25 mM Tris-HCl 200 mM Glycin 3.5 mM SDS	Carl Roth, Karlsruhe, Germany Sigma Aldrich, Hamburg, Germany Carl Roth, Karlsruhe, Germany
Size Exclusion Chromatography (SEC) buffer	20 mM HEPES pH 6.9 150 mM NaCl 5% Glycerol 1mM TCEP 10 μM ATP	Sigma-Aldrich GmbH, Seelze, Germany VWR Chemicals, Darmstadt, Germany GERBU Biotechnik GmbH, Heidelberg, Germany Biosynth AG; Staad; Switzerland Sigma-Aldrich GmbH, Steinheim, Germany
Taxol		Sigma-Aldrich GmbH, Steinheim, Germany
TCEP (tris(2-carboxyethyl)phosphine)		Biosynth AG; Staad; Switzerland
Tris-Acetate-EDTA (TAE) buffer (50X)	50 mM Tris-Base 57.1 ml Glacial acetic acid 0.5 M EDTA (pH 8)	Carl Roth, Karlsruhe, Germany Sigma-Aldrich GmbH, Hamburg,Germany GERBU Biotechnik GmbH, Heidelberg, Germany
Tetramethylethylenediamine (TEMED)		SERVA Electrophoresis GmbH, Heidelberg, Germany
Tertracycline		Sigma-Aldrich GmbH, Steinheim, Germany
Thymidine		Sigma-Aldrich GmbH, Steinheim, Germany
Triton X-100		Thermo Fisher Scientific, Waltham, U.S.A.
Trypan blue solution		Thermo Fisher Scientific,

(0.4 %)		Waltham, U.S.A.
Trypsin-EDTA		PAN-Biotech GmbH, Aidenbach, Germany
Tween-20		SERVA Electrophoresis GmbH, Heidelberg, Germany
Wash buffer for pull-downs	20 mM HEPES 500 mM NaCl 5% Glycerol 0.1% Triton X-100 1mM TCEP	Sigma-Aldrich GmbH, Seelze, Germany VWR Chemicals, Darmstadt, Germany GERBU Biotechnik GmbH, Heidelberg, Germany Thermo Fisher Scientific, Waltham, U.S.A Biosynth AG; Staad; Switzerland
Western transfer buffer	25 mM Tris 190 mM Glycin 10 % Methanol	Carl Roth, Karlsruhe, Germany Carl Roth, Karlsruhe, Germany Sigma Aldrich, Hamburg, Germany
X-Galactoside		Sigma-Aldrich GmbH, Steinheim, Germany
β-Mercaptoethanol		Serva Electrophoresis GmbH, Heidelberg, Germany

6.2 Instruments and devices

Table 6-2. List of instrument and devices

Device	Model	Company
-80° freezer	MDF-U5386S	SANYO Electric Co., Ltd.; Moriguchi, Japan
Cell Counter	Countess	Invitrogen GmbH, Karlsruhe, Germany
Cell Counter	Scepter Handheld Automated Cell counter 2.0	Merck Chemicals GmbH; Darmstadt; Germany

Centrifuge	Mini Spin plus	Eppendorf GmbH; Wesseling-Berzdorf; Germany
Centrifuge	5418	Eppendorf GmbH; Hamburg Germany
Centrifuge	5417 R	Eppendorf GmbH; Wesseling-Berzdorf; Germany
Centrifuge	5804 R	Eppendorf GmbH; Wesseling-Berzdorf; Germany
Centrifuge	Avanti J-20 XP	Beckman and Coulter GmbH; Krefeld, Germany
Centrifuge	Allegra J-30 I New	Beckmann and Coulter GmbH; Engelsdorf, Germany
Centrifuge (high speed)	Avanti J-30 I Old	Beckman and Coulter GmbH; Krefeld, Germany
Cryogenic Freezer	MDF-1156-PE Ultra Low Temperature Freezer	Panasonic Biomedical Sales Europe B.V
DNA Electrophoresis Unit	CRHU10, Min-Plus Horizontal	Carl Roth, Karlsruhe, Germany
Electrophoresis power supply	Power SourceTM 300V	VWR International GmbH; Langenfeld; Germany
Flake ice machine	AF 100	Scotsman Ice Systems; Milan; Italy
Fluorescence Microscopy	EVOS® FL Imaging System	Life Technologies; Thermo Fisher Scientific, Waltham, U.S.A.
Freezer -20 °C	LGex 3410 MediLine	Liebherr-Elektronik GmbH; Lindau; Deutschland
Freezer -20 °C	LGUex 1500 MediLine	Liebherr-Elektronik GmbH; Lindau; Deutschland
Fridge 4 °C	LKexv 1800	Liebherr-Elektronik GmbH; Lindau; Deutschland
Fridge 4 °C	LKUexv 1610 MediLine	Liebherr-Elektronik GmbH; Lindau; Deutschland
Imaging System	ChemiDoc MP	Bio-Rad Laboratories GmbH, Munich, Germany
Incubator	Heraeus B6030	Thermo Electron LED GmbH;

		Langenselbold Germany
Incubator CO_2-DH Autoflow	NU-5500	NuAir
ibidi Imaging chamber	15 µ-Slide 8 well	iBidi, Martinsried, Germany
ibidi Imaging chamber	µ-Dish 35 mm dish	iBidi, Martinsried, Germany
Incubator shaker	Multitron Standard	Infors HAT AG; Bottmingen; Switzerland
Incubator shaker	Minitron	Infors HAT AG; Bottmingen; Switzerland
Mini Rocker Shaker	MR1	BioSan
PCR cycler	T3000 Thermocylcer	Biometra GmbH; Göttingen; Germany
Photometer	NanoDrop 2000	Thermo Electron LED GmbH; Langenselbold Germany
Photometer	Biophotometer 6131	Eppendorf GmbH; Wesseling-Berzdorf; Germany
SDS Page Electrophoresis Unit	Mini Protean Tetra Cell	Biorad, China
Scale	BL150 S	Sartorius
Scale	PE 3600	Mettler
See-saw rocker	SSL4	Bibby Scientific Limited; Staffordshire; UK
Sonicator	Sonifier 450	Branson Ultraschall- Emerson Technologies GmbH; Dietzenbach; Germany
Sterile bench	Herasafe™ KS	Thermo Electron LED GmbH; Langenselbold Germany
Sterile Bench	NU-437 (Nuaire)	Ibs tecnomara GmbH; Fernwald; Germany
Thermostat-Metal	Techne Dri-Block D13.3	Germany
Thermostat	BT 100	Kleinfeld Labortechnik, Germany
Thermostat	MBT 250	ETG-Ilmenau; Illmenau; Germany
Thermomixer	Thermomixer comfort	Eppendorf GmbH; Wesseling-Berzdorf;

		Germany
Thermomixer	Thermomixer 5436	Eppendorf GmbH; Wesseling-Berzdorf; Germany
Ultracentrifuge Optimal TL	TL361547	Beckman Coulter
Vortex	Vortex-Genie 2	Scientific Industries, Inc; New York; U.S.A.
Water bath	WNB7	Memmert (Shanghai) Trading Co. Ltd; Shanghai City; China
Waterbath	TW8	Julabo
Western Blot electrophoresis chamber	Mini Protean II ™	Biorad, Italy

6.3 Cloning using restriction enzyme digestion and ligation.

Primers are attached with restriction enzyme sequence corresponding to the targeted vectors. Genes of interest were amplified by PCR using Q5 2X Master Mix. To clean DNA after PCR, DNA was purified using PCR clean up kit after and digested by restriction enzymes for few hour or overnight at 37 °C. DNA was purified again by PCR clean up kit before ligation.

Table 6-3. Standard program for PCR amplification

Step	Temperature	Time	
Denaturation	98 °C	2 min	
	98 °C	30 s	30-35x
Annealing	52 °C – 65 °C	30 s	
Elongation	72 °C	1 -3 min (10 min for site-direct mutagenesis)	
	72 °C	5 min	
Pause	4 °C	~	

Table 6-4. Standard scheme for ligation

Component	Volume for 10 µL ligation reaction
Vector:Insert	1:3 (molar ratio)

T4 DNA Ligase	1 μL
5X T4 Ligase Buffer	2 μL
ddH_2O	X μL

6.4 Transformation

The competent cells were placed on ice to thaw. The plasmid DNA was incubated with competent cells for 5 min on ice and then perfromed heat shock at 42 °C for 45 sec. 1ml fresh LB medium was added into bacterial cells following heat shock, and incubated at 37 °C with shaking for 1 hour before plating on LB agar plates containing antibiotics.

Table 6-5. List of competent cells for transformation

Bacteria	Strain	Company
E. coli	Rosetta 2(DE3)	Max-Planck Institute, DPF, Dortmund, Germany.
E. coli	OmniMax (chemically competent cells)	Max-Planck Institute, DPF, Dortmund, Germany.
E. coli	Top10 (chemically competent cells)	Thermo Fisher Scientific (Gibco), Waltham, USA
E. coli	Max Efficiency DH10Bac™ Chemically competent cells (EMBACY)	Thermo Fisher Scientific (Gibco), Waltham, USA

Table 6-6. List of DNA constructs, vectors and primers

Construct name	Vector & company	Primers (5'-3')
pGEX-6p-1 CHC 1-330	pGEX-6p-1 GE healthcare	Fwd-aaaGGATCCATGGCCCAGATTCTGCCAATTCGT Rev-aaaGTCGACTTCCACACACACTGACAGAACTTG
pGEX-6p-1 CHC 1-364	pGEX-6p-1 GE healthcare	Fwd-aaaGGATCCATGGCCCAGATTCTGCCAATTCGT Rev-aaaGTCGACTTAAAAGAGTTCTTCAGCACCGG (STOP)
pGEX-6p-1 CHC	pGEX-6p-1 GE	Fwd-aaaGGATCCATGGCCCAGATTCTGCCAATTCGT

1-642	healthcare	Rev- aaaGTCGACGTGAACCACTGCACGTTTTAT
pET28a- GTSE1 (1-460)	pET28a (+) Novagen	Fwd- aaaGGATCCATGGAAGGAGGCGGCGGCCG Rev- aaaGTCGACTGTCTTGGAATTTAGACAGGAA
pET28a- GTSE1 (463-739)	pET28a (+) Novagen	Fwd- aaaGGATCCATGCCTACTCCTACAAATCA Rev- aaaGTCGACGAACTTGAGGAGTGGGGAAT
pET28a- GTSE1 (639-739)	pET28a (+) Novagen	Fwd- aaaGGATCCATGGCCCCTAGTGAGGCTCTTCT Rev- aaaGTCGACGAACTTGAGGAGTGGGGAAT
pGEX-6P- 1-GTSE1-C (639-739)	pGEX-6p-1 GE healthcare	Fwd- aaaGGATCCATGGCCCCTAGTGAGGCTCTTCT Rev- aaaGTCGACTTAGAACTTGAGGAGTGGGGA (stop)
pGEX-6P- 1-GTSE1- C1 (652- 687)	pGEX-6p-1 GE healthcare	Fwd- aaaGGATCCCCACTCGCGGTCACTCCAGAT Rev- aaaGTCGACCTACCTGCTTTCAGATCCTACA (stop)
pGEX-6P- 1-GTSE1- C2 (672- 708)	pGEX-6p-1 GE healthcare	Fwd- aaaGGATCCTTCTGCGATACCCCAGAAG Rev- aaaGTCGACTTACGGTGAAGGTTTGGCCACATTTT (stop)
pGEX-6P- 1-GTSE1- C3 (693- 739)	pGEX-6p-1 GE healthcare	Fwd- aaaGGATCCATGGAAGGAGGCGGCGGCCGCGAT Rev- aaaGTCGACTTAGAACTTGAGTGGGGAATCCAC (STOP)

6.5 Site-direct mutagenesis

Mutations were generated by site-direct mutagenesis using Q5 2X Master Mix. Wild-type plasmids were used as templates for DNA amplification. The PCR products were digested by DpnI for 2 hour and then performed transformation.

Table 6-7. List of mutants and primers

Construct name	Original template	Primers (5'-3')
pGEX-6p-1 CHC 1-330 (S1M)	pGEX-6p-1 CHC 1-330	T87A_Q89A_Fwd AAGCTCTTGCGATTTTTAACATTGAAA T87A_Q89A_Rev AAATCGCAAGAGCTTTCCCAGCTTTCAGT K96E_K98E_Fwd AAATGGAAAGTGAAATGAAGGCTCATA K96E_K98E_Rev TTCATTTCACTTTCCATTTCAATGTTAAAAA
pGEX-6p-1 CHC 1-330 (S2M)	pGEX-6p-1 CHC 1-330	Q152L_I154Q_Fwd TGCCTGATTCAAAATTACCGTACAGATGCA Q152L_I154Q_Rev GTAATTTTGAATCAGGCACCCTGCAAGGCTAGAA
pGEX-6p-1 CHC 1-330 (S3M)	pGEX-6p-1 CHC 1-330	R188A_Q192A_Fwd TGCGAAAGTGTCTGCGCCCATTGAAGGACATGC R188A_Q192A_Rev GGGCGCAGACACTTTCGCATCTACAGAATATAGCTGCAT
pGEX-6P-1-GTSE1-C1 (652-687) A	pGEX-6P1-GTSE1-C1 (652-687	Fwd- AAGCCAGCCCGCCGCTGCCCTTCCTCTCATCGACTTCTGCG Rev- GAAGGGCAGCGGCGGGCTGGCTTGCAGCATCTGGAG
pGEX-6P-1-GTSE1-C1 (652-687) B	pGEX-6P-1-GTSE1-C1 (652-687	Fwd- CCTGCCGCCGCCTTCTGCGATACCCCAGAAGCA Rev- AGAAGGCGGCGGCAGGAAGGTCAATGAGGGGCTGGCT

pGEX-6P-1-GTSE1-C1 (652-687) AB	pGEX-6P-1-GTSE1-C1 (652-687	Fwd-CCCGCCGCTGCCCTTCCTGCCGCCGCCTTCTGCGATACCCCAGA Rev-AAGGCGGCGGCAGGAAGGGCAGCGGCGGGCTGGCTTGCAGCATCT
pGEX-6P-1-GTSE1-C3 (693-739) D-LID	pGEX-6P-1-GTSE1-C3 (693-739)	Fwd-CCGCAGCCCTGAGCTCCCCTCTGATCCAGCTGA Rev-GGAGCTCAGGGCTGCGGCCTGTCCCACCACCGGT
pGEX-6P-1-GTSE1-C3 (693-739) D-IDL	pGEX-6P-1-GTSE1-C3 (693-739)	Fwd-GGACAGCTCGCAGCCGCGAGCTCCCCTCTGATCC Rev-GGGGAGCTCGCGGCTGCGAGCTGTCCCACCACCGGT
pGEX-6P-1-GTSE1-C3 (693-739) D-LIDxL	pGEX-6P-1-GTSE1-C3 (693-739)	Fwd-GGGACAGGCCGCAGACGCGAGCTCCCCTCTG Rev-AGCTCGCGTCTGCGGCCTGTCCCACCACCGGT
pGEX-6P-1-GTSE1-C3 (693-739) E	pGEX-6P-1-GTSE1-C3 (693-739)	Fwd-CTCCCCTGCGGCCGCGCTGAGCCCTGAGGCTGA Rev-AGGGCTCAGCGCGGCCGCAGGGGAGCTCAGG

6.6 Cloning using Gibson Assembly

Gibson Master mix which contains dNTPs, T5 exonuclease, Phusion polymerase, Taq ligase was made in house (Ingrid Hoffmann). DNA fragments were amplified by PCR. Fragments that join together need to overlap at least 15 nucleotides. 5 µl mixture of DNA was mixed

with 15 µl of Gibson Master mix and incubated at 50 °C for 1 hour. 5-10 µL of this Gibson assembly reaction mix was transformed into competent cells.

6.7 Plasmid extraction and DNA purification

Plasmids and DNA were extracted using the following kits according to manufacturer's protocol.

Table 6-8. List of kits for plasmid/BAC DNA extraction

Kit Name	Company
NucleoSpin Plasmid (NoLid)	Macherey-Nagel GmbH; Düren, Germany
Roti-Prep Plasmid MINI	Carl Roth GmbH, Karlsruhe, Germany
Zymoclean Gel DNA Recovery Kit	**Zymo Research Corporation,** Irvine, U.S.A.
GeneJET Plasmid Miniprep Kit	**Thermo Scientific, Baltics, U.S.A**
QiaQuick PCR Purification Kit	**Qiagen, Hilden, Germany**
Wizard SV Gel and PCR Clean-up system	**Qiagen, Hilden, Germany**

6.8 Proteins purification from bacteria

Genes of interest were cloned into pGEX-6p-1 or pET28(A)+ vectors and expressed in Rosetta. Bacteria were grown in TB medium until they reached an $O.D_{600}$ of 0.8 and added 1 mM IPTG overnight at 20 °C for protein expression. The bacterial cells were pelleted by centrifugation at 6000 rpm for 10 min at room temperature. Cells were resuspended in GST binding buffer (25 mM HEPES pH 7.5, 300 mM NaCl, 1 mM EDTA, 5% glycerol, 1% Triton X-100, DNase) with 1 mM PMSF, lysed by sonication and cleared by centrifugation at 30,000 rpm for 30 min at 4 °C. The supernatant after the centrifugation was incubated with Glutathione resin (Amintra) for 4~8 hour at 4 °C. The beads were washed with GST binding buffer and the purified protein was used for experiments.

6.9 GST pull-down experiments

In vitro GST pull-downs were performed in GST binding buffer by incubating proteins of interest with GST alone or GST-tagged proteins (immobilized on Glutathione resin) for 1~3 hour at 4 °C. The reactions were washed with 1 ml GST binding buffer for three times, and samples were analyzed by SDS-page or Western blotting.

6.10 Protein expression in insect cells (Shweta Bendre's protocol)

The gene of interest was cloned into pFG vector and confirmed by sequencing. The

recombinant DNA was transformed into EMBACY *E.Coli* competent cells using heat shock method, and incubated at 37 °C for 6 hour. Bacterial cells were plated onto LB agar plates supplemented with 10 g/mL Gentamycin, 7 g/mL Tetracycline, 50 g/mL Kanamycin, 40 g/mL IPTG and 100 g/mL X-Gal. The EMBACY cells contain a BAC that harbors the Baculovirus genome along with a helper plasmid containing the Tn7 transposon enzyme complex under an IPTG inducible promoter. In the pFG vector, our gene of interest is flanked by Tn7R and Tn7L transposon sequences. In EMBACY cells after induction with IPTG, Tn7 transposon enzyme complex allows integration of our gene from the pFG vector to a site on the BAC, which disrupts the *LacZα* gene. Bacteria containing the recombinant BAC were identified using blue/white screening. One white colony was grown in liquid culture containing 10 g/mL Gentamycin, 7 g/mL Tetracycline, 50 g/mL Kanamycin overnight at 37 °C. The purified BAC was precipitated using isopropanol for 30 min on ice and further washed twice using 70% ethanol. The ethanol was removed under sterile conditions and the BAC was resuspended in Tris-EDTA buffer. Transfections were performed in 6 well dishes containing Sf9 cells ($1*10^6$ cells/mL; immortalized cell line from *Spodoptera frugiperda*) using FuGENE transfection reagent. The cells after transfection were incubated for 3 days at 27 °C. After 72 h, cells were resuspended and added to a 10 cm dish containing $1*10^6$ Sf9 cells/mL and incubated for 4 days at 27 °C for amplification of the virus. After 96 h, the cells were harvested and centrifuged at 2500 rpm for 5 min at 27 °C. Thereafter, 5% FBS was added to the supernatant, which was then sterile filtered and stored at 4 °C as V0 (Virus0). The virus was further amplified by adding 1:50 of the V0 to 50 mL $1*10^6$ Sf9 cells/mL and incubated for 4 days at 27 °C. The 50 mL culture was harvested by centrifugation and the supernatant was stored at 4 °C as V1. Similarly, the V1 was further amplified to produce V2, by adding 1:50 V1 in 50 mL Sf9 culture. This V2 was further used for large-scale expression of proteins in Tnao38 (*Trichoplusia ni*) cells.

6.11 *In vitro* proteins phosphorylation

Proteins of interest were phosphorylated by Aurora A, Aurora or Cdk1 using a molar ratio 1:100 (kinase: protein) overnight on ice in the buffer further supplemented with 10 mM $MgCl_2$, 1 mM sodium orthovanadate and 2 mM ATP. The phosphorylation reaction was stopped by adding 5 μM RO-3306 (Cdk1 inhibitor) or 500 nM MLN8054 (Aurora A inhibitor) for 10 min on ice. The proteins were then either used for GST pulldown.

6.12 ProQ Diamond staining

Phosphorylation of GTSE1 was confirmed using ProQ diamond staining. Equimolar concentrations (2 μM) of all proteins phosphorylated and unphosphorylated were resolved on a SDS PAGE gel. The gels were incubated with fixing solution overnight following which they were washed three times with water to remove all traces of fixing solution. Next the gels were incubated with ProQ Diamond phospho-specific stain for 90 min with shaking in dark. Gels were destained thrice for 30 min each with destaining solution followed by washing with water for 10 min thrice. All the steps were performed at room temperature. The signal for ProQ was detected using the BioRad developer. The gel was then stained with Coomassie blue (CB) to confirm equal protein loading.

6.13 Cell culture and cell expressing BAC lines

U2OS and U2OS BAC-transgene lines were grown in DMEM media containing 10% fetal bovine serum, 2 mM L-Glutamine, 100U/mL Penicillin and 0.1mg/mL streptomycin at 37 °C in 5% CO_2. U2OS cells expressing GTSE1-WT-GFP or GTSE1-5xLID-GFP were generated by transfecting the respective BACs using Effectene transfection reagent according to manufacturers protocol, and selecting for stable lines.

6.14 Gene silencing using RNA interference (RNAi)

Cells were seeded into 3,5 cm dishes one day before siRNA treatment. 3,0 μl lipofectamine RNAiMax and 25-50 nM siRNA were pre-incubated with 200 μl Opti-MEM for 5 min. These two mixtures were mixed and further incubated for 25 min. Cells were wished with PBS for 2 times, and added 1,6 ml Opti-MEM into the dishes. The siRNA/lipofectamine RNAiMax mixtures were further added into dishes. These reagents were replaced with culture medium following incubating for 6-8 hour. Cells were analyzed 48 to 60 hour after siRNA treatment. Sequences of siRNAs were shown below. GTSE1: 5′-GAUUCAUACAGGAGUCAAA-3′ (Ambion), CHC: 5′-GGUUGCUCUUGUUACGGAUtt-3′, Hec1-No.1: 5′-AACCCUGGGUCGUCAGGAA-3′, Hec1-No.2: 5′-AAGAGUAGAACUAGAAUGUGAA-3′.

6.15 Antibodies

Table 6-9. List of primary and secondary antibodies

Primary antibody	Directed to	Made in	Dilution		Clone number and Company
			WB	IF	
DM1α	Human	Mouse	1:10,000	1:400	Sigma Aldrich

Anti-GTSE1 3753	Human	Rabbit	1:30,000	1:1000	MPI CBG, Dresden (Scolz et al., 2012)
Anti-CREST	Human	Human	-	1:500	CS1058; Europa Bioproducts Ltd.
Anti-GFP		Rabit	1:10,000	1:500	Abcam (ab6556)
Anti-His		Mouse	1:5000		Qiagen
Anti-MCAK	Human	Mouse	1:100	1:200	Clone 1G2; Abnova Corporation
Anti-CHC	Human	Mouse	1:1000	1:500	Abcam (X22)
Anti-GST		Mouse	1:10,000		Novagen #71097-3
Anti-TACC3	Human	Rabbit	1:5000	1:500	Santa Cruz Biotechnlogy, H-300
Anti-pTACC3	Human	Rabbit	1:1000	1:2000	Kind gift from Kazu Kinoshita
Anti-MBP		Mouse	1:10000		NEB #E8032S
Anti-Aurora A	Human	Rabbit	1:2000		Abcam #12875
Texas Red (594) dye-conjugated AffinityPure	Mouse	Donkey	-	1:500	Jackson ImmunoResearch Europe Ltd., UK
Texas Red (594) dye-conjugated AffinityPure	Rabbit	Donkey		1:500	Bethyl Laboratories, Inc. Montgomery, USA
Texas Red (594) dye-conjugated AffinityPure	Human	Donkey		1:500	Jackson ImmunoResearch Laboratories
Alexa 488-conjugated AffinityPure	Mouse	Donkey		1:500	Bethyl Laboratories, Inc. Montgomery, USA
Alexa 488-conjugated AffinityPure	Rabbit	Donkey	-	1:500	Bethyl Laboratories, Inc. Montgomery, USA
Cy5-conjugated AffinityPure	Mouse	Donkey		1:300	Bethyl Laboratories, Inc. Montgomery,

					USA
Cy5-conjugated AffinityPure	Rabbit	Donkey		1:300	Bethyl Laboratories, Inc. Montgomery, USA
Cy5-conjugated AffinityPure	Human	Donkey		1:500	Jackson ImmunoResearch Laboratories
HRP-conjugated	Mouse	Goat	1:5000	-	GE/Amersham
HRP-conjugated	Rabbit	Donkey	1:5000	-	GE/Amersham

6.16 Immunofluorescence

Cells on coverslips were fixed using −20 °C methanol or 4% PFA/PIPES. For methanol fixation, cells were fixed using −20 °C methanol for 10 min and wished with PBS for 3 times to remove methanol. To prepare PFA/PIPES, 4% PFA dissolved in Pipes (50 mM Pipes, pH 7.2, 10 mM EGTA, 1 mM MgCl2, and 0.2% Triton X-100). For fixation, cells were incubated with 4% PFA/PIPES at room temperature for 10 min and then further incubated with 0.25% Triton X-100 for 5 min. Cells were then wished with PBS to remove the reagents. For immunofluorescence, cells were incubated with primary antibodies in 0.5% BSA in PBST for overnight at 4 °C in a humidified chamber. They were then washed for 30 min with PBST, and the same process was repeated with secondary antibodies. Coverslips were mounted with ProLong gold containing DAPI.

6.17 Immunoprecipitation

To prepare mitotic cells, 80% confluence of cells was arrested by adding 3.3 μM nocodazole for 18 hour and then harvested by shake-off. Cells were lysed using cell lysis buffer with protease inhibitor followed by centrifugation at 13,000 rpm for 10 min at 4 °C. Final concentration of the cell lysate was around 1mg/ml. 1-2 μg of the indicated antibody was added to ~900 μL of the cell lysate and incubated for 2 hour at 4 °C with rotation. 25 μL of Dynabeads coupled to protein G was washed with cell lysis buffer for 3 times and then added to the extracts to incubate for 4 hour at 4 °C. The beads were washed three times with 1 mL of cell lysis buffer and once with 1X PBS and then resuspended in hot Laemmli buffer to be analyzed by Western blotting.

6.18 Sodium dodecyl sulfate (SDS) electrophoresis

Proteins are denatured using Laemmli buffer, which contains a negatively charged detergent SDS that coats the polypeptide chains. Due to this the proteins obtain a net negative charge. These negatively charged proteins move with different speeds towards the anode. The speed at which they move depends on the molecular weight of proteins and the percentage of acrylamide in the gel. Smaller proteins move faster through the pores towards the anode, whereas, the motion of larger proteins is retarded due to the small pore size of the acrylamide gel. SDS PAGE gels were run using SDS-PAGE running buffer at 120-180 V for 1-1.5 hour.

6.19 Western blot

Proteins from SDS-PAGE gels were transferred onto nitrocellulose membrane using Western transfer buffer at 300 mA for 2 hour at 4 °C. The membrane was blocked with 5 % skimmed milk in 1X PBS containing 0.1% Tween20 (PBS-T) and incubated with primary antibodies overnight at 4 °C. The membrane was then washed three times for 10 min each using PBS-T followed by incubation with appropriate secondary antibodies for 1 h at room temperature. The membrane was washed three times for 15 min each with PBS-T. Protein signals were detected using enhanced chemiluminescence.

6.20 Proximity ligation assay (PLA)

Experiments were performed using the PLA kits (Sigma) according to manufacturer's protocol. In Brief, Cells on coverslips were fixed by 4% PFA/PIPES and wished with PBS. Fixed cells were performed blocking by the blocking reagent from the kit at 37 °C for 1 hour. Diluted MCAK and GFP antibodies for 100 times in the antibody dilution buffer from the kit, and coverslips were incubated with primary antibodies at 4 °C overnight. Coverslips were washed with 1xBuffer A from kit for 2 times (5 min for each time). Anti-mouse and anti-rabbit PLA probes were diluted for 5 times in the dilution buffer, and coverslips were incubated with the PLA probes at 37 °C for 1 hour. After the incubation, samples were wished with 1xBuffer A from kit for 2 times (5 min for each time). Samples with PLA probes were further preformed the ligation by ligase (1:40 dilution) from the kit at 37 °C for 30 min and then wished with 1xBuffer A from kit for 2 times (5 min for each time). To amplify the PLA signal, coverslips were incubated with amplification enzyme (1:80 dilution) from the kit at 37 °C for 100 min. Coverslips were washed with 1X Buffer B from the kit for 2 times (10 min for each time) and coverslips were mounted with mounting medium following washed with 0.01X Buffer B for 2 mim.

6.21 Fluorescence microtubule binding assay

Rhodamine-labeled tubulin, biotin-labeled tubulin and unlabeled tubulin were mixed (the final concentration of tubulin is 10 μm) and polymerized in the presence of 1 mM GTP in BRB buffer at 34 °C for 15 min. The microtubules were then stabilized by adding 20 μm and incubated for 5 more min. Microtubules were diluted 10 times in BRB buffer with 10 mM 2-mercaptoethanol. Coverslips for flow cells were incubated with 2% biotinylated poly-L-Lysine-PEG at room temperature for half hour, and try with N2 gas. Coated coverslips were assembled as flow cells. The surface of the flow cell was passivated with 1% pluronic F-127 at room temperature in a humility chamber for 1 hour. 0.1mg/ml avidin in BRB80 with 10uM taxol was added into the flow cell and incubated at room temperature for 10 min, and subsequently washed with at least 5 chamber volumes of BRB80 containing 10 uM taxol. Microtubules were added into the flow cell for 10 min. Protein of interest was then added into the flow cell. The flow cell was then imagined under microscopy.

6.22 Microscopy

Images were acquired using a Marianas (3i) spinning disk confocal system based on an Axio Observer Z1 microscopy (Zeiss) equipped with a Hamamatsu ORCA-Flash 4.0 Camera. Images were taken using 63x 1.4 NA Apochromat objective (Zeiss) and Slidebook software 6.0. All other images were acquired using a DeltaVision imaging system (GE Healthcare) equipped with an sCMOS camera (PCO edge 5.5). Images were taken using a 60x 1.42 NA PlanApo-N objective (Olympus) at room temperature. Serial Z-stacks of 0.2 μm thickness were obtained and deconvolved using SoftWoRx 6.1.1 software.

Bibliography

Akhmanova, A., and M.O. Steinmetz. 2008. Tracking the ends: a dynamic protein network controls the fate of microtubule tips. *Nat Rev Mol Cell Biol*. 9:309-322.

Akhmanova, A., and M.O. Steinmetz. 2015. Control of microtubule organization and dynamics: two ends in the limelight. *Nat Rev Mol Cell Biol*. 16:711-726.

Al-Bassam, J., H. Kim, G. Brouhard, A. van Oijen, S.C. Harrison, and F. Chang. 2010. CLASP promotes microtubule rescue by recruiting tubulin dimers to the microtubule. *Dev Cell*. 19:245-258.

Alfaro-Aco, R., A. Thawani, and S. Petry. 2017. Structural analysis of the role of TPX2 in branching microtubule nucleation. *J Cell Biol*. 216:983-997.

Alushin, G.M., V.H. Ramey, S. Pasqualato, D.A. Ball, N. Grigorieff, A. Musacchio, and E. Nogales. 2010. The Ndc80 kinetochore complex forms oligomeric arrays along microtubules. *Nature*. 467:805-810.

Asbury, C.L. 2017. Anaphase A: Disassembling Microtubules Move Chromosomes toward Spindle Poles. *Biology (Basel)*. 6.

Bakhoum, S.F., G. Genovese, and D.A. Compton. 2009a. Deviant kinetochore microtubule dynamics underlie chromosomal instability. *Curr Biol*. 19:1937-1942.

Bakhoum, S.F., S.L. Thompson, A.L. Manning, and D.A. Compton. 2009b. Genome stability is ensured by temporal control of kinetochore-microtubule dynamics. *Nat Cell Biol*. 11:27-35.

Barr, A.R., and F. Gergely. 2007. Aurora-A: the maker and breaker of spindle poles. *J Cell Sci*. 120:2987-2996.

Bendre, S., A. Rondelet, C. Hall, N. Schmidt, Y.C. Lin, G.J. Brouhard, and A.W. Bird. 2016. GTSE1 tunes microtubule stability for chromosome alignment and segregation by inhibiting the microtubule depolymerase MCAK. *J Cell Biol*. 215:631-647.

Bird, A.W., and A.A. Hyman. 2008. Building a spindle of the correct length in human cells requires the interaction between TPX2 and Aurora A. *J Cell Biol*. 182:289-300.

Booth, D.G., F.E. Hood, I.A. Prior, and S.J. Royle. 2011. A TACC3/ch-TOG/clathrin complex stabilises kinetochore fibres by inter-microtubule bridging. *EMBO J*. 30:906-919.

Borner, G.H., R. Antrobus, J. Hirst, G.S. Bhumbra, P. Kozik, L.P. Jackson, D.A. Sahlender, and M.S. Robinson. 2012. Multivariate proteomic profiling identifies novel accessory proteins of coated vesicles. *J Cell Biol*. 197:141-160.

Braun, M., D.R. Drummond, R.A. Cross, and A.D. McAinsh. 2009. The kinesin-14 Klp2 organizes microtubules into parallel bundles by an ATP-dependent sorting mechanism. *Nat Cell Biol*. 11:724-730.

Brodsky, F.M. 2012. Diversity of clathrin function: new tricks for an old protein. *Annu Rev Cell Dev Biol*. 28:309-336.

Brouhard, G., and D. Sept. 2012. Microtubules: sizing up the GTP cap. *Curr Biol*. 22:R802-803.

Brouhard, G.J., J.H. Stear, T.L. Noetzel, J. Al-Bassam, K. Kinoshita, S.C. Harrison, J. Howard, and A.A. Hyman. 2008. XMAP215 is a processive microtubule polymerase. *Cell*. 132:79-88.

Carmena, M., S. Ruchaud, and W.C. Earnshaw. 2009. Making the Auroras glow: regulation of Aurora A and B kinase function by interacting proteins. *Curr Opin Cell Biol*. 21:796-805.

Chao, W.T., and J. Kunz. 2009. Focal adhesion disassembly requires clathrin-dependent endocytosis of integrins. *FEBS Lett*. 583:1337-1343.

Cheeseman, I.M., and A. Desai. 2008. Molecular architecture of the kinetochore-microtubule interface. *Nat Rev Mol Cell Biol*. 9:33-46.

Cheeseman, L.P., E.F. Harry, A.D. McAinsh, I.A. Prior, and S.J. Royle. 2013. Specific removal of TACC3-ch-TOG-clathrin at metaphase deregulates kinetochore fiber tension. *J Cell Sci*. 126:2102-2113.

Ciferri, C., J. De Luca, S. Monzani, K.J. Ferrari, D. Ristic, C. Wyman, H. Stark, J. Kilmartin, E.D. Salmon, and A. Musacchio. 2005. Architecture of the human ndc80-hec1 complex, a critical constituent of the outer kinetochore. *J Biol Chem*. 280:29088-29095.

Ciferri, C., S. Pasqualato, E. Screpanti, G. Varetti, S. Santaguida, G. Dos Reis, A. Maiolica, J. Polka, J.G. De Luca, P. De Wulf, M. Salek, J. Rappsilber, C.A. Moores, E.D. Salmon, and A. Musacchio. 2008. Implications for kinetochore-microtubule attachment from the structure of an engineered Ndc80 complex. *Cell*. 133:427-439.

Cimini, D., L.A. Cameron, and E.D. Salmon. 2004. Anaphase spindle mechanics prevent mis-segregation of merotelically oriented chromosomes. *Curr Biol*. 14:2149-2155.

Cimini, D., X. Wan, C.B. Hirel, and E.D. Salmon. 2006. Aurora kinase promotes turnover of kinetochore microtubules to reduce chromosome segregation errors. *Curr Biol*. 16:1711-1718.

Cleghorn, W.M., K.M. Branch, S. Kook, C. Arnette, N. Bulus, R. Zent, I. Kaverina, E.V. Gurevich, A.M. Weaver, and V.V. Gurevich. 2015. Arrestins regulate cell spreading and motility via focal adhesion dynamics. *Mol Biol Cell*. 26:622-635.

Cleveland, D.W., Y. Mao, and K.F. Sullivan. 2003. Centromeres and kinetochores: from epigenetics to mitotic checkpoint signaling. *Cell*. 112:407-421.

Collavin, L., M. Monte, R. Verardo, C. Pfleger, and C. Schneider. 2000. Cell-cycle regulation of the p53-inducible gene B99. *FEBS Lett*. 481:57-62.

Crowther, R.A., and B.M. Pearse. 1981. Assembly and packing of clathrin into coats. *J Cell Biol*. 91:790-797.

D'Assoro, A.B., T. Haddad, and E. Galanis. 2015. Aurora-A Kinase as a Promising Therapeutic Target in Cancer. *Front Oncol*. 5:295.

Dannhauser, P.N., S.M. Camus, K. Sakamoto, L.A. Sadacca, J.A. Torres, M.D. Camus, K. Briant, S. Vassilopoulos, A. Rothnie, C.J. Smith, and F.M. Brodsky. 2017. CHC22 and CHC17 clathrins have distinct biochemical properties and display differential regulation and function. *J Biol Chem*. 292:20834-20844.

DeLuca, J.G., W.E. Gall, C. Ciferri, D. Cimini, A. Musacchio, and E.D. Salmon. 2006. Kinetochore microtubule dynamics and attachment stability are regulated by Hec1. *Cell*. 127:969-982.

DeLuca, K.F., S.M. Lens, and J.G. DeLuca. 2011. Temporal changes in Hec1 phosphorylation control kinetochore-microtubule attachment stability during mitosis. *J Cell Sci*. 124:622-634.

Domnitz, S.B., M. Wagenbach, J. Decarreau, and L. Wordeman. 2012. MCAK activity at microtubule tips regulates spindle microtubule length to promote robust kinetochore attachment. *J Cell Biol*. 197:231-237.

Dutertre, S., S. Descamps, and C. Prigent. 2002. On the role of aurora-A in centrosome function. *Oncogene*. 21:6175-6183.

Ertych, N., A. Stolz, A. Stenzinger, W. Weichert, S. Kaulfuss, P. Burfeind, A. Aigner, L. Wordeman, and H. Bastians. 2014. Increased microtubule assembly rates influence chromosomal instability in colorectal cancer cells. *Nat Cell Biol*. 16:779-791.

Ezratty, E.J., C. Bertaux, E.E. Marcantonio, and G.G. Gundersen. 2009. Clathrin mediates integrin endocytosis for focal adhesion disassembly in migrating cells. *J Cell Biol*. 187:733-747.

Fotin, A., Y. Cheng, N. Grigorieff, T. Walz, S.C. Harrison, and T. Kirchhausen. 2004. Structure of an auxilin-bound clathrin coat and its implications for the mechanism of uncoating. *Nature*. 432:649-653.

Fu, J., M. Bian, J. Liu, Q. Jiang, and C. Zhang. 2009. A single amino acid change converts Aurora-A into Aurora-B-like kinase in terms of partner specificity and cellular function. *Proc Natl Acad Sci U S A*. 106:6939-6944.

Fu, W., W. Tao, P. Zheng, J. Fu, M. Bian, Q. Jiang, P.R. Clarke, and C. Zhang. 2010. Clathrin recruits phosphorylated TACC3 to spindle poles for bipolar spindle assembly and chromosome alignment. *J Cell Sci*. 123:3645-3651.

Gergely, F. 2002. Centrosomal TACCtics. *Bioessays*. 24:915-925.

Gergely, F., V.M. Draviam, and J.W. Raff. 2003. The ch-TOG/XMAP215 protein is essential for spindle pole organization in human somatic cells. *Genes Dev*. 17:336-341.

Gergely, F., C. Karlsson, I. Still, J. Cowell, J. Kilmartin, and J.W. Raff. 2000a. The TACC domain identifies a family of centrosomal proteins that can interact with microtubules. *Proc Natl Acad Sci U S A*. 97:14352-14357.

Gergely, F., D. Kidd, K. Jeffers, J.G. Wakefield, and J.W. Raff. 2000b. D-TACC: a novel centrosomal protein required for normal spindle function in the early Drosophila embryo. *EMBO J*. 19:241-252.

Gulluni, F., M. Martini, M.C. De Santis, C.C. Campa, A. Ghigo, J.P. Margaria, E. Ciraolo, I. Franco, U. Ala, L. Annaratone, D. Disalvatore, G. Bertalot, G. Viale, A. Noatynska, M. Compagno, S. Sigismund, F. Montemurro, M. Thelen, F. Fan, P. Meraldi, C. Marchio, S. Pece, A. Sapino, R. Chiarle, P.P. Di Fiore, and E. Hirsch. 2017. Mitotic Spindle Assembly and Genomic Stability in Breast Cancer Require PI3K-C2alpha Scaffolding Function. *Cancer Cell*. 32:444-459 e447.

Guo, L., S. Zhang, B. Zhang, W. Chen, X. Li, W. Zhang, C. Zhou, J. Zhang, N. Ren, and Q. Ye. 2016. Silencing GTSE-1 expression inhibits proliferation and invasion of hepatocellular carcinoma cells. *Cell Biol Toxicol*. 32:263-274.

Gutierrez-Caballero, C., S.G. Burgess, R. Bayliss, and S.J. Royle. 2015. TACC3-ch-TOG track the growing tips of microtubules independently of clathrin and Aurora-A phosphorylation. *Biol Open*. 4:170-179.

Hans, F., D.A. Skoufias, S. Dimitrov, and R.L. Margolis. 2009. Molecular distinctions between Aurora A and B: a single residue change transforms Aurora A into correctly localized and functional Aurora B. *Mol Biol Cell*. 20:3491-3502.

Hauf, S., R.W. Cole, S. LaTerra, C. Zimmer, G. Schnapp, R. Walter, A. Heckel, J. van Meel, C.L. Rieder, and J.M. Peters. 2003. The small molecule Hesperadin reveals a role for Aurora B in correcting kinetochore-microtubule attachment and in maintaining the spindle assembly checkpoint. *J Cell Biol*. 161:281-294.

Heald, R., and A. Khodjakov. 2015. Thirty years of search and capture: The complex simplicity of mitotic spindle assembly. *J Cell Biol*. 211:1103-1111.

Honnappa, S., S.M. Gouveia, A. Weisbrich, F.F. Damberger, N.S. Bhavesh, H. Jawhari, I. Grigoriev, F.J. van Rijssel, R.M. Buey, A. Lawera, I. Jelesarov, F.K. Winkler, K. Wuthrich, A. Akhmanova, and M.O. Steinmetz. 2009. An EB1-binding motif acts as a microtubule tip localization signal. *Cell*. 138:366-376.

Hood, F.E., and S.J. Royle. 2009. Functional equivalence of the clathrin heavy chains CHC17 and CHC22 in endocytosis and mitosis. *J Cell Sci*. 122:2185-2190.

Hood, F.E., S.J. Williams, S.G. Burgess, M.W. Richards, D. Roth, A. Straube, M. Pfuhl, R. Bayliss, and S.J. Royle. 2013. Coordination of adjacent domains mediates TACC3-ch-TOG-clathrin assembly and mitotic spindle binding. *J Cell Biol*. 202:463-478.

Hsu, K.S., and T. Toda. 2011. Ndc80 internal loop interacts with Dis1/TOG to ensure proper kinetochore-spindle attachment in fission yeast. *Curr Biol*. 21:214-220.

Huang, H., J. Feng, J. Famulski, J.B. Rattner, S.T. Liu, G.D. Kao, R. Muschel, G.K. Chan, and T.J. Yen. 2007. Tripin/hSgo2 recruits MCAK to the inner centromere to correct defective kinetochore attachments. *J Cell Biol*. 177:413-424.

Hubner, N.C., A.W. Bird, J. Cox, B. Splettstoesser, P. Bandilla, I. Poser, A. Hyman, and M. Mann. 2010. Quantitative proteomics combined with BAC TransgeneOmics reveals in vivo protein interactions. *J Cell Biol*. 189:739-754.

Janke, C., and J.C. Bulinski. 2011. Post-translational regulation of the microtubule cytoskeleton: mechanisms and functions. *Nat Rev Mol Cell Biol*. 12:773-786.

Kajtez, J., A. Solomatina, M. Novak, B. Polak, K. Vukusic, J. Rudiger, G. Cojoc, A. Milas, I. Sumanovac Sestak, P. Risteski, F. Tavano, A.H. Klemm, E. Roscioli, J. Welburn, D. Cimini, M. Gluncic, N. Pavin, and I.M. Tolic. 2016. Overlap microtubules link sister k-fibres and balance the forces on bi-oriented kinetochores. *Nat Commun*. 7:10298.

Kang, D.S., R.C. Kern, M.A. Puthenveedu, M. von Zastrow, J.C. Williams, and J.L. Benovic. 2009. Structure of an arrestin2-clathrin complex reveals a novel clathrin binding domain that modulates receptor trafficking. *J Biol Chem*. 284:29860-29872.

Keen, J.H. 1990. Clathrin and associated assembly and disassembly proteins. *Annu Rev Biochem*. 59:415-438.

Kinoshita, K., T.L. Noetzel, L. Pelletier, K. Mechtler, D.N. Drechsel, A. Schwager, M. Lee, J.W. Raff, and A.A. Hyman. 2005. Aurora A phosphorylation of TACC3/maskin is required for centrosome-dependent microtubule assembly in mitosis. *J Cell Biol*. 170:1047-1055.

Kirchhausen, T., D. Owen, and S.C. Harrison. 2014. Molecular structure, function, and dynamics of clathrin-mediated membrane traffic. *Cold Spring Harb Perspect Biol*. 6:a016725.

Knowlton, A.L., W. Lan, and P.T. Stukenberg. 2006. Aurora B is enriched at merotelic attachment sites, where it regulates MCAK. *Curr Biol*. 16:1705-1710.

Lampson, M.A., and I.M. Cheeseman. 2011. Sensing centromere tension: Aurora B and the regulation of kinetochore function. *Trends Cell Biol*. 21:133-140.

Lan, W., X. Zhang, S.L. Kline-Smith, S.E. Rosasco, G.A. Barrett-Wilt, J. Shabanowitz, D.F. Hunt, C.E. Walczak, and P.T. Stukenberg. 2004. Aurora B phosphorylates centromeric MCAK and regulates its localization and microtubule depolymerization activity. *Curr Biol*. 14:273-286.

Lara-Gonzalez, P., F.G. Westhorpe, and S.S. Taylor. 2012. The spindle assembly checkpoint. *Curr Biol*. 22:R966-980.

Li, X., and R.B. Nicklas. 1995. Mitotic forces control a cell-cycle checkpoint. *Nature*. 373:630-632.

Lin, C.H., C.K. Hu, and H.M. Shih. 2010. Clathrin heavy chain mediates TACC3 targeting to mitotic spindles to ensure spindle stability. *J Cell Biol*. 189:1097-1105.

Liu, D., G. Vader, M.J. Vromans, M.A. Lampson, and S.M. Lens. 2009. Sensing chromosome bi-orientation by spatial separation of aurora B kinase from kinetochore substrates. *Science*. 323:1350-1353.

Liu, X., and R.L. Erikson. 2002. Activation of Cdc2/cyclin B and inhibition of centrosome amplification in cells depleted of Plk1 by siRNA. *Proc Natl Acad Sci U S A*. 99:8672-8676.

Liu, X.S., H. Li, B. Song, and X. Liu. 2010. Polo-like kinase 1 phosphorylation of G2 and S-phase-expressed 1 protein is essential for p53 inactivation during G2 checkpoint recovery. *EMBO Rep*. 11:626-632.

Macurek, L., A. Lindqvist, D. Lim, M.A. Lampson, R. Klompmaker, R. Freire, C. Clouin, S.S. Taylor, M.B. Yaffe, and R.H. Medema. 2008. Polo-like kinase-1 is activated by aurora A to promote checkpoint recovery. *Nature*. 455:119-123.

Magidson, V., C.B. O'Connell, J. Loncarek, R. Paul, A. Mogilner, and A. Khodjakov. 2011. The spatial arrangement of chromosomes during prometaphase facilitates spindle assembly. *Cell*. 146:555-567.

Maney, T., A.W. Hunter, M. Wagenbach, and L. Wordeman. 1998. Mitotic centromere-associated kinesin is important for anaphase chromosome segregation. *J Cell Biol*. 142:787-801.

Manning, A.L., and D.A. Compton. 2008. Structural and regulatory roles of nonmotor spindle proteins. *Curr Opin Cell Biol*. 20:101-106.

Maro, B., M.H. Johnson, S.J. Pickering, and D. Louvard. 1985. Changes in the distribution of membranous organelles during mouse early development. *J Embryol Exp Morphol*. 90:287-309.

Marumoto, T., D. Zhang, and H. Saya. 2005. Aurora-A - a guardian of poles. *Nat Rev Cancer*. 5:42-50.

Mastronarde, D.N., K.L. McDonald, R. Ding, and J.R. McIntosh. 1993. Interpolar spindle microtubules in PTK cells. *J Cell Biol*. 123:1475-1489.

McClelland, S.E., S. Borusu, A.C. Amaro, J.R. Winter, M. Belwal, A.D. McAinsh, and P. Meraldi. 2007. The CENP-A NAC/CAD kinetochore complex controls chromosome congression and spindle bipolarity. *EMBO J*. 26:5033-5047.

Meraldi, P., R. Honda, and E.A. Nigg. 2002. Aurora-A overexpression reveals tetraploidization as a major route to centrosome amplification in p53-/- cells. *EMBO J*. 21:483-492.

Miele, A.E., P.J. Watson, P.R. Evans, L.M. Traub, and D.J. Owen. 2004. Two distinct interaction motifs in amphiphysin bind two independent sites on the clathrin terminal domain beta-propeller. *Nat Struct Mol Biol*. 11:242-248.

Miller, M.P., C.L. Asbury, and S. Biggins. 2016. A TOG Protein Confers Tension Sensitivity to Kinetochore-Microtubule Attachments. *Cell*. 165:1428-1439.

Mitchison, T., and M. Kirschner. 1984. Dynamic instability of microtubule growth. *Nature*. 312:237-242.

Monte, M., R. Benetti, G. Buscemi, P. Sandy, G. Del Sal, and C. Schneider. 2003. The cell cycle-regulated protein human GTSE-1 controls DNA damage-induced apoptosis by affecting p53 function. *J Biol Chem*. 278:30356-30364.

Muenzner, J., L.M. Traub, B.T. Kelly, and S.C. Graham. 2017. Cellular and viral peptides bind multiple sites on the N-terminal domain of clathrin. *Traffic*. 18:44-57.

Musacchio, A., and A. Desai. 2017. A Molecular View of Kinetochore Assembly and Function. *Biology (Basel)*. 6.

Nicklas, R.B., and S.C. Ward. 1994. Elements of error correction in mitosis: microtubule capture, release, and tension. *J Cell Biol*. 126:1241-1253.

Nishimura, T., and K. Kaibuchi. 2007. Numb controls integrin endocytosis for directional cell migration with aPKC and PAR-3. *Dev Cell*. 13:15-28.

Nixon, F.M., C. Gutierrez-Caballero, F.E. Hood, D.G. Booth, I.A. Prior, and S.J. Royle. 2015. The mesh is a network of microtubule connectors that stabilizes individual kinetochore fibers of the mitotic spindle. *Elife*. 4.

Okamoto, C.T., J. McKinney, and Y.Y. Jeng. 2000. Clathrin in mitotic spindles. *Am J Physiol Cell Physiol*. 279:C369-374.

Olmsted, J.B. 1986. Microtubule-associated proteins. *Annu Rev Cell Biol*. 2:421-457.

Parra, M.T., R. Gomez, A. Viera, J. Page, A. Calvente, L. Wordeman, J.S. Rufas, and J.A. Suja. 2006. A perikinetochoric ring defined by MCAK and Aurora-B as a novel centromere domain. *PLoS Genet*. 2:e84.

Parsons, J.T., A.R. Horwitz, and M.A. Schwartz. 2010. Cell adhesion: integrating cytoskeletal dynamics and cellular tension. *Nat Rev Mol Cell Biol*. 11:633-643.

Pesenti, M.E., J.R. Weir, and A. Musacchio. 2016. Progress in the structural and functional characterization of kinetochores. *Curr Opin Struct Biol*. 37:152-163.

Peterman, E.J., and J.M. Scholey. 2009. Mitotic microtubule crosslinkers: insights from mechanistic studies. *Curr Biol*. 19:R1089-1094.

Petrovic, A., J. Keller, Y. Liu, K. Overlack, J. John, Y.N. Dimitrova, S. Jenni, S. van Gerwen, P. Stege, S. Wohlgemuth, P. Rombaut, F. Herzog, S.C. Harrison, I.R. Vetter, and A. Musacchio. 2016. Structure of the MIS12 Complex and Molecular Basis of Its Interaction with CENP-C at Human Kinetochores. *Cell*. 167:1028-1040 e1015.

Pfleger, C.M., and M.W. Kirschner. 2000. The KEN box: an APC recognition signal distinct from the D box targeted by Cdh1. *Genes Dev*. 14:655-665.

Prosser, S.L., and L. Pelletier. 2017. Mitotic spindle assembly in animal cells: a fine balancing act. *Nat Rev Mol Cell Biol*. 18:187-201.

Raff, J.W., and R. Basto. 2017. Centrosome Amplification and Cancer: A Question of Sufficiency. *Dev Cell*. 40:217-218.

Reed, N.A., D. Cai, T.L. Blasius, G.T. Jih, E. Meyhofer, J. Gaertig, and K.J. Verhey. 2006. Microtubule acetylation promotes kinesin-1 binding and transport. *Curr Biol*. 16:2166-2172.

Rieder, C.L. 1981. The structure of the cold-stable kinetochore fiber in metaphase PtK1 cells. *Chromosoma*. 84:145-158.

Royle, S.J. 2012. The role of clathrin in mitotic spindle organisation. *J Cell Sci*. 125:19-28.

Royle, S.J. 2013. Protein adaptation: mitotic functions for membrane trafficking proteins. *Nat Rev Mol Cell Biol*. 14:592-599.

Royle, S.J., N.A. Bright, and L. Lagnado. 2005. Clathrin is required for the function of the mitotic spindle. *Nature*. 434:1152-1157.

Royle, S.J., and L. Lagnado. 2006. Trimerisation is important for the function of clathrin at the mitotic spindle. *J Cell Sci*. 119:4071-4078.

Ruchaud, S., M. Carmena, and W.C. Earnshaw. 2007. Chromosomal passengers: conducting cell division. *Nat Rev Mol Cell Biol*. 8:798-812.

Scolz, M., P.O. Widlund, S. Piazza, D.R. Bublik, S. Reber, L.Y. Peche, Y. Ciani, N. Hubner, M. Isokane, M. Monte, J. Ellenberg, A.A. Hyman, C. Schneider, and A.W. Bird. 2012. GTSE1 is a microtubule plus-end tracking protein that regulates EB1-dependent cell migration. *PLoS One*. 7:e51259.

Sharma, A., A. Aher, N.J. Dynes, D. Frey, E.A. Katrukha, R. Jaussi, I. Grigoriev, M. Croisier, R.A. Kammerer, A. Akhmanova, P. Gonczy, and M.O. Steinmetz. 2016. Centriolar CPAP/SAS-4 Imparts Slow Processive Microtubule Growth. *Dev Cell*. 37:362-376.

Shimizu, H., I. Nagamori, N. Yabuta, and H. Nojima. 2009. GAK, a regulator of clathrin-mediated membrane traffic, also controls centrosome integrity and chromosome congression. *J Cell Sci*. 122:3145-3152.

Singh, P., G.E. Thomas, K.K. Gireesh, and T.K. Manna. 2014. TACC3 protein regulates microtubule nucleation by affecting gamma-tubulin ring complexes. *J Biol Chem*. 289:31719-31735.

Slep, K.C. 2009. The role of TOG domains in microtubule plus end dynamics. *Biochem Soc Trans*. 37:1002-1006.

Smith, C.M., V. Haucke, A. McCluskey, P.J. Robinson, and M. Chircop. 2013. Inhibition of clathrin by pitstop 2 activates the spindle assembly checkpoint and induces cell death in dividing HeLa cancer cells. *Mol Cancer*. 12:4.

Tanaka, T.U., M.J. Stark, and K. Tanaka. 2005. Kinetochore capture and bi-orientation on the mitotic spindle. *Nat Rev Mol Cell Biol*. 6:929-942.

Tanenbaum, M.E., T. Vallenius, E.F. Geers, L. Greene, T.P. Makela, and R.H. Medema. 2010. Cyclin G-associated kinase promotes microtubule outgrowth from chromosomes during spindle assembly. *Chromosoma*. 119:415-424.

ter Haar, E., S.C. Harrison, and T. Kirchhausen. 2000. Peptide-in-groove interactions link target proteins to the beta-propeller of clathrin. *Proc Natl Acad Sci U S A*. 97:1096-1100.

ter Haar, E., A. Musacchio, S.C. Harrison, and T. Kirchhausen. 1998. Atomic structure of clathrin: a beta propeller terminal domain joins an alpha zigzag linker. *Cell*. 95:563-573.

Thakur, H.C., M. Singh, L. Nagel-Steger, J. Kremer, D. Prumbaum, E.K. Fansa, H. Ezzahoini, K. Nouri, L. Gremer, A. Abts, L. Schmitt, S. Raunser, M.R. Ahmadian, and R.P. Piekorz. 2014. The centrosomal adaptor TACC3 and the microtubule polymerase chTOG interact via defined C-terminal subdomains in an Aurora-A kinase-independent manner. *J Biol Chem*. 289:74-88.

Tian, T., E. Zhang, F. Fei, X. Li, X. Guo, B. Liu, J. Li, Z. Chen, and J. Xing. 2011. Up-regulation of GTSE1 lacks a relationship with clinical data in lung cancer. *Asian Pac J Cancer Prev*. 12:2039-2043.

Tolic, I.M. 2017. Mitotic spindle: kinetochore fibers hold on tight to interpolar bundles. *Eur Biophys J*.

Ungewickell, E., and D. Branton. 1981. Assembly units of clathrin coats. *Nature*. 289:420-422.

Utrera, R., L. Collavin, D. Lazarevic, D. Delia, and C. Schneider. 1998. A novel p53-inducible gene coding for a microtubule-localized protein with G2-phase-specific expression. *EMBO J*. 17:5015-5025.

Vader, G., R.H. Medema, and S.M. Lens. 2006. The chromosomal passenger complex: guiding Aurora-B through mitosis. *J Cell Biol*. 173:833-837.

Vaughan, K.T. 2005. TIP maker and TIP marker; EB1 as a master controller of microtubule plus ends. *J Cell Biol*. 171:197-200.

von Kleist, L., W. Stahlschmidt, H. Bulut, K. Gromova, D. Puchkov, M.J. Robertson, K.A. MacGregor, N. Tomilin, A. Pechstein, N. Chau, M. Chircop, J. Sakoff, J.P. von Kries, W. Saenger, H.G. Krausslich, O. Shupliakov, P.J. Robinson, A. McCluskey, and V.

Haucke. 2011. Role of the clathrin terminal domain in regulating coated pit dynamics revealed by small molecule inhibition. *Cell*. 146:471-484.

Wang, E., E.R. Ballister, and M.A. Lampson. 2011. Aurora B dynamics at centromeres create a diffusion-based phosphorylation gradient. *J Cell Biol*. 194:539-549.

Wang, G., Q. Jiang, and C. Zhang. 2014. The role of mitotic kinases in coupling the centrosome cycle with the assembly of the mitotic spindle. *J Cell Sci*. 127:4111-4122.

Wei, R.R., P.K. Sorger, and S.C. Harrison. 2005. Molecular organization of the Ndc80 complex, an essential kinetochore component. *Proc Natl Acad Sci U S A*. 102:5363-5367.

Widlund, P.O., J.H. Stear, A. Pozniakovsky, M. Zanic, S. Reber, G.J. Brouhard, A.A. Hyman, and J. Howard. 2011. XMAP215 polymerase activity is built by combining multiple tubulin-binding TOG domains and a basic lattice-binding region. *Proc Natl Acad Sci U S A*. 108:2741-2746.

Wilde, A., and F.M. Brodsky. 1996. In vivo phosphorylation of adaptors regulates their interaction with clathrin. *J Cell Biol*. 135:635-645.

Willox, A.K., and S.J. Royle. 2012. Functional analysis of interaction sites on the N-terminal domain of clathrin heavy chain. *Traffic*. 13:70-81.

Wood, L.A., G. Larocque, N.I. Clarke, S. Sarkar, and S.J. Royle. 2017. New tools for "hot-wiring" clathrin-mediated endocytosis with temporal and spatial precision. *J Cell Biol*. 216:4351-4365.

Wordeman, L., and T.J. Mitchison. 1995. Identification and partial characterization of mitotic centromere-associated kinesin, a kinesin-related protein that associates with centromeres during mitosis. *J Cell Biol*. 128:95-104.

Wu, X., A. Kodama, and E. Fuchs. 2008. ACF7 regulates cytoskeletal-focal adhesion dynamics and migration and has ATPase activity. *Cell*. 135:137-148.

Wu, X., Q.T. Shen, D.S. Oristian, C.P. Lu, Q. Zheng, H.W. Wang, and E. Fuchs. 2011. Skin stem cells orchestrate directional migration by regulating microtubule-ACF7 connections through GSK3beta. *Cell*. 144:341-352.

Wu, X., H. Wang, Y. Lian, L. Chen, L. Gu, J. Wang, Y. Huang, M. Deng, Z. Gao, and Y. Huang. 2017. GTSE1 promotes cell migration and invasion by regulating EMT in hepatocellular carcinoma and is associated with poor prognosis. *Sci Rep*. 7:5129.

Yue, J., Y. Zhang, W.G. Liang, X. Gou, P. Lee, H. Liu, W. Lyu, W.J. Tang, S.Y. Chen, F. Yang, H. Liang, and X. Wu. 2016. In vivo epidermal migration requires focal adhesion targeting of ACF7. *Nat Commun*. 7:11692.

Acknowledgements

First of all, I would like to thank my supervisor Dr. Alex Bird. Thank Alex for giving me the opportunity to join his lab. Alex is always very supportive and let me experience any techniques in different fields of biology. I would like to express my sincere gratitude to him for all the scientific discussions, efforts and help during my Ph.D.

I would like to thank my thesis committee Prof. Andrea Musacchio, Prof. Hemmo Meyer and Prof. Stefan Westermann for the valuable suggestions and discussions. I am grateful to Dr. Arthur Porfetye and Dr. Ingrid Vetter for their help in the crystallization and the contributions to the CHC-GTSE1 structure.

I want to thank present and past members in Bird lab. Because of you we have the wonderful atmosphere in the lab. I would like to acknowledge Dr. Arnaud Rondelet for his contributions to the project and the joyful cooperation. I am thankful to Pia Brinkert who identified the CHC-binding mutant on GTSE1. I appreciate her constant supports for the work and my private life. I am grateful to Dr. Shweta Bendre who gives me the big help for the thesis writing, and also her accompaniment when we got started in Dortmund. I would like to thank Nadine Schmidt for her help in generating cell line, and her friendship for sharing the good and bad times. I would like to thank Divya Singh for the identification of GTSE1 phosphorylation and her lovely singing and smiles in the lab. I am thankful to the past members who created nice homely environment in the lab, especially, Brenda Aguero, Julian Berlitz, Lisa Mazul, Eugenie Werbenko and Dominic Heinecke. A big thank you goes to Lisa-Marie Kuhl, Maria-Ascension Villar-Fernandez, Vivek Raina, Dr. Richard Cardoso da Silva and Annika Sarembe. The time in lab would not be so interesting without you guys. I would like to thank Yen-Chun Lee, a dear friend, who always understands me and supports me. I am thankful to Christa Hornemann, Dr. Lucia Sironi and Antje Peukert for all their help in any difficulties and the administration.

It has been pleasent working in Prof. Andrea Musacchio's department. He is always willing to share all reagents and equipment from his lab, and attending his group meetings is very helpful to get new ideas for my work. I would also like to thank colleagues from his lab for all the trouble-shootings and scientific discussions.

Last but not least, I am thankful to Taiwanese government for offering me the fellowship during my Ph.D. I would especially like to thank my family for the endless support and let me follow my dreams. I would like to express my gratitude to Karsten who always stands by me. It would have been much difficult to complete this thesis without his accompany, constant help and support.

Curriculum vitae

Der Lebenslauf ist in der Online-Version aus Gründen des Datenschutzes nicht enthalten.

Affidavit

Hiermit erkläre ich, Yu-Chih Lin gem. § 7 Abs. (2) d) + f) der Promotionsordnung der Fakultät für Biologie zur Erlangung des Dr. rer. nat., dass ich die vorliegende Dissertation selbständig verfasst und mich keiner anderen als der angegebenen Hilfsmittel bedient, bei der Abfassung der Dissertation nur die angegeben Hilfsmittel benutzt und alle wörtlich oder inhaltlich übernommenen Stellen als solche gekennzeichnet habe.

Essen, den _____ _____

Unterschrift des/r Doktoranden/in

Erklärung:

Hiermit erkläre ich, Yu-Chih Lin gem. § 7 Abs. (2) e) + g) der Promotionsordnung der Fakultät für Biologie zur Erlangung des Dr. rer. nat., dass ich keine anderen Promotionen bzw. Promotionsversuche in der Vergangenheit durchgeführt habe und dass diese Arbeit von keiner anderen Fakultät/Fachbereich abgelehnt worden ist.

Essen, den _____ _____

Unterschrift des Doktoranden

Erklärung:

Hiermit erkläre ich, Prof. Dr. Andrea Musacchio gem. § 6 Abs. (2) g) der Promotionsordnung der Fakultät für Biologie zur Erlangung der Dr. rer. nat., dass ich das Arbeitsgebiet, dem das Thema "GTSE1 regulates microtubule stability during mitosis through inhibition of the microtubule depolymerase MCAK", zuzuordnen ist, in Forschung und Lehre vertrete und den Antrag von Shweta Bendre befürworte und die Betreuung auch im Falle eines Weggangs, wenn nicht wichtige Gründe dem entgegenstehen, weiterführen werde.

Essen, den _____ _____

Unterschrift eines Mitglieds der Universität Duisburg-Essen